


6-2015

Chlorinated Tyrosine Species as Markers of Inflammation: A Kinetic Study

Matthew Peter Curtis

Follow this and additional works at: <http://scholarsrepository.llu.edu/etd>

 Part of the [Anatomy Commons](#), and the [Medical Biochemistry Commons](#)

Recommended Citation

Curtis, Matthew Peter, "Chlorinated Tyrosine Species as Markers of Inflammation: A Kinetic Study" (2015). *Loma Linda University Electronic Theses, Dissertations & Projects*. 259.
<http://scholarsrepository.llu.edu/etd/259>

This Dissertation is brought to you for free and open access by TheScholarsRepository@LLU: Digital Archive of Research, Scholarship & Creative Works. It has been accepted for inclusion in Loma Linda University Electronic Theses, Dissertations & Projects by an authorized administrator of TheScholarsRepository@LLU: Digital Archive of Research, Scholarship & Creative Works. For more information, please contact scholarsrepository@llu.edu.

LOMA LINDA UNIVERSITY
School of Medicine
in conjunction with the
Faculty of Graduate Studies

Chlorinated Tyrosine Species as Markers of Inflammation: A Kinetic Study

by

Matthew Peter Curtis

A Dissertation submitted in partial satisfaction of
the requirements for the degree
Doctor of Philosophy in Biochemistry

June 2015

© 2015

Matthew Peter Curtis
All Rights Reserved

Each person whose signature appears below certifies that this dissertation in his/her opinion is adequate, in scope and quality, as a dissertation for the degree Doctor of Philosophy.

_____, Chairperson
Jonathan Neidigh, Assistant Professor of Biochemistry

Paul Herrmann, Associate Professor of Pathology and Human Anatomy

Christopher Perry, Assistant Professor of Biochemistry

Nathan Wall, Assistant Professor of Biochemistry

David Weldon, Associate Professor of Pharmaceutical and Administrative Sciences,
School of Pharmacy

ACKNOWLEDGEMENTS

My gratitude goes to my mentor and professor, Dr. Jonathan Neidigh. He fostered in me the tools to tackle most any challenge, helped me develop proficiency and independence, and found opportunities for me to use the skills I gained to collaborate with other researchers. Over past seven years, I've appreciated his forthrightness, his intelligence, and his encouragement.

I would like to thank Loma Linda University Department of Biochemistry for allowing me the use of their facilities and the members of my committee: Jonathan Neidigh, Paul Herrmann, Christopher Perry, Nathan Wall, and David Weldon for their guidance and support. I am also grateful to Kerby Oberg, Penelope Duerksen-Hughes, and Marissa Fulache for their guidance and assistance over the years.

Lastly, I would like to thank my family. To my siblings and parents, thank you for your love and support. To my in-laws, thank you for your acceptance and your care. My beloved wife, Gennaya, deserves the greatest appreciation. She has been by my side these past six years and encouraged me when even the smallest problem seemed insurmountable. I pray that whatever the future holds for us, we will be able to meet it together with God's grace.

CONTENTS

Approval Page.....	iii
Acknowledgements.....	iv
Contents	v
List of Figures	ix
List of Tables	xi
List of Abbreviations	xii
Abstract.....	xiv
Chapter	
1. Introduction.....	1
Inflammation Contributes to Disease Pathology	1
Myeloperoxidase Creates Chlorinating and Nitrating Species	2
Tyrosine Analogues as Markers of MPO Activity	3
The Purpose of These Studies.....	5
References.....	8
2. Kinetics of Formation and Degradation of 3-Chlorotyrosine by Hypochlorous Acid and Chloramines.....	14
Abstract.....	15
Introduction.....	16
Experimental Procedures	19
Materials	19
Synthesis of N-acetyl-3-chlorotyrosine	19
Synthesis of N-acetyl-3,5-dichlorotyrosine	21
Synthesis of Ac-KGNYAE-NH ₂	22
Methods.....	22
UV/Vis Spectroscopy of Tyrosine Chlorination by HOCl	23
Reactions of Tyrosine Analogues with HOCl or Chloramines.....	23
HPLC Measurement of Chlorination Products	24
Analysis of Kinetics Data and Determination of Rate Constants	25

Dependence of Kinetics on Presence of Chloride and Solution pH.....	25
Chlorination of Tyrosine by HOCl in a Lysine-Containing Peptide.....	26
Results.....	27
HOCl Reacts with 3ClTyr to form Cl ₂ Tyr.....	27
HOCl Chlorinate 3ClTyr More Rapidly than Tyr.....	32
Chloride Increases Tyr Chlorination at Acidic pH Values.....	35
Chloramines Chlorinate 3ClTyr More Rapidly than Tyr.....	38
Lysine Chloramine Rapidly Chlorinates Tyrosine in the Context of a Peptide.....	39
Discussion.....	41
References.....	48
3. Kinetics of 3-Nitrotyrosine Chlorination by Hypochlorous Acid and Chloramines.....	55
Abstract.....	56
Introduction.....	57
Experimental Procedures.....	58
Materials.....	58
Synthesis of N-acetyl-3-nitrotyrosine.....	59
Synthesis of N-acetyl-3-chloro-5-nitrotyrosine.....	61
Synthesis of N-FMOC-3-nitrotyrosine.....	61
Peptide Synthesis and Purification.....	62
Methods.....	62
Reactions of AcNO ₂ Tyr with HOCl or Chloramines.....	63
UV/Vis Spectroscopy of AcClNO ₂ Tyr Chlorination by HOCl.....	64
Reaction of Peptides with HOCl.....	64
HPLC Quantitation of Reaction Products.....	64
Determination of Initial Reaction Rate and Reaction Order.....	65
Analysis of Kinetics Data and Determination of Rate Constants.....	65
Results.....	66
HOCl Reacts with NO ₂ Tyr to Form ClNO ₂ Tyr.....	66
HOCl Reacts with AcClNO ₂ Tyr to Form Unknown Products.....	70
Rate of NO ₂ Tyr Chlorination by HOCl Increases in Peptides.....	73

NO ₂ Tyr Chlorination by HOCl in Peptides is a First Order Reaction	73
Discussion.....	76
References.....	82
4. Effect of Primary and Secondary Structure on the Rate of Tyrosine Chlorination by Hypochlorous Acid.....	86
Abstract.....	87
Introduction	88
Experimental Procedures	90
Materials	90
Linear Peptide Synthesis and Purification	90
Synthesis of ^D Phe-chlorotrityl Resin	91
Cyclic Peptide Synthesis and Purification	92
Methods.....	94
Reaction of Peptides with HOCl.....	94
HPLC Quantitation of Reaction Products.....	95
Analysis of Kinetics Data and Determination of Rate Constants	95
Characterization of Secondary Structure by Circular Dichroism	97
Results.....	98
Spacing of Lysine and Tyrosine Residues Alters Rate of Chlorination	98
CD Spectra of Cyclic Peptide Indicates Gramicidin S Homology	98
Rate of Tyrosine Chlorination by Lysine Chloramine Increased in Cyclic Peptide	101
Discussion.....	101
References.....	107
5. Discussion.....	112
Loss of 3ClTyr and NO ₂ Tyr by HOCl.....	112
Chlorination of Tyrosine by Chloramines	114
Effect of Peptide Primary Structure on Tyrosine Chlorination by HOCl.....	118
Effect of Peptide Secondary Structure on Tyrosine Chlorination by HOCl.....	120
Overall Trends in the Kinetics of Chlorination of Tyrosine Analogues.....	121

Future Directions	123
References.....	125

Appendices

A. Characterization of Ac-KGNYAE-NH ₂ Chlorination Products by MALDI-TOF	130
B. GC-MS of Tyr, 3ClTyr, and Cl ₂ Tyr.....	131
C. Chlorination of Tyrosine Lowers the pKa Value of the Phenol Hydroxyl	132
D. Chlorination of AcNO ₂ Tyr Lowers the pKa Value of the Phenol Hydroxyl	133
E. pH-Dependence of the Apparent Rate Constant of AcNO ₂ Tyr Chlorination by HOCl.....	134
F. Confirmation of Cyclic Structure of cyclo-P(OH)TKLDFP(OH)TYLDF- by MS/MS.....	135
G. CD Spectra of Peptides Containing Lysine and NO ₂ Y	136

FIGURES

Figures	Page
Chapter 1	
1. Potential Pathways of Tyrosine Chlorination and Nitration by MPO	4
Chapter 2	
1. Synthesis of Ac3ClTyr and AcCl ₂ Tyr	20
2. UV Spectroscopy of AcTyr or Ac3ClTyr Reacting with HOCl	29
3. UV Spectrum of Tyrosine Analogues in Varying pH Values.....	30
4. HPLC Detection of Products Formed when AcTyr Reacts with HOCl	31
5. Kinetics of AcTyr Chlorination by HOCl and AcHisCl.....	33
6. Kinetic Scheme for Modeling the Chlorination of AcTyr	34
7. Effect of Chloride and pH on Rate of Tyrosine Chlorination.....	37
8. Rapid Chlorination of Tyrosine by Lysine Chloramine in a Peptide.....	40
9. Summary of Reactions by HOCl that Compete with 3ClTyr Formation.....	45
Chapter 3	
1. Synthesis of AcNO ₂ Tyr and AcClNO ₂ Tyr	60
2. Separation and Quantitation of AcNO ₂ Tyr and AcClNO ₂ Tyr by HPLC	68
3. Kinetics of AcNO ₂ Tyr Chlorination by HOCl or AcHisCl	69
4. UV/Vis Analysis of AcClNO ₂ Tyr Reacting with HOCl.....	72
5. Acceleration of NO ₂ Tyr Chlorination by His Chloramine in a Peptide	74
6. Determining the Rate Order of NO ₂ Tyr Chlorination by Chloramines within a Peptide.....	75
7. Kinetics Schemes for the Chlorination of NO ₂ Tyr by HOCl	80

Chapter 4

1. Structure of cyclo-P(OH)TKL^DFP(OH)TYL^DF93
2. Kinetic Scheme of Intramolecular Tyrosine Chlorination.....96
3. CD Spectra of cyclo-P(OH)TKL^DFP(OH)TYL^DF100
4. Kinetics of cyclo-P(OH)TKL^DFP(OH)TYL^DF Chlorination by HOCl.....102

Chapter 5

1. Products of 3ClTyr and NO₂Tyr Reacting with HOCl or Chloramines113
2. Summary of Reactions by HOCl that Compete with 3ClTyr Formation.....117

TABLES

Tables	Page
Chapter 2	
1. Rate Constants for Chlorination of Tyr Analogues by HOCl and Chloramines	36
Chapter 3	
1. Rate Constants for Chlorination of Tyrosine, 3ClTyr, and NO ₂ Tyr.....	71
2. Rate Constants for Chlorination of Tyr and NO ₂ Tyr within a Peptide.....	77
Chapter 4	
1. Rate Constants for Chlorination of NO ₂ Tyr by Lysine Chloramine within a Peptide.....	99
Chapter 5	
1. Summary of Tyrosine Analogue Chlorination as Free Amino Acids.....	116
2. Summary of Tyrosine Analogue Chlorination in Peptides	119

LIST OF ABBREVIATIONS

$^1\text{H-NMR}$	Proton Nuclear Magnetic Resonance
3ClTyr	3-Chlorotyrosine
Ac ₂ O	Acetic Anhydride
Ac3ClTyr	N-Acetyl-3-Chlorotyrosine
AcCl ₂ Tyr	N-Acetyl-3,5-Dichlorotyrosine
AcClNO ₂ Tyr	N-Acetyl-3-Chloro-5-Nitrotyrosine
AcHis	N- α -Acetylhistidine
AcHisCl	N- α -Acetyl-N- δ -Chlorohistidine
AcLys	N- α -Acetyllysine
AcLysCl	N- α -Acetyl-N- ϵ -Chlorolysine
AcLysCl ₂	N- α -Acetyl-N,N- ϵ,ϵ -Dichlorolysine
AcNO ₂ Tyr	N-Acetyl-3-Nitrotyrosine
AcTyr	N-Acetyltyrosine
BOC	<i>tert</i> -Butyloxycarbonyl
CD	Circular Dichroism
Cl ⁻	Chloride
Cl ₂	Chlorine
Cl ₂ Tyr	3,5-Dichlorotyrosine
ClNO ₂ Tyr	3-Chloro-5-Nitrotyrosine
DCM	Dichloromethane
DIPEA	N,N-Diisopropylethylamine
Fmoc	Fluorenylmethyloxycarbonylchloride

H ₂ O ₂	Hydrogen Peroxide
H ₂ SO ₄	Sulfuric Acid
HOCl	Hypochlorous Acid
HPLC	High Pressure Liquid Chromatography
iNOS	Inducible Nitric Oxide Synthase
MPO	Myeloperoxidase
NaNO ₃	Sodium Nitrate
NO•	Nitric Oxide
NO ₂ •	Nitrogen Dioxide
NO ₂ ⁻	Nitrite
NO ₂ Cl	Nitryl Chloride
NO ₂ Tyr	3-Nitrotyrosine
O ₂ •	Superoxide
ONOO ⁻	Peroxynitrite.
RNS	Reactive Nitrogen Species
SO ₂ Cl ₂	Sulfuryl Chloride
SPE	Solid Phase Extraction
SSD	Sum of Squared Differences
TFA	Trifluoroacetic Acid
Tyr	Tyrosine
UV/Vis	Ultraviolet-Visible Light
V ₀	Initial Reaction Rate

ABSTRACT OF THE DISSERTATION

Chlorinated Tyrosine Species as Markers of Inflammation: A Kinetic Study

by

Matthew Peter Curtis

Doctor of Philosophy, Graduate Program in Biochemistry

Loma Linda University, June 2015

Dr. Jonathan W. Neidigh, Chairperson

Chronic inflammation is associated with numerous human diseases. During inflammation, leukocytes release the enzyme myeloperoxidase (MPO) which generates reactive oxygen species such as hypochlorous acid (HOCl). Additionally, MPO generates reactive nitrogen species. These reactive species can damage host fats, proteins, and DNA, contributing to disease pathology.

Because of the reactivity and short half-lives of reactive species, measurement of surrogate markers is necessary to determine their extent and source. Chlorination of the tyrosine phenol ring by HOCl to produce 3-chlorotyrosine (3ClTyr) or nitration of the phenol ring by reactive nitrogen species to produce 3-nitrotyrosine (NO₂Tyr) are two such markers. Both are stable byproducts of MPO activity and are readily measurable.

Some studies, however, have called into question their use as biomarkers of inflammation. Concentrations of 3ClTyr or NO₂Tyr reportedly decrease upon exposure to HOCl, suggesting that any measurement of these *in vivo* would be underestimated. These studies, however, failed to quantify the rate of degradation and did not identify the products.

Furthermore, there is some evidence to suggest that, *in vivo*, chlorination of tyrosine by HOCl occurs through chloramine intermediates rather than directly. This is

evidenced by the preferential chlorination of tyrosine residues that are nearby lysine or histidine, whose side-chain amines react with HOCl to become chloramines. This contradicts the relatively slow reactions kinetics of tyrosine chlorination by histidine or lysine chloramine and warrants further investigation.

In these studies, we identify the product of 3ClTyr and NO₂Tyr reacting with HOCl as 3,5-dichlorotyrosine (Cl₂Tyr) and 3-chloro-5-nitrotyrosine (ClNO₂Tyr), respectively. The second-order rate constants of the chlorination of tyrosine, 3ClTyr, and NO₂Tyr by HOCl, histidine chloramine, and lysine chloramine are reported. The relevance of Cl₂Tyr and ClNO₂Tyr *in vivo* are discussed.

Additionally, we investigate the kinetics of tyrosine chlorination in the context of a lysine- or histidine-containing peptide. The rate of chlorination of tyrosine within a peptide is dependent on the primary and secondary structure and is a first-order, intramolecular reaction. These studies further support the role of chloramines in the chlorination of protein-bound tyrosine and, to our knowledge, are the first to provide rate constants.

CHAPTER ONE

INTRODUCTION

Inflammation Contributes to Disease Pathology

Inflammation is a defensive response triggered by damage to living tissues. Its purpose is to localize and eliminate any harmful agents and remove damaged components so that the body can begin the healing process. However, prolonged periods of inflammation can be more harmful than beneficial. Chronic inflammation can eventually lead to tissue destruction and the functional impairments that characterize many human disease conditions.¹ The generation of reactive oxygen species (ROS) in inflammatory tissue is thought to drive proinflammatory cytokine production, thus prolonging the duration of the inflammatory process and contributing to the pathogenesis of human diseases.²

The human diseases that are associated with chronic inflammation and reactive oxygen species are varied, affecting numerous organ systems with different presentations. Chronic inflammation has been implicated in the pathology of disorders including psoriasis of the skin,³ arthritis of the joints,⁴ lung diseases,⁵⁻⁷ cardiovascular disease,⁸⁻¹⁰ and neurodegenerative diseases.¹¹⁻¹³ Even cancers are associated with chronic inflammation, as seen in the increased incidence of colorectal cancer in patients with inflammatory bowel disease,^{14, 15} increased production of reactive species in breast tumors,^{16, 17} and studies linking inflammation with tumorigenesis.¹⁸⁻²¹ As reactive species have been implicated in more and more disease pathologies, there has been a greater effort to study their generation and to measure their effects in tissue.

Myeloperoxidase Creates Chlorinating and Nitrating Species

Neutrophils are a major source of reactive oxygen species and are likely contributors to the diseases in which inflammatory cells participate.²² Neutrophils that have been activated by cytokines during inflammation generate superoxide and its dismutase byproduct, hydrogen peroxide. In addition, the heme enzyme myeloperoxidase (MPO) is released which has the unique ability to catalyze the reaction between chloride ions and hydrogen peroxide to create hypochlorous acid (HOCl).²³

HOCl is a highly reactive species that can react to form either oxidized or chlorinated products. *In vivo*, there are many potential targets of HOCl including nucleic acids, lipids, and proteins.^{24, 25} Reactions with proteins are especially common due to their relative abundance. HOCl reacts rapidly with thiols or thioesters on cysteine or methionine side-chains,²⁶ with free amines on the N-terminus or lysine and histidine side-chains to give chloramines,²⁷ and with the phenol ring of tyrosine producing 3-chlorotyrosine (3ClTyr).²⁸ These reactions damage proteins thus impairing their normal function.²⁹ For example, apolipoprotein A-I, which normally removes cholesterol from macrophages, can be oxidized by HOCl, impairing its ability to remove cholesterol and contributing to atherosclerosis of arteries.³⁰

In addition to oxidation and chlorination, MPO participates in the generation of reactive nitrating agents. Two such species are nitrogen dioxide (NO_2^\bullet), which is generated by the oxidation of nitrite (NO_2^-) by MPO,³¹ and nitryl chloride (NO_2Cl_2), which is generated by the oxidation of NO_2^- by MPO-derived HOCl.^{32, 33} These reactive nitrogen species can result in modulation of the catalytic activity of enzymes through nitration. For example, nitration of cyclooxygenase-2 results in inhibition, shortening the

inflammatory response,³⁴ or nitration can inhibit mitochondrial respiration, leading to cell death.³⁵⁻³⁷ Nitration of tyrosine by NO_2Cl or NO_2^* results in the formation of 3-nitrotyrosine (NO_2Tyr). **Figure 1** provides a summary of reactions involving MPO that results in the generation of reactive nitrogen species and ROS.

Tyrosine Analogues as Markers of MPO Activity

Biomarkers of reactant species have the potential to allow researchers and clinicians the ability to determine the extent of oxidative injury and identify the source of the oxidative stress. Unfortunately, finding an appropriate biomarker can be challenging. Expression of MPO, for example, has been correlated to disease pathology,³⁸⁻⁴⁰ but its use as a potential biomarker of reactive species is complicated by the presence of both active and inactive forms of the enzyme.⁴¹⁻⁴³ Direct measurement of oxidative species themselves is also difficult because of their high reactivity and short lifetime in biological environments.⁴⁴ Instead, surrogate markers, often the product of a reactive species with a biological molecule, need to be measured to study the role of reactive species in disease pathology.^{45, 46}

The characteristics of a good biomarker include specificity, stability, and measurability.²⁴ Specificity means that the marker is only produced by the reactive species or enzyme in question. For example, MPO is the only human enzyme to produce HOCl and is present predominantly in neutrophils and monocytes.⁴⁷ Thus, HOCl or HOCl-derived byproducts would be specific markers of the oxidant activity of neutrophils and other MPO-containing cells.

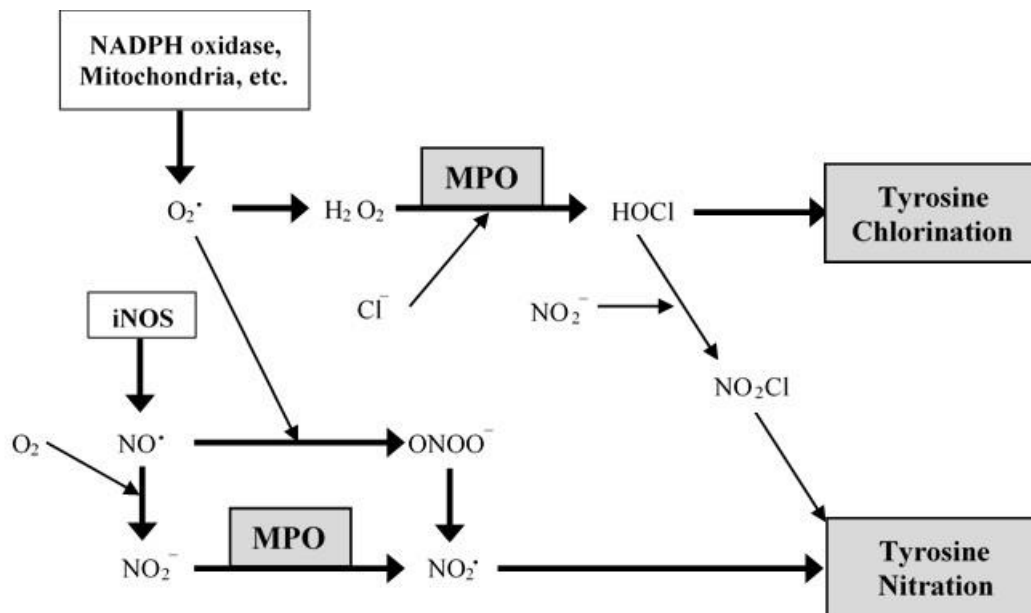


Figure 1: Potential Pathways of Tyrosine Chlorination and Nitration by MPO. Cl^- , chloride; H_2O_2 , hydrogen peroxide; HOCl , hypochlorous acid; iNOS , inducible nitric oxide synthase; MPO , myeloperoxidase; NO^* , nitric oxide; NO_2^* , nitrogen dioxide; NO_2^- , nitrite; NO_2Cl , nitryl chloride; O_2^* , superoxide; ONOO^- , peroxynitrite.

Stability implies that a molecule is able to persist for great lengths of time in physiologic conditions, without degrading further, reacting with other molecules, or being enzymatically repaired. DNA bases, for instance, are oxidized or chlorinated by HOCl to form hydroxyuracil, 5-hydroxycytosine, 8-chloroadenosine, 5-chlorocytosine, and more.⁴⁸⁻⁵⁰ However, the repair of damaged DNA molecules, with the possible exception of 5-chlorocytosine,⁵¹ precludes their use as biomarkers of HOCl. Chloramines, the byproduct of HOCl with free protein amines, also continue to react with other molecules at high rates and have relatively short half-lives.^{52, 53} Chlorination or nitration of tyrosine by MPO-derived compounds to make 3ClTyr or NO₂Tyr, however, produce more stable end products that persist for long periods of time *in vivo*.^{54, 55}

Measurability of a potential biomarker means that there are laboratory techniques or instruments to measure the marker that are consistent and sensitive. In the case of 3ClTyr and NO₂Tyr, several methods of measuring these compounds exist. 3ClTyr can be measured qualitatively by antibody-based immunoassays^{56, 57} or quantitatively measured by mass spectrometry⁵⁸ and HPLC.⁵⁹ NO₂Tyr can likewise be measured using HPLC⁶⁰ and tandem mass spectrometry,^{61, 62} while its measurement by immunoassays is still undergoing investigation.⁶³ Because they are unique byproducts of MPO activity, stable, and quantifiable, both 3ClTyr and NO₂Tyr are promising potential biomarkers of the extent of MPO activity in inflamed tissue.

The Purpose of These Studies

While much of the literature appears to support the role of 3ClTyr and NO₂Tyr as biomarkers of MPO in inflamed tissue, two studies in particular have called into question

their stability and usefulness as biomarkers. One study qualitatively describes the loss of measurable 3CITyr upon exposure to HOCl.⁵⁹ Likewise, the second study shows concentrations of NO₂Tyr decrease when exposed to HOCl.⁶⁴ These studies suggest a more complicated relationship with HOCl and implicate that these markers have been underestimated in previous reports. Neither of these studies, however, quantitatively measured the rate of disappearance nor suggested what the products of such a reaction would be.

In addition, it has been suggested by other studies that, *in vivo*, tyrosine is more likely to be chlorinated by HOCl-derived chloramines than by HOCl directly.^{44, 47} Even though the rate of tyrosine chlorination by lysine chloramine as free amino acids appears too slow to be of significance,⁶⁵ several different groups have shown preferential chlorination of tyrosine residues within proteins that are near in space to histidine or lysine residues.^{55, 65, 66} Though this pattern has been established, there have been no studies into the exact mechanism of tyrosine chlorination in this context nor the quantification of the rates of chlorination.

Our purpose in these studies is to investigate the disappearance of 3CITyr and NO₂Tyr on exposure to HOCl, to determine what role chloramines play in tyrosine chlorination, and to investigate how tyrosine chlorination differs in the context of a peptide. Our first study identifies the product of 3CITyr reacting with HOCl, measures the rate at which 3CITyr disappears, and shows how lysine and histidine chloramines are able to accomplish tyrosine chlorination as well, albeit slower than HOCl (**Chapter 2**). The second study focuses on the disappearance of NO₂Tyr when it reacts with HOCl, again investigating the role of chloramines, but this study further investigates the

mechanism of how chloramines are able to more favorably chlorinate tyrosine when they are located on the same peptide (**Chapter 3**). Our last study looks at how changes in the primary or secondary structure of a peptide that place tyrosine and chloramine residues closer in space are able to change the reaction kinetics, significantly speeding up the rate of chlorination when compared to free amino acids (**Chapter 4**). Finally, our conclusions are summarized and the relevance of our findings in regards to the role of 3ClTyr and NO₂Tyr as biomarkers of MPO activity are discussed in the context of our current understanding of the literature (**Chapter 5**).

References

1. Karin, M., Lawrence, T., and Nizet, V. (2006) Innate immunity gone awry: linking microbial infections to chronic inflammation and cancer. *Cell*, 124, 823-835.
2. Naik, E., and Dixit, V. M. (2011) Mitochondrial reactive oxygen species drive proinflammatory cytokine production. *The Journal of experimental medicine*, 208, 417-420.
3. Lynde, C. W., Poulin, Y., Vender, R., Bourcier, M., and Khalil, S. (2014) Interleukin 17A: toward a new understanding of psoriasis pathogenesis. *Journal of the American Academy of Dermatology*, 71, 141-150.
4. Komatsu, N., and Takayanagi, H. (2012) Autoimmune arthritis: the interface between the immune system and joints. *Advances in immunology*, 115, 45-71.
5. Yamamoto, M., Tochino, Y., Chibana, K., Trudeau, J. B., Holguin, F., and Wenzel, S. E. (2012) Nitric oxide and related enzymes in asthma: relation to severity, enzyme function and inflammation. *Clinical and experimental allergy : journal of the British Society for Allergy and Clinical Immunology*, 42, 760-768.
6. Ricciardolo, F. L., Caramori, G., Ito, K., Capelli, A., Brun, P., Abatangelo, G., Papi, A., Chung, K. F., Adcock, I., Barnes, P. J., Donner, C. F., Rossi, A., and Di Stefano, A. (2005) Nitrosative stress in the bronchial mucosa of severe chronic obstructive pulmonary disease. *The Journal of allergy and clinical immunology*, 116, 1028-1035.
7. Wijnhoven, H. J., Heunks, L. M., Geraedts, M. C., Hafmans, T., Vina, J. R., and Dekhuijzen, P. N. (2006) Oxidative and nitrosative stress in the diaphragm of patients with COPD. *International journal of chronic obstructive pulmonary disease*, 1, 173-179.
8. Upmacis, R. K. (2008) Atherosclerosis: A Link Between Lipid Intake and Protein Tyrosine Nitration. *Lipid insights*, 2008, 75.
9. Tao, L., Gao, E., Jiao, X., Yuan, Y., Li, S., Christopher, T. A., Lopez, B. L., Koch, W., Chan, L., Goldstein, B. J., and Ma, X. L. (2007) Adiponectin cardioprotection after myocardial ischemia/reperfusion involves the reduction of oxidative/nitritative stress. *Circulation*, 115, 1408-1416.
10. Stocker, R., and Keaney, J. F., Jr. (2004) Role of oxidative modifications in atherosclerosis. *Physiological reviews*, 84, 1381-1478.
11. Bombeiro, A. L., D'Imperio Lima, M. R., Chadi, G., and Alvarez, J. M. (2010) Neurodegeneration and increased production of nitrotyrosine, nitric oxide synthase, IFN-gamma and S100beta protein in the spinal cord of IL-12p40-deficient mice infected with *Trypanosoma cruzi*. *Neuroimmunomodulation*, 17, 67-78.

12. Iravani, M. M., Kashefi, K., Mander, P., Rose, S., and Jenner, P. (2002) Involvement of inducible nitric oxide synthase in inflammation-induced dopaminergic neurodegeneration. *Neuroscience*, 110, 49-58.
13. Halliwell, B. (2006) Oxidative stress and neurodegeneration: where are we now? *Journal of neurochemistry*, 97, 1634-1658.
14. Itzkowitz, S. H., and Yio, X. (2004) Inflammation and cancer IV. Colorectal cancer in inflammatory bowel disease: the role of inflammation. *American journal of physiology. Gastrointestinal and liver physiology*, 287, G7-17.
15. Payne, C. M., Bernstein, C., Bernstein, H., Gerner, E. W., and Garewal, H. (1999) Reactive nitrogen species in colon carcinogenesis. *Antioxidants & redox signaling*, 1, 449-467.
16. Harris, R. E., Casto, B. C., and Harris, Z. M. (2014) Cyclooxygenase-2 and the inflammogenesis of breast cancer. *World journal of clinical oncology*, 5, 677-692.
17. Haklar, G., Sayin-Ozveri, E., Yuksel, M., Aktan, A. O., and Yalcin, A. S. (2001) Different kinds of reactive oxygen and nitrogen species were detected in colon and breast tumors. *Cancer letters*, 165, 219-224.
18. Reuter, S., Gupta, S. C., Chaturvedi, M. M., and Aggarwal, B. B. (2010) Oxidative stress, inflammation, and cancer: how are they linked? *Free radical biology & medicine*, 49, 1603-1616.
19. Sun, B., and Karin, M. (2013) Inflammation and liver tumorigenesis. *Frontiers of medicine*, 7, 242-254.
20. Kamp, D. W., Shacter, E., and Weitzman, S. A. (2011) Chronic inflammation and cancer: the role of the mitochondria. *Oncology*, 25, 400-410, 413.
21. Ohshima, H., Tatemichi, M., and Sawa, T. (2003) Chemical basis of inflammation-induced carcinogenesis. *Archives of biochemistry and biophysics*, 417, 3-11.
22. Dahlgren, C., and Karlsson, A. (1999) Respiratory burst in human neutrophils. *Journal of immunological methods*, 232, 3-14.
23. Harrison, J. E., and Schultz, J. (1976) Studies on the chlorinating activity of myeloperoxidase. *The Journal of biological chemistry*, 251, 1371-1374.
24. Winterbourn, C. C., and Kettle, A. J. (2000) Biomarkers of myeloperoxidase-derived hypochlorous acid. *Free radical biology & medicine*, 29, 403-409.
25. Hawkins, C. L., Pattison, D. I., and Davies, M. J. (2003) Hypochlorite-induced oxidation of amino acids, peptides and proteins. *Amino acids*, 25, 259-274.

26. Winterbourn, C. C. (1985) Comparative reactivities of various biological compounds with myeloperoxidase-hydrogen peroxide-chloride, and similarity of the oxidant to hypochlorite. *Biochimica et biophysica acta*, 840, 204-210.
27. Prutz, W. A. (1996) Hypochlorous acid interactions with thiols, nucleotides, DNA, and other biological substrates. *Archives of biochemistry and biophysics*, 332, 110-120.
28. Kettle, A. J. (1996) Neutrophils convert tyrosyl residues in albumin to chlorotyrosine. *FEBS letters*, 379, 103-106.
29. Pattison, D. I., and Davies, M. J. (2006) Reactions of myeloperoxidase-derived oxidants with biological substrates: gaining chemical insight into human inflammatory diseases. *Current medicinal chemistry*, 13, 3271-3290.
30. Shao, B., Tang, C., Heinecke, J. W., and Oram, J. F. (2010) Oxidation of apolipoprotein A-I by myeloperoxidase impairs the initial interactions with ABCA1 required for signaling and cholesterol export. *Journal of lipid research*, 51, 1849-1858.
31. van der Vliet, A., Eiserich, J. P., Halliwell, B., and Cross, C. E. (1997) Formation of reactive nitrogen species during peroxidase-catalyzed oxidation of nitrite. A potential additional mechanism of nitric oxide-dependent toxicity. *The Journal of biological chemistry*, 272, 7617-7625.
32. Eiserich, J. P., Hristova, M., Cross, C. E., Jones, A. D., Freeman, B. A., Halliwell, B., and van der Vliet, A. (1998) Formation of nitric oxide-derived inflammatory oxidants by myeloperoxidase in neutrophils. *Nature*, 391, 393-397.
33. Hazen, S. L., Zhang, R., Shen, Z., Wu, W., Podrez, E. A., MacPherson, J. C., Schmitt, D., Mitra, S. N., Mukhopadhyay, C., Chen, Y., Cohen, P. A., Hoff, H. F., and Abu-Soud, H. M. (1999) Formation of nitric oxide-derived oxidants by myeloperoxidase in monocytes: pathways for monocyte-mediated protein nitration and lipid peroxidation *In vivo*. *Circulation research*, 85, 950-958.
34. Clancy, R., Varenika, B., Huang, W., Ballou, L., Attur, M., Amin, A. R., and Abramson, S. B. (2000) Nitric oxide synthase/COX cross-talk: nitric oxide activates COX-1 but inhibits COX-2-derived prostaglandin production. *Journal of immunology*, 165, 1582-1587.
35. Schopfer, F. J., Baker, P. R., and Freeman, B. A. (2003) NO-dependent protein nitration: a cell signaling event or an oxidative inflammatory response? *Trends in biochemical sciences*, 28, 646-654.
36. Greenacre, S. A., and Ischiropoulos, H. (2001) Tyrosine nitration: localisation, quantification, consequences for protein function and signal transduction. *Free radical research*, 34, 541-581.

37. Virag, L., Szabo, E., Gergely, P., and Szabo, C. (2003) Peroxynitrite-induced cytotoxicity: mechanism and opportunities for intervention. *Toxicology letters*, 140-141, 113-124.
38. Choi, D. K., Pennathur, S., Perier, C., Tieu, K., Teismann, P., Wu, D. C., Jackson-Lewis, V., Vila, M., Vonsattel, J. P., Heinecke, J. W., and Przedborski, S. (2005) Ablation of the inflammatory enzyme myeloperoxidase mitigates features of Parkinson's disease in mice. *The Journal of neuroscience: the official journal of the Society for Neuroscience*, 25, 6594-6600.
39. Rainis, T., Maor, I., Lanir, A., Shnizer, S., and Lavy, A. (2007) Enhanced oxidative stress and leucocyte activation in neoplastic tissues of the colon. *Digestive diseases and sciences*, 52, 526-530.
40. Sugiyama, S., Okada, Y., Sukhova, G. K., Virmani, R., Heinecke, J. W., and Libby, P. (2001) Macrophage myeloperoxidase regulation by granulocyte macrophage colony-stimulating factor in human atherosclerosis and implications in acute coronary syndromes. *The American journal of pathology*, 158, 879-891.
41. Lefkowitz, D. L., and Lefkowitz, S. S. (2001) Macrophage-neutrophil interaction: a paradigm for chronic inflammation revisited. *Immunology and cell biology*, 79, 502-506.
42. King, C. C., Jefferson, M. M., and Thomas, E. L. (1997) Secretion and inactivation of myeloperoxidase by isolated neutrophils. *Journal of leukocyte biology*, 61, 293-302.
43. Edwards, S. W., Hughes, V., Barlow, J., and Bucknall, R. (1988) Immunological detection of myeloperoxidase in synovial fluid from patients with rheumatoid arthritis. *The Biochemical journal*, 250, 81-85.
44. Dalle-Donne, I., Scaloni, A., Giustarini, D., Cavarra, E., Tell, G., Lungarella, G., Colombo, R., Rossi, R., and Milzani, A. (2005) Proteins as biomarkers of oxidative/nitrosative stress in diseases: the contribution of redox proteomics. *Mass spectrometry reviews*, 24, 55-99.
45. Dalle-Donne, I., Rossi, R., Colombo, R., Giustarini, D., and Milzani, A. (2006) Biomarkers of oxidative damage in human disease. *Clinical chemistry*, 52, 601-623.
46. Lesko, L. J., and Atkinson, A. J., Jr. (2001) Use of biomarkers and surrogate endpoints in drug development and regulatory decision making: criteria, validation, strategies. *Annual review of pharmacology and toxicology*, 41, 347-366.
47. Klebanoff, S. J. (2005) Myeloperoxidase: friend and foe. *Journal of leukocyte biology*, 77, 598-625.

48. Whiteman, M., Jenner, A., and Halliwell, B. (1997) Hypochlorous acid-induced base modifications in isolated calf thymus DNA. *Chemical research in toxicology*, 10, 1240-1246.
49. Badouard, C., Masuda, M., Nishino, H., Cadet, J., Favier, A., and Ravanat, J. L. (2005) Detection of chlorinated DNA and RNA nucleosides by HPLC coupled to tandem mass spectrometry as potential biomarkers of inflammation. *Journal of chromatography. B, Analytical technologies in the biomedical and life sciences*, 827, 26-31.
50. Kang, J. I., Jr., and Sowers, L. C. (2008) Examination of hypochlorous acid-induced damage to cytosine residues in a CpG dinucleotide in DNA. *Chemical research in toxicology*, 21, 1211-1218.
51. Valinluck, V., Liu, P., Kang, J. I., Jr., Burdzy, A., and Sowers, L. C. (2005) 5-halogenated pyrimidine lesions within a CpG sequence context mimic 5-methylcytosine by enhancing the binding of the methyl-CpG-binding domain of methyl-CpG-binding protein 2 (MeCP2). *Nucleic acids research*, 33, 3057-3064.
52. Hazen, S. L., Hsu, F. F., d'Avignon, A., and Heinecke, J. W. (1998) Human neutrophils employ myeloperoxidase to convert alpha-amino acids to a battery of reactive aldehydes: a pathway for aldehyde generation at sites of inflammation. *Biochemistry*, 37, 6864-6873.
53. Zgliczynski, J. M., Stelmaszynska, T., Ostrowski, W., Naskalski, J., and Sznajd, J. (1968) Myeloperoxidase of human leukaemic leucocytes. Oxidation of amino acids in the presence of hydrogen peroxide. *European journal of biochemistry / FEBS*, 4, 540-547.
54. Haqqani, A. S., Kelly, J. F., and Birnboim, H. C. (2002) Selective nitration of histone tyrosine residues in vivo in mutatact tumors. *The Journal of biological chemistry*, 277, 3614-3621.
55. Kang, J. I., Jr., and Neidigh, J. W. (2008) Hypochlorous acid damages histone proteins forming 3-chlorotyrosine and 3,5-dichlorotyrosine. *Chemical research in toxicology*, 21, 1028-1038.
56. Malle, E., Hazell, L., Stocker, R., Sattler, W., Esterbauer, H., and Waeg, G. (1995) Immunologic detection and measurement of hypochlorite-modified LDL with specific monoclonal antibodies. *Arteriosclerosis, thrombosis, and vascular biology*, 15, 982-989.
57. Malle, E., Waeg, G., Schreiber, R., Grone, E. F., Sattler, W., and Grone, H. J. (2000) Immunohistochemical evidence for the myeloperoxidase/H₂O₂/halide system in human atherosclerotic lesions: colocalization of myeloperoxidase and hypochlorite-modified proteins. *European journal of biochemistry / FEBS*, 267, 4495-4503.

58. Hazen, S. L., Crowley, J. R., Mueller, D. M., and Heinecke, J. W. (1997) Mass spectrometric quantification of 3-chlorotyrosine in human tissues with attomole sensitivity: a sensitive and specific marker for myeloperoxidase-catalyzed chlorination at sites of inflammation. *Free radical biology & medicine*, 23, 909-916.
59. Whiteman, M., and Spencer, J. P. (2008) Loss of 3-chlorotyrosine by inflammatory oxidants: implications for the use of 3-chlorotyrosine as a bio-marker in vivo. *Biochemical and biophysical research communications*, 371, 50-53.
60. Herce-Pagliai, C., Kotecha, S., and Shuker, D. E. (1998) Analytical methods for 3-nitrotyrosine as a marker of exposure to reactive nitrogen species: a review. *Nitric oxide: biology and chemistry / official journal of the Nitric Oxide Society*, 2, 324-336.
61. Nicholls, S. J., Shen, Z., Fu, X., Levison, B. S., and Hazen, S. L. (2005) Quantification of 3-nitrotyrosine levels using a benchtop ion trap mass spectrometry method. *Methods in enzymology*, 396, 245-266.
62. Tsikas, D., Mitschke, A., and Gutzki, F. M. (2012) Measurement of 3-nitro-tyrosine in human plasma and urine by gas chromatography-tandem mass spectrometry. *Methods in molecular biology*, 828, 255-270.
63. Safinowski, M., Wilhelm, B., Reimer, T., Weise, A., Thome, N., Hanel, H., Forst, T., and Pfutzner, A. (2009) Determination of nitrotyrosine concentrations in plasma samples of diabetes mellitus patients by four different immunoassays leads to contradictive results and disqualifies the majority of the tests. *Clinical chemistry and laboratory medicine: CCLM / FESCC*, 47, 483-488.
64. Whiteman, M., and Halliwell, B. (1999) Loss of 3-nitrotyrosine on exposure to hypochlorous acid: implications for the use of 3-nitrotyrosine as a bio-marker in vivo. *Biochemical and biophysical research communications*, 258, 168-172.
65. Pattison, D. I., and Davies, M. J. (2005) Kinetic analysis of the role of histidine chloramines in hypochlorous acid mediated protein oxidation. *Biochemistry*, 44, 7378-7387.

CHAPTER TWO
KINETICS OF FORMATION AND DEGRADATION OF 3-CHLOROTYROSINE
BY HYPOCHLOROUS ACID AND CHLORAMINES

Matthew P. Curtis, Andrew J. Hicks, Jonathan W. Neidigh

Department of Basic Sciences, Loma Linda University School of Medicine

Loma Linda, CA 92350

Adapted from Curtis, M.P., Hicks, A.J., and Neidigh, J.W. (2011). *Chem Res Toxicol.*

24(3): p. 418-428.

Abstract

The persistent activation of innate immune cells in chronic inflammation is gaining recognition as a contributing factor in a number of human diseases. A distinguishing feature of activated leukocytes at sites of inflammation is their production of reactive species such as hypochlorous acid (HOCl). Investigating the role of reactive molecules like HOCl in inflammation and human disease requires appropriate biomarkers. The preferred biomarker for HOCl, and by extension its synthesizing enzyme myeloperoxidase, is 3-chlorotyrosine. 3-Chlorotyrosine is a chemically stable product formed when HOCl, or a HOCl-induced chloramine, reacts with the tyrosine side-chain and is readily measured by sensitive mass spectrometry methods. However, Whiteman and Spencer¹ recently noted that 3-chlorotyrosine is degraded by HOCl, calling into question its use as a biomarker. The kinetic rate constants of HOCl, histidine chloramine, and lysine chloramine reacting with 3-chlorotyrosine to form 3,5-dichlorotyrosine are reported. The kinetics of tyrosine chlorination in the context of a peptide with a nearby lysine residue was also determined and further supports the role of chloramines in the chlorination of protein-bound tyrosine residues. The likelihood of free 3,5-dichlorotyrosine occurring *in vivo*, given the reported rate constants, is discussed.

Introduction

The persistent activation of innate immune cells in chronic inflammation is gaining recognition as a contributing factor in numerous human diseases including diabetes, neurodegeneration, atherosclerosis, and cancer.²⁻⁷ The reactive species superoxide, hydrogen peroxide, hypochlorous acid (HOCl), and hypobromous acid are generated by human leukocytes.⁸ Myeloperoxidase (MPO), found in neutrophils, monocytes, and macrophages, generates HOCl using hydrogen peroxide to oxidize chloride ions.⁹ While HOCl kills invading microorganisms, it is also toxic to host cells.¹⁰ ¹¹ These reactive species, produced at sites of inflammation, are thought to contribute to the pathology of human disease.¹²

However, the direct measurement of HOCl is not feasible because of its reactivity and short half-life in biological environments.¹³ While expression of MPO correlates with pathologies including cardiovascular disease,^{14, 15} cancer,^{7, 16} and neurodegenerative disease,¹⁷⁻¹⁹ measurement of MPO as a biomarker for reactive species is complicated by the presence of both active and inactive forms of the enzyme.²⁰⁻²² The products that result when reactive species damage biological molecules are instead used as surrogate markers to investigate the role of reactive species in disease pathology.^{23,24}

Surrogate markers of HOCl result from the reaction of HOCl with nucleic acids, proteins, and lipids.²⁵ HOCl oxidizes DNA bases forming 5-hydroxyuracil, 5-hydroxycytosine, and thymine glycol.²⁶ HOCl can also chlorinate DNA forming 8-chloroguanosine, 8-chloroadenosine, and 5-chlorocytosine.²⁷ HOCl-generated DNA damage will result in mutations if not repaired.^{28, 29} However, the repair of damaged DNA, with the possible exception of 5-chlorocytosine,³⁰ likely precludes the use of these

HOCl damage products as a biomarker of HOCl. Furthermore, DNA and lipid oxidation or chlorination are slower than the reactions of HOCl with protein side-chains suggesting that protein damage will reach higher concentrations *in vivo*.³¹⁻³⁴

Products of both oxidation and chlorination damage occur when proteins or amino acids are exposed to HOCl.³⁵ The preferred marker of HOCl *in vivo* is 3-chlorotyrosine (3ClTyr); a stable and unique product qualitatively measured by antibody-based methods^{36, 37} or quantitatively measured by mass spectrometry.³⁸ As most tyrosine is incorporated into cellular proteins, *in vivo* measurements of 3ClTyr focus on protein-bound tyrosine and 3ClTyr. Measurements of 3ClTyr in human tissues were found to correlate with other measurements of disease.³⁹⁻⁴¹ Given the clinical connection between inflammation and human diseases, researchers will continue to use 3ClTyr as a biomarker to determine the role of HOCl in the etiology of these diseases.

The reported kinetics of tyrosine chlorination by HOCl is slow relative to the rate of reaction with other protein side-chains.³¹ The observation of 3ClTyr *in vivo* indicates that HOCl was formed in sufficient quantities to chlorinate tyrosine despite the slow rate measured *in vitro*. However, Whiteman and Spencer report that 3ClTyr is lost when exposed to HOCl suggesting a more complicated relationship between HOCl and 3ClTyr, calling into question the use of 3ClTyr as a biomarker.¹ Previous articles suggested that 3ClTyr reacts with HOCl to form 3,5-dichlorotyrosine (Cl₂Tyr).⁴²⁻⁴⁶ However, the kinetics of HOCl reacting with 3ClTyr is not known nor did the above cited papers attempt to measure Cl₂Tyr *in vivo*. In this study we report the kinetics of 3ClTyr chlorination to form Cl₂Tyr.

Our early experiments also noted a discrepancy with the previously reported model used to calculate the kinetics of tyrosine chlorination; the appearance of UV/Vis absorbance bands at 240 and 300 nm was observed and attributed to an intermediate product preceding formation of 3ClTyr.³¹ However, we have observed that authentic samples of Cl₂Tyr, not 3ClTyr or some unknown intermediate, contain UV/Vis absorption peaks near 240 and 300 nm indicating the formation of Cl₂Tyr during the experiments reported to measure the chlorination of tyrosine to form 3ClTyr. Furthermore, the buffer used in this previous study lacked chloride ions raising the concern that their reported rate constants may not reflect the physiological rate if chloride ions participate in the chlorination reaction. In this study we used an HPLC method and authentic standards to remove ambiguity when determining the kinetics of tyrosine and 3ClTyr chlorination by HOCl and determined the impact of chloride ions on the kinetics as a function of pH.

One solution to the slow rate of direct chlorination of tyrosine by HOCl is the suggestion that the rapid chlorination of a lysine residue or N-terminal amino group to form a chloramine will in turn rapidly chlorinate a nearby tyrosine residue.^{44, 47} However, Pattison and Davies found that the chloramine of a lysine side-chain analogue very slowly chlorinated tyrosine over nine days with low levels of chlorine incorporation.⁴⁸ In this study, we examine the kinetics whereby lysine chloramines chlorinate tyrosine residues, both as individual amino acids and in the context of a polypeptide using mass spectrometry to characterize the peptide products following reaction with HOCl.

At this time, an accurate estimate of the physiological quantities and concentrations of HOCl reached *in vivo* is missing. The relative kinetics of reactions

between HOCl and biological molecules is important for defining the normal and pathological ranges of HOCl production in human tissues. The rate constants of 3ClTyr chlorination, we argue, will allow more accurate estimates of HOCl formation *in vivo*.

Experimental Procedures

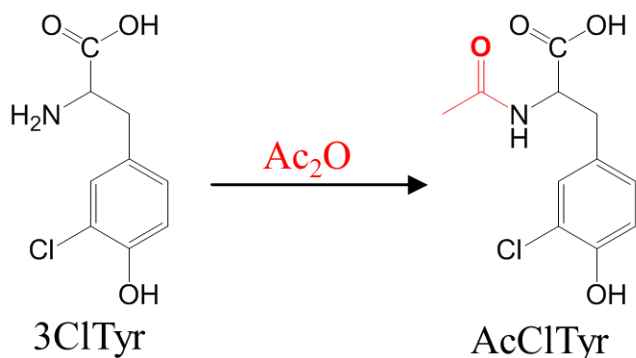
Materials

L-Tyrosine, N-acetyl-L-tyrosine (AcTyr), N- α -acetyl-L-lysine (AcLys), and N-acetyl-L-histidine (AcHis) were purchased from Novabiochem (San Diego, CA). Fluorenylmethyloxycarbonylchloride (Fmoc)-amide resin was purchased from Applied Biosystems, Inc. (Foster City, CA). Fmoc-Lys(Boc)-OH, and all other Fmoc-amino acids were purchased from Advanced ChemTech (Louisville, KY). α -Cyano-4-hydroxycinnamic acid matrix and peptide calibration standards were purchased from Bruker (Billerica, MA). Sodium hypochlorite, 3-chloro-L-tyrosine, L-methionine, N-acetylglycine, N-acetyl-L-alanine, N-acetyl-L-glutamic acid, N- α -acetyl-L-asparagine, and all other laboratory chemicals were purchased from Sigma-Aldrich (St. Louis, MO).

Synthesis of N-acetyl-3-chlorotyrosine

3-Chloro-L-tyrosine (1 g, 4.6 mmol) was acetylated with excess acetic anhydride (4 ml, 42 mmol) in 100 ml acetone at room temperature (**Figure 1**). The crude product containing N,O-diacetyl-3-chlorotyrosine was formed after reacting overnight and is soluble in acetone. The acetone was removed using rotary evaporation after filtering off any remaining insoluble impurities. Remaining acetic anhydride was hydrolyzed by addition of water. The phenol acetate ester was rapidly hydrolyzed for one hour by addition of 1M NaOH until the solution pH was between 8 and 9 resulting in the

A. Synthesis of Ac3ClTyr



B. Synthesis of AcCl₂Tyr

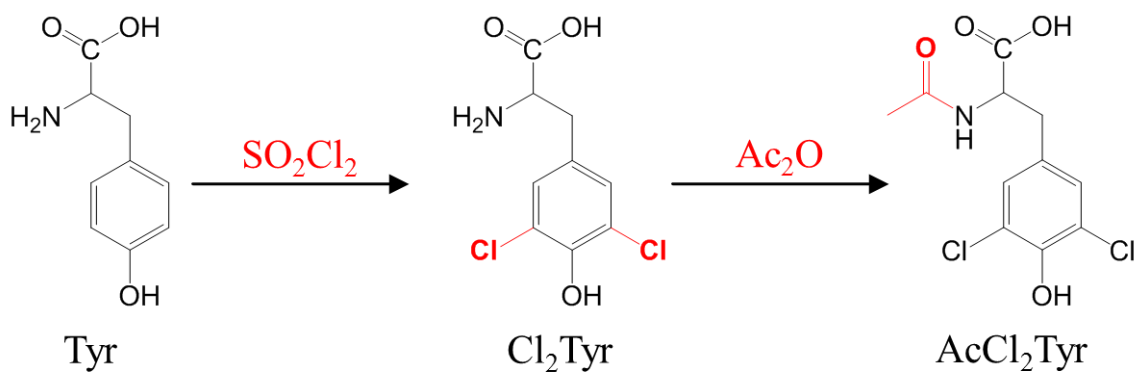


Figure 1: Synthesis of Ac3ClTyr and AcCl₂Tyr. Ac3ClTyr was synthesized by acetylation of 3ClTyr with excess acetic anhydride (Ac₂O) (A). AcCl₂Tyr was synthesized by chlorination of tyrosine with excess sulfuryl chloride (SO₂Cl₂) with subsequent acetylation with excess Ac₂O (B).

formation of N-acetyl-3-chlorotyrosine (Ac3ClTyr) in high purity (> 95% pure). The aqueous solution was acidified to a pH < 2 with concentrated hydrochloric acid and then added to a SupelClean, LC-18 packing, solid phase extraction (SPE) column (Supelco, Bellefonte, PA). Following washing with aqueous 0.1% trifluoroacetic acid (TFA), the desired compound was eluted with 5-10% methanol, 0.1% TFA solution. Fractions of \geq 98% purity, as determined by analytical HPLC, were dried by vacuum centrifugation and stored for later use. The compound gave the expected UV/Vis absorbance maximum at 279 nm.⁴⁹ ¹H-NMR (500 MHz, DMSO-d₆), δ : 9.79 (s, 1H, -OH), 8.17 (d, J = 8.1 Hz, 1H, NH), 7.16 (d, J = 1.8 Hz, H₂), 6.98 (dd, J = 1.8, 8.3 Hz, 1H, H₆), 6.86 (d, J = 8.3 Hz, 1H, H₅), 4.33 (m, 1H, J = 5.0, 8.3, 9.5 Hz, H α), 2.92 (dd, 1H, J = 5.0, 13.9 Hz, H β), 2.72 (dd, J = 9.5, 13.9 Hz, H β), 1.79 (s, 3H, CH₃).

Synthesis of N-acetyl-3,5-dichlorotyrosine

The procedure of Allevi *et al.* was used to synthesize 3,5-dichlorotyrosine (Cl₂Tyr) from tyrosine, which was then used without further purification.⁵⁰ Cl₂Tyr was acetylated as described above for the acetylation of 3ClTyr (**Figure 1**). The desired compound eluted from the C18 SPE column with a solution consisting of 20% methanol and 0.1% TFA. The UV/Vis spectrum in 0.1 M HCl showed the expected absorbance maximums at 281 and 287 nm.⁴⁹ ¹H-NMR (500 MHz, DMSO-d₆), δ : 9.94 (s, 1H, -OH), 8.15 (d, J = 8.2 Hz, 1H, NH), 7.21 (s, 2H, H_{2,6}), 4.36 (m, J = 5.0, 8.2, 9.5 Hz, 1H, H α), 2.94 (dd, J = 5.0, 13.8 Hz, 1H, H β), 2.73 (dd, J = 9.5, 13.8 Hz, H β), 1.78 (s, 3H, CH₃).

Synthesis of Ac-KGNYAE-NH₂

A small peptide, Ac-KGNYAE-NH₂, was synthesized using solid phase synthesis and fast Fmoc chemistry on an Applied Biosystems (Foster City, CA) 433A peptide synthesizer. The sequence of this peptide is identical to residues 36 to 41 of human histone H2A. We used an Fmoc-amide resin and Fmoc-protected amino acids with the lysine side-chain protected by a *tert*-butyloxycarbonyl (BOC) protecting group. After synthesis, the N-terminal Fmoc-group was removed with piperidine and acetylated by acetic anhydride and triethylamine in dimethylformamide. The peptide was cleaved from the resin and purified by HPLC as previously described.⁴³ Following purification, the peptide was characterized by MALDI-TOF in positive-ion mode and determined that the peptide monoisotopic mass (M+H⁺) was 722.34 m/z; the expected monoisotopic mass is 722.35 m/z. The purity of the peptide was determined to be $\geq 97\%$ by analytical HPLC.

Methods

Sodium hypochlorite was stored at 4 °C. The pK_a of HOCl is 7.5 resulting in equal concentrations of hypochlorous acid and its conjugate base, hypochlorite, at physiological pH. The term “hypochlorous acid” is thus used in this article to refer to both the acid and its conjugate base. The concentration of the HOCl stock was determined daily using the absorbance at 292 nm ($\epsilon_{292 \text{ nm}} = 350 \text{ M}^{-1}\text{cm}^{-1}$) for a fresh dilution of the stock into 0.1 M NaOH.⁵¹ Dilutions of the HOCl stock were then made into buffer. All reactions were initiated by the addition of HOCl and quenched by adding 10-fold excess methionine, which reacts rapidly with HOCl ($\sim 10^8 \text{ M}^{-1}\text{s}^{-1}$).³¹

Tyrosine analogues with acetylated amine groups were used to avoid reaction with HOCl forming a chloramine with subsequent degradation to aldehyde products.⁴⁵ AcTyr, Ac3ClTyr, and N-acetyl-3,5-dichlorotyrosine (AcCl₂Tyr) in 0.1 M HCl displayed UV/Vis absorbance's maximums at 274, 279, 287 nm with molar absorptivity values of $\epsilon_{274 \text{ nm}} = 1368 \text{ M}^{-1} \text{ cm}^{-1}$, $\epsilon_{279 \text{ nm}} = 1879 \text{ M}^{-1} \text{ cm}^{-1}$ and $\epsilon_{287 \text{ nm}} = 1424 \text{ M}^{-1} \text{ cm}^{-1}$, respectively.⁴⁹

UV/Vis Spectroscopy of Tyrosine Chlorination by HOCl

The UV-spectra of AcTyr reacting with HOCl was measured on a Varian (Palo Alto, CA) Cary 100 Bio UV-Visible Spectrophotometer in a 1-cm micro quartz cell. 350 μM Ac3ClTyr and 70 – 350 μM AcTyr were reacted with 200 μM HOCl at room temperature and the spectra between 230 and 350 nm was measured every 22 seconds.

Reactions of Tyrosine Analogues with HOCl or Chloramines

Like previously published kinetics reports, all reactions were buffered with 100 mM phosphate buffer.^{31, 48} Most reactions added 200 μM HOCl to concentrations between 300 and 1500 μM of AcTyr, Ac3ClTyr, and AcCl₂Tyr. Reactions with N-acetylhistidine chloramine (AcHisCl) and N- α -acetyllysine chloramine (AcLysCl) were done by premixing tyrosine analogues with excess AcHis or AcLys and then adding 200 μM HOCl for a final concentration of 1000 μM AcHis or AcLys. Reactions with N- α -acetyllysine dichloramine (AcLysCl₂) were done by premixing AcLys with tyrosine analogues and then adding 200 μM HOCl for a final concentration of 105 μM AcLys. Reaction times between 1 and 120 seconds were mixed using a KinTek RQF-3 Rapid

Quench Flow apparatus (Austin, TX) maintained at 37 °C while manual mixing was used for reaction times longer than 15 seconds in an aluminum block maintained at 37 °C. The sample, reaction, and exit loops of the KinTek Quench Flow system were calibrated using a solution of AcTyr with known concentration according to the manufacturer's directions. The collected calibration samples were dried by vacuum centrifugation and then a known volume of water was added to each sample and analyzed by UV/Vis to calculate the loop volumes.

HPLC Measurement of Chlorination Products

The concentration of products and reactants in kinetics samples were measured using a ThermoFinnigan (Waltham, MA) Surveyor HPLC system containing a MS Pump, Autosampler, and PDA detector. Standard curves were generated using pure stocks ($\geq 98\%$ pure) of AcTyr, Ac3ClTyr, and AcCl₂Tyr ($r^2 \geq 0.999$). Separation of each analyte was accomplished by using a Restek Ultra IBD column (C18, 3 μ m, 150 x 2.1 mm). The initial solvent mix was 95% mobile phase A (0.1% aqueous TFA) and 5% mobile phase B (0.85% TFA in acetonitrile) for 5 minutes followed by a linear gradient to 50% B over 20 minutes at a flow rate of 200 μ L/min. The limit of detection ($S/N \geq 3$) was $\approx 0.5 \mu$ M while the limit of quantitation was 100 - 200 μ M depending on the analyte. Kinetics samples were diluted as necessary to achieve a final concentration of analyte less than the limit of quantitation. The Qual browser module of Xcalibur, ver. 1.3 (Thermo-Finnigan, Ontario, Canada) was used to analyze the HPLC chromatogram. Standard curves were obtained periodically to ensure that measured concentrations were accurate.

Analysis of Kinetics Data and Determination of Rate Constants

Microsoft Excel was used to analyze all kinetics data using a model comparison method.⁵² A time interval of 0.1 seconds was used to numerically model the differential equations. The chemical models for chlorination of phenol analogues by HOCl are presented in the Results section. The sum of the squared differences (SSD) was calculated between the experimental and modeled concentrations for time points in a kinetics experiment. The Solver tool in Excel was used to determine the optimized second order rate constants that minimized the SSD giving SSD_{opt} . The error in each rate constant was estimated by determining the two rate constants that gave $SSD = SSD_{opt} * (F(P/(N-P))+1)$ where F is the critical value of the F distribution, P is the number of model parameters, and N is the number of data points.⁵² We chose a value of F corresponding to the 95% confidence level. When multiple rate constants were used to model the kinetics, the error in each rate constant was estimated while all other rate constants were held at their optimized value. The rate constant values are reported as the middle value $\pm \frac{1}{2} * \text{range}$; the middle value was calculated from the high and low SSD values calculated above that defined the range of certainty (95% confidence level) and were within 1% of the optimized value in most cases.

Dependence of Kinetics on Presence of Chloride and Solution pH

The reaction pH was varied from pH 4.0 to pH 10.5 and the kinetics of chlorination were determined when 200 μM HOCl reacted with 690 μM AcTyr or 680 μM Ac3ClTyr at 37 °C. HOCl was prepared in phosphate buffer with or without chloride (Cl^-) so that the final concentration of Cl^- during reaction was 140 mM. The reactions

were stopped with a 10-fold excess of methionine after 1, 5, 10, 15, and 30 seconds using the KinTek Quench flow system. The apparent rate constant was modeled as described in the previous paragraph. The pH dependence of chlorination for tyrosine analogues was fit to the equation $k_{\text{apparent}} = k_w[\text{phenol}][\text{HOCl}] + k_x([\text{phenol}][\text{OCl}^-] + [\text{phenolate}][\text{HOCl}]) + k_y[\text{phenolate}][\text{OCl}^-] + k_z[\text{H}^+][\text{HOCl}][\text{Cl}^-]$ where the concentrations of the acid and conjugate base of the tyrosine analogue or HOCl were determined by their pK_a values. The terms $[\text{phenol}][\text{OCl}^-]$ and $[\text{phenolate}][\text{HOCl}]$ were combined because the optimized rate constant for each term, when separated, was dependent on the value of the other term. The concentration of chlorine (Cl_2) formed at equilibrium is small relative to HOCl/OCl⁻ at the examined pH values indicating that any effect of chloride ion on the chlorination kinetics was due to either the rate limiting reaction of Cl_2 formation or the rate of Cl_2 reacting with tyrosine analogues.⁵³ As the effect of chloride on chlorination kinetics was observed to be a function of the rate of Cl_2 formation, we included the effect of chloride using the previously determined rate law.⁵³

Chlorination of Tyrosine by HOCl in a Lysine-Containing Peptide

The concentration of the peptide, Ac-KGNYAE-NH₂, was determined using UV/Vis spectrometry and the molar absorptivity of tyrosine at 274 nm ($\epsilon_{274 \text{ nm}} = 1368 \text{ M}^{-1} \text{cm}^{-1}$). Reactions contained 125 μM peptide and 65 – 400 μM of HOCl and were quenched with at least 10-fold excess methionine. Likewise, a mixture of the N- α -acetyl analogues of lysine, glycine, asparagine, tyrosine, alanine, and glutamic acid, where each amino acid was present at a concentration of 125 μM , was reacted with 65 – 400 μM HOCl. Reactants were combined manually for reaction times between 15 seconds and 60

minutes in an aluminum block maintained at 37 °C. The reactant and products were quantitated by UV-detected HPLC. The peptide reaction products were identified by isolating HPLC chromatographic peaks and by using MALDI-TOF mass spectrometry as described in **Appendix A**.

Quantitation of Ac-KGNYAE-NH₂ and its chloro- and dichlorotyrosine analogues were based on the standard curve of the AcTyr analogues. While the retention times were different, quantitation by this method closely matched initial quantitation by UV/Vis and the sum of the peptide analogues remained constant throughout the reaction. Our experience with Tyr and AcTyr indicated that differences in retention time, and thus acetonitrile content of the solvent during elution from the column, did not result in significant ($p \leq 0.05$) changes in the calibration slope. Furthermore, our HPLC quantitation method was compared with a previously established GC-MS method to quantitating Tyr, 3ClTyr, and Cl₂Tyr and showed no significant difference in concentration (**Appendix B**). The apparent rate constant of tyrosine chlorination in the peptide Ac-KGNYAE-NH₂ or the equivalent mixture of N-acetyl amino acids was determined as described above.

Results

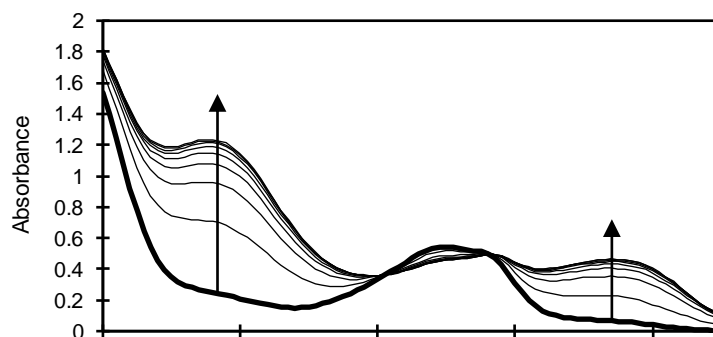
HOCl Reacts with 3ClTyr to form Cl₂Tyr

The reported loss of 3ClTyr in the presence of HOCl suggested caution when using 3ClTyr as a biomarker for active MPO and HOCl *in vivo*.¹ While the previous reports showed that HOCl reacts with 3ClTyr to form Cl₂Tyr,^{42, 44-46, 48} the kinetics of this reaction and thus the likelihood that formation of Cl₂Tyr is physiologically relevant are

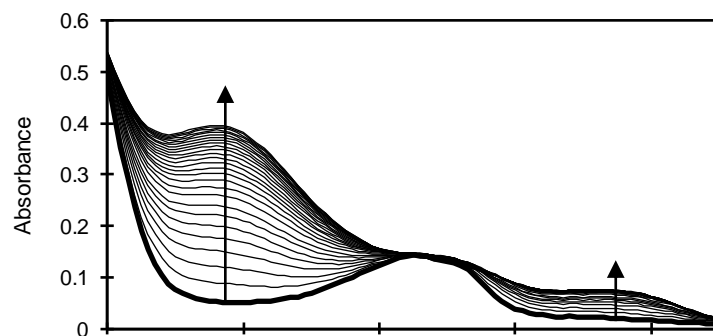
unknown. The changes in the UV spectrum when Ac3ClTyr is reacted with HOCl are shown in **Figure 2a**. The product formed when HOCl reacts with Ac3ClTyr has absorbance peaks at 247 and 305 nm, consistent with the UV spectrum of synthetic AcCl₂Tyr. However, the kinetics of tyrosine chlorination by HOCl reported by Pattison and Davies attributed these absorbance peak to an intermediate compound following the reaction of HOCl with the phenol ring of tyrosine and preceding the formation of 3ClTyr. We therefore reexamined the kinetics of Tyr chlorination by HOCl to determine if AcCl₂Tyr was formed during the published experiments.³¹ **Figures 2b** and **2c** show the changes in the UV spectrum when AcTyr reacts with HOCl, matching the previously described reaction conditions and results. The kinetics of UV spectra changes indicates that HOCl reacts faster with Ac3ClTyr than with AcTyr. As Cl₂Tyr was apparently formed during the published kinetics experiments, the reported rate constant of tyrosine chlorination may be in error.

The UV spectrum of authentic AcTyr, Ac3ClTyr, and AcCl₂Tyr is shown in **Figure 3** at acidic, basic, and neutral pH values. The pH-dependence of the UV spectra for AcTyr, Ac3ClTyr, and AcCl₂Tyr was used to determine the phenol pK_a values of 9.8, 8.5, and 6.7, respectively (**Appendix C**). The final purity of all compounds was $\geq 98\%$ as determined by analytical HPLC at the maximum absorbance circa 280 nm. These spectra indicate the formation of both Ac3ClTyr and AcCl₂Tyr when AcTyr reacts with HOCl (**Figure 2**). As the UV spectra of these compounds overlap at pH 7.4, we instead used an HPLC method to quantitate the formation of reaction products. The HPLC chromatogram shown in **Figure 4** confirms that both Ac3ClTyr and AcCl₂Tyr are formed after 30 seconds when HOCl reacts with AcTyr under the same conditions as those reported while

A. 350 μM Ac3ClTyr + 200 μM HOCl



B. 70 μM AcTyr + 200 μM HOCl



C. 350 μM AcTyr + 200 μM HOCl

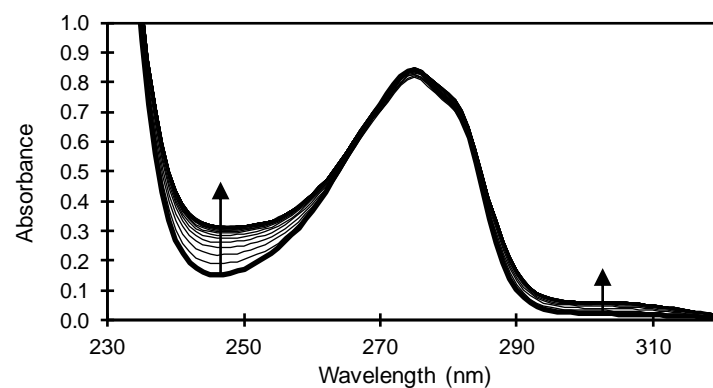


Figure 2: UV Spectroscopy of AcTyr or Ac3ClTyr Reacting with HOCl. HOCl reacts with Ac3ClTyr more rapidly than with AcTyr. The initial spectrum is shown as a bold line while the arrows show the changes in the spectra collected every subsequent 22 seconds. All reactions were performed at room temperature (approximately 22 $^{\circ}\text{C}$) with 200 μM HOCl and (A) 350 μM Ac3ClTyr, (B) 70 μM AcTyr, or (C) 350 μM AcTyr. The product of the reaction of Ac3ClTyr with HOCl has peaks at 246 and 305 nm (panel A). These peaks are also seen when HOCl reacts with small amounts of AcTyr (panel B) or with excess AcTyr (panel C).

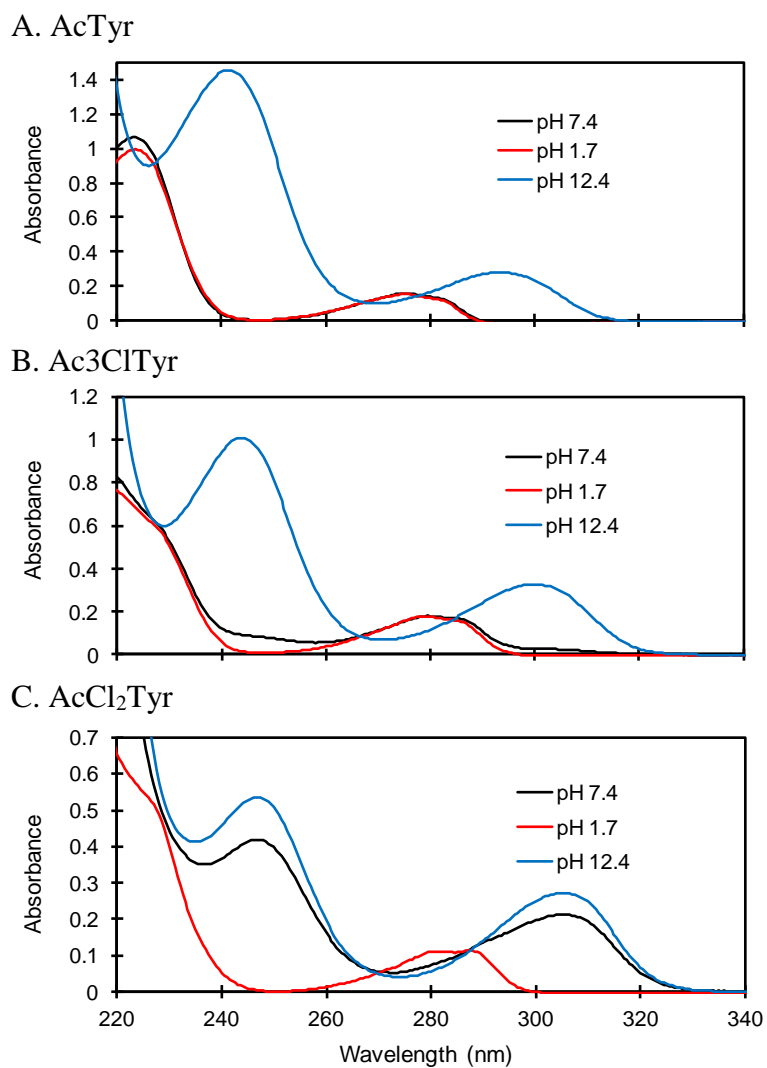


Figure 3: UV Spectrum of Tyrosine Analogues at Varying pH Values. Phosphate buffer at 100 mM was used to buffer the compounds in acidic, basic, and physiologic pH values. The spectrum of (A) AcTyr and (B) Ac3ClTyr at physiological pH is similar to the spectrum at acidic pH while the spectrum of (C) AcCl₂Tyr is most similar to the spectrum at basic pH.

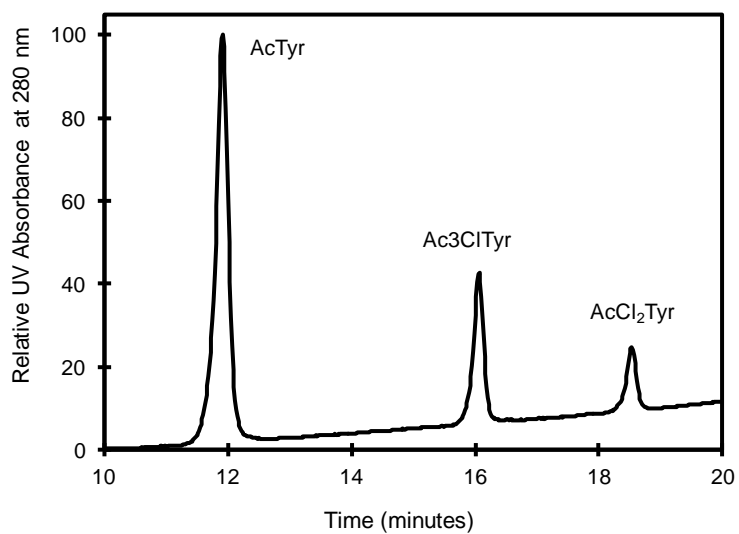


Figure 4: HPLC Detection of Products Formed when AcTyr Reacts with HOCl. Both Ac3ClTyr and AcCl2Tyr are formed after 30 seconds when 350 μ M AcTyr is reacted with 200 μ M HOCl at 37 $^{\circ}$ C, pH 7.4. The peaks at 11.9, 16.1, and 18.6 minutes display identical UV spectra and coelute with authentic standards of AcTyr, Ac3ClTyr, and AcCl2Tyr, respectively.

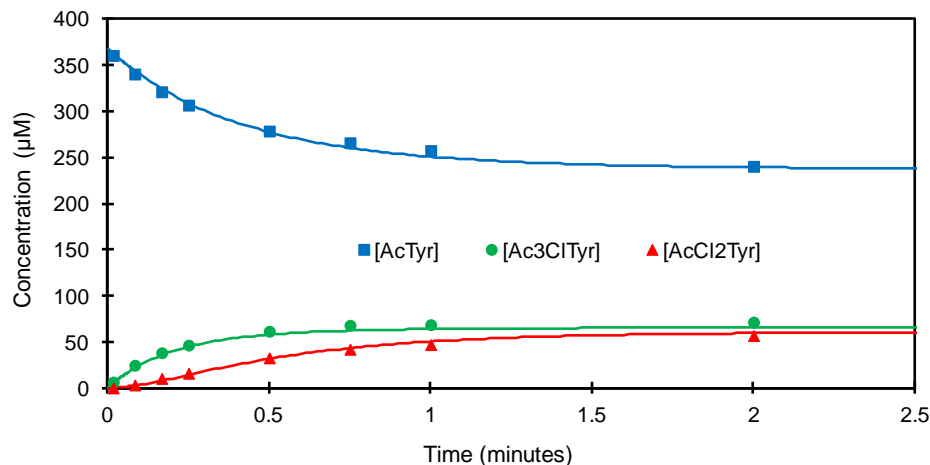
determining the published rate constants.³¹ The standards were important to verify the identity of products and generate the standard curves for quantitation as described in the Experimental Procedures section.

HOCl Chlorinates 3ClTyr More Rapidly than Tyr

The time course of tyrosine analogue chlorination was monitored using UV-detected HPLC. In all cases excess AcTyr, Ac3ClTyr, or AcCl₂Tyr at nominal concentrations of 350, 500, and 1000 μ M were exposed to chlorinating agent in 100 mM phosphate buffer, pH 7.4. The chlorinating agent HOCl was rapidly consumed by addition of excess methionine to stop the reaction at the desired reaction time, usually between 1 second and 60 minutes. The chlorinating agents examined included HOCl, the monochloramine of N-acetylhistidine (AcHisCl), and the mono- and dichloramines of N-acetyllysine. **Figure 5a** shows a representative kinetic experiment for the chlorination of AcTyr by HOCl where first Ac3ClTyr and then AcCl₂Tyr are formed.

The time-dependence of product formation was modeled using the differential equations shown in **Figure 6** to determine the rate constants. The reaction progress was modeled numerically as described in the Experimental Procedures section. The rate constants were determined by minimizing differences between the model and experimental reaction progress curves. For reactions with excess AcTyr or Ac3ClTyr, the loss of phenol reactant was equal to the formation of chlorinated products. However, the loss of AcCl₂Tyr following reaction with HOCl was less than the added chlorinating agent, presumably due to the reaction of the unknown product with chlorinating agent. Therefore, only the first 2 minutes, 15 minutes, or 48 hours were modeled for HOCl,

A. AcTyr + HOCl



B. AcTyr + AcHisCl

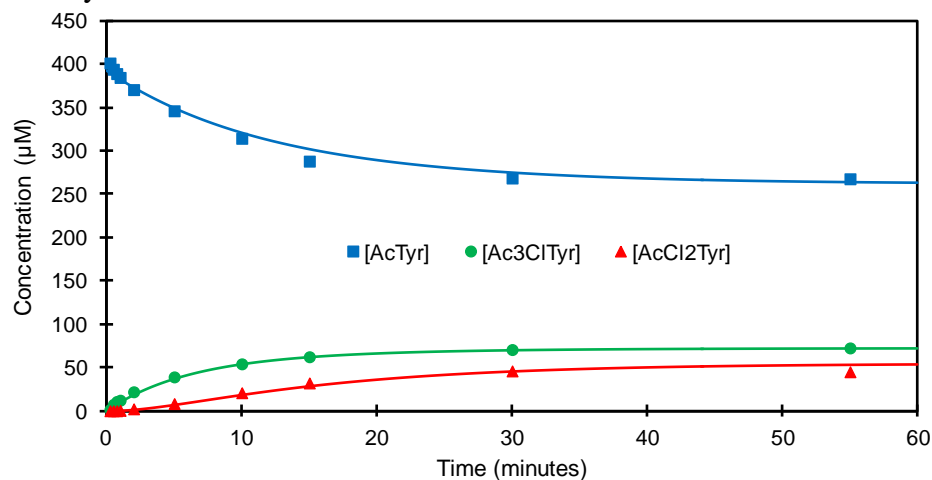
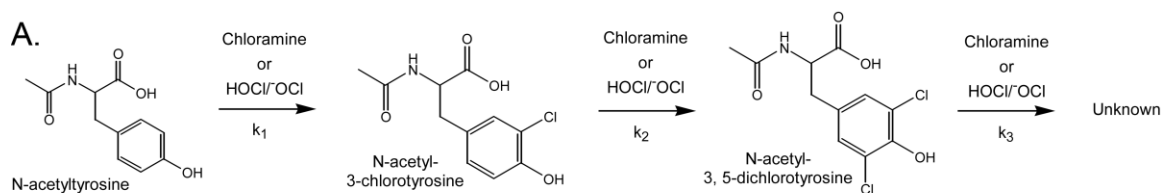


Figure 5: Kinetics of AcTyr Chlorination by HOCl and AcHisCl. (A) 350 μM AcTyr or (B) 400 μM AcTyr with 1000 μM AcHis were reacted with 200 μM HOCl at 37 $^{\circ}\text{C}$ for the indicated time; the reaction was stopped with excess methionine and the products were quantitated by UV- detected HPLC. The solid lines in each panel represent the modeled reaction progress with optimized rate constants. The rate constants k_1 , k_2 , and k_3 for AcTyr, Ac3ClTyr, and AcCl₂Tyr, respectively, reacting with HOCl in panel A are 71, 238, and 32 $\text{M}^{-1}\text{s}^{-1}$. The rate constants k_1 , k_2 , and k_3 for AcTyr, Ac3ClTyr, and AcCl₂Tyr, respectively, reacting with AcHisCl in panel B are 2.3, 7.0, and 1.7 $\text{M}^{-1}\text{s}^{-1}$.



B.
$$\frac{d[\text{AcTyr}]}{dt} = -k_1[\text{HOCl/Chloramine}][\text{AcTyr}]$$

$$\frac{d[\text{Ac3ClTyr}]}{dt} = k_1[\text{HOCl/Chloramine}][\text{AcTyr}] - k_2[\text{HOCl/Chloramine}][\text{Ac3ClTyr}]$$

$$\frac{d[\text{AcCl}_2\text{Tyr}]}{dt} = k_2[\text{HOCl/Chloramine}][\text{Ac3ClTyr}] - k_3[\text{HOCl/Chloramine}][\text{AcCl}_2\text{Tyr}]$$

Figure 6: Kinetic Scheme for Modeling the Chlorination of AcTyr. (A) AcTyr is converted to Ac3ClTyr that can also react with HOCl or chloramine to form AcCl₂Tyr. AcCl₂Tyr is consumed when exposed to HOCl or chloramine to form unknown products. (B) The differential equations describing the change in AcTyr, Ac3ClTyr, and AcCl₂Tyr concentration used to numerically model the experimental data.

AcHisCl, or the lysine chloramines, respectively, to determine the rate constants for AcCl₂Tyr chlorination. For each chlorinating agent, all kinetics experiments at a given temperature with at least three different concentrations of AcTyr, Ac3ClTyr, and AcCl₂Tyr were simultaneously modeled when determining the rate constants. The rate constants are summarized in **Table 1**.

Chloride Increases Tyr Chlorination at Acidic pH Values

The effect of chloride ions on the kinetics of tyrosine analogue chlorination was next investigated to determine the effect of chloride on the *in vivo* chlorination of protein-bound tyrosine. Approximate chloride concentrations *in vivo* range from 20 mM inside cells, 116 mM in interstitial fluid, 100 mM in plasma, and up to 160 mM in the stomach. In the presence of chloride, HOCl is in equilibrium with Cl₂ as shown in equation 1.⁵³



The pH-dependent nature of this equilibrium prompted an investigation of the pH dependence of AcTyr and Ac3ClTyr chlorination by HOCl with and without chloride as shown in **Figure 7**. The effect of chloride is only significant at acidic pH values as the formation of Cl₂ becomes favorable. In the absence of chloride, the apparent rate constant was decomposed to species specific terms for the reaction of the phenol or phenolate ion with HOCl or hypochlorite. Initial efforts indicated that the reaction of phenol with hypochlorite was not distinguishable from the reaction of phenolate with HOCl prompting combination of these two terms with a single rate constant. The modeled species-specific rate constants indicate that chlorination of tyrosine occurs when the ^oCl reacts with the phenol or HOCl reacts with the phenolate as expected for an electrophilic

Table 1. Rate Constants for Chlorination of Tyr Analogues by HOCl and Chloramines. This table shows the rate constants calculated for AcTyr, Ac3ClTyr, and AcCl₂Tyr reacting with HOCl, AcHisCl, AcLysCl, and AcLysCl₂. Rate constants are second order (M⁻¹s⁻¹) and were determined at pH 7.4 in 100 mM phosphate buffer.

Analogue	Temp (°C)	HOCl	AcHisCl	AcLysCl	AcLysCl ₂	Reference
AcTyr	22	47 ± 14	9 ± 2	-	-	31, 48
	22	23 ± 2	2.0 ± 0.1	0.002 ± 0.001	0.002 ± 0.002	This Study
	37	71 ± 8	3.0 ± 0.3	0.004 ± 0.003	0.003 ± 0.002	This Study
Ac3ClTyr	22	82 ± 7	6.6 ± 0.4	0.003 ± 0.001	0.009 ± 0.005	This Study
	37	238 ± 27	10.4 ± 1.0	0.008 ± 0.002	0.012 ± 0.007	This Study
AcCl ₂ Tyr	22	26 ± 3	1.2 ± 0.1	0.002 ± 0.002	0.004 ± 0.004	This Study
	37	32 ± 6	1.7 ± 0.2	0.003 ± 0.002	0.006 ± 0.006	This Study

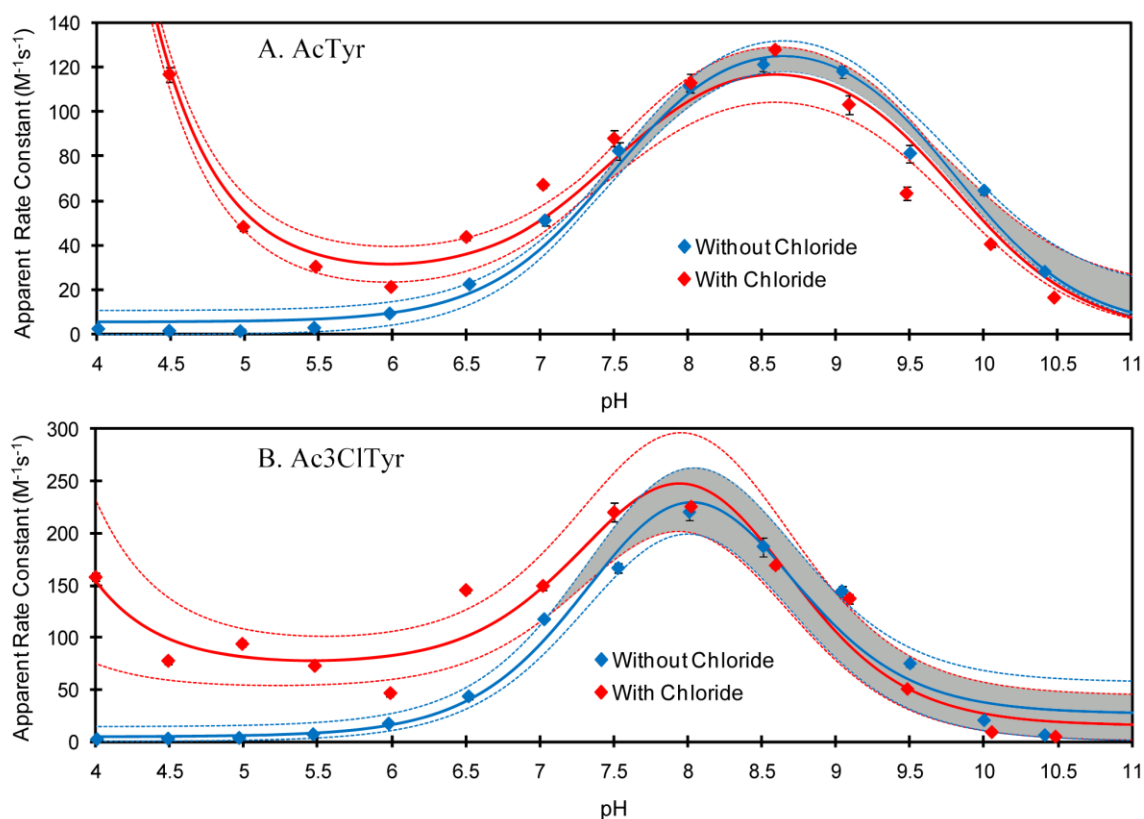


Figure 7: Effect of Chloride and pH on Rate of Tyrosine Chlorination. Chloride causes an increase in the apparent rate constant for the chlorination of tyrosine analogues by HOCl at a low pH. (A) AcTyr and (B) Ac3ClTyr were reacted with HOCl with (red curve) and without (blue curve) the presence of 140 mM chloride and modeled as described in the Experimental Procedures section. The solid curves represent the optimized model while the dashed lines represent the 95% confidence limits; overlap of these limits for the presence and absence of chloride is shaded grey. The presence of chloride only causes a significant increase in the apparent rate constant at acidic pH values. The AcTyr rate constants without chloride, k_w , k_x , and k_y , are 5.3, 142, $1.3\text{M}^{-1}\text{s}^{-1}$, respectively. With chloride, the AcTyr rate constants, k_w , k_x , k_y , and k_z , are 25, 141, 0 $\text{M}^{-1}\text{s}^{-1}$, and $14026\text{M}^{-2}\text{s}^{-1}$, respectively. The Ac3ClTyr rate constants without chloride, k_w , k_x , k_y , are 4.8, 353, 27 $\text{M}^{-1}\text{s}^{-1}$. With chloride present, the Ac3ClTyr rate constants, k_w , k_x , k_y , and k_z , become 72, 363, 15 $\text{M}^{-1}\text{s}^{-1}$, and $3930\text{M}^{-2}\text{s}^{-1}$, respectively.

aromatic substitution reaction. As the equilibrium concentration of Cl_2 prior to reaction initiation is small relative to the quantity of chlorination product observed, the influence of chloride was modeled by adding a term for the rate of Cl_2 formation. The modeled value of this chloride-dependent rate constant is similar to the reported rate constant of Cl_2 formation indicating that Cl_2 formation, not phenol chlorination by Cl_2 , is the rate-limiting step in tyrosine chlorination at acidic pH values.⁵³

Chloramines Chlorinate 3ClTyr More Rapidly than Tyr

Recent reports indicate that chlorination of protein-bound tyrosine is preferred when a His or Lys residue is nearby, suggesting that the formation of 3ClTyr *in vivo* is accelerated by first forming a histidine or lysine chloramine.^{43, 44, 47} The monochloramines of AcHis and AcLys as well as the dichloramine of AcLys were reacted with the tyrosine analogues AcTyr, Ac3ClTyr, and AcCl₂Tyr. At the concentrations used in this study, HOCl will rapidly react to form AcHisCl, AcLysCl, or AcLysCl₂ within one second. **Figure 5b** shows the chlorination of AcTyr by AcHisCl where first Ac3ClTyr and then AcCl₂Tyr are formed. All chlorinating agents also caused AcCl₂Tyr to disappear forming one or more unknown products. As this article focuses on the use of 3ClTyr as a biomarker, the identity of these unknown products were not pursued. The relative rate of chlorination in all cases by chlorinating agents was HOCl > AcHisCl >> AcLysCl ≈ AcLysCl₂. The kinetics of these reactions were determined as described in the Experimental Procedures section above and were analogous to the chlorination of tyrosine analogues by HOCl.

Analysis of AcLysCl₂ kinetics is complicated due to the interaction between the three species of lysine. When AcLysCl₂ chlorinates a tyrosine analogue, it becomes AcLysCl that in turn can chlorinate a tyrosine analogue. Additionally, when AcLysCl chlorinates AcTyr, it becomes AcLys, which can be rapidly chlorinated by AcLysCl₂ to become AcLysCl again.⁵⁴ The complete data set of AcLysCl and AcLysCl₂ reactions were thus simultaneously modeled to determine separate rate constants for the mono- and dichloramine of lysine. The complete progress curve for AcTyr or Ac3ClTyr was modeled; only the first 15 minutes, 48 hours, or 48 hours of the progress curves of AcCl₂Tyr reacting with AcHisCl, AcLysCl, or AcLysCl₂, respectively, were modeled due to the apparent reaction of HOCl or chloramine with the unknown products. The rate constants for AcHisCl are approximately 10- to 30-fold slower than those for HOCl and the lysine chloramine rates are more than 10,000-fold slower (**Table 1**).

Lysine Chloramine Rapidly Chlorinates Tyrosine in the Context of a Peptide

The slow chlorination of AcTyr by lysine chloramines conflicts with the selective, and more rapid, chlorination of tyrosine residues near a lysine residue in a peptide or protein.^{43, 44} The effect of a nearby lysine residue on the kinetics of tyrosine chlorination was examined in the context of the peptide Ac-KGNYAE-NH₂. A mixture of N- α -acetyl analogues corresponding to the amino acid content of this peptide was also reacted with HOCl to serve as a control. **Figure 8a** shows the HPLC of 125 μ M Ac-KGNYAE-NH₂ after it has reacted with 0, 130, or 260 μ M HOCl for 60 minutes at 37 °C. Each peak was collected and analyzed by MALDI-TOF in positive- and negative-ion mode. The three largest HPLC peaks had mass spectra peaks of 722.3, 756.2, and 790.2 m/z that

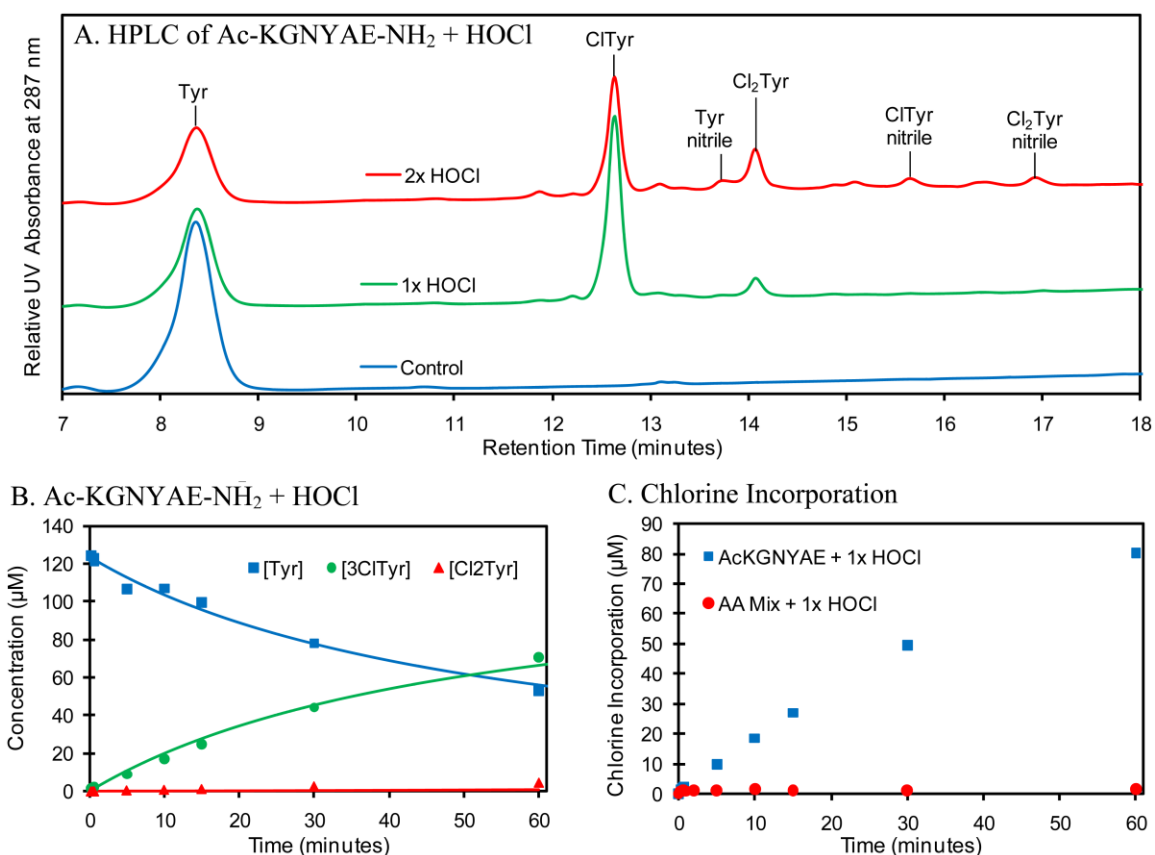


Figure 8: Rapid Chlorination of Tyrosine by Lysine Chloramine in a Peptide. Tyrosine in a peptide is more rapidly chlorinated by a nearby lysine chloramine than by free AcLysCl. (A) HPLC of 125 μM Ac-KGNYAE-NH₂ after a 60 minute reaction with either 0, 130, or 260 μM HOCl. The peaks at 8.3, 12.6, and 14.0 minutes correspond to Ac-KGNXAE-NH₂ with tyrosine, 3-chlorotyrosine, or 3,5-dichlorotyrosine, respectively, at residue four. The peaks at 13.6, 15.6, and 16.8 minutes correspond to the lysine nitrile form of the peptide with tyrosine, 3-chlorotyrosine, or 3,5-dichlorotyrosine, respectively. (B) 125 μM Ac-KGNYAE-NH₂ was reacted with 130 μM HOCl, stopped with excess methionine at the indicated time and then quantitated by UV-detected HPLC. The apparent rate constant k_1 was found to be $2.4 \text{ M}^{-1}\text{s}^{-1}$. (C) 125 μM Ac-KGNYAE-NH₂ or 130 μM of an equivalent N-acetyl amino acid mixture was reacted with 130 μM HOCl. Chlorination incorporation was measured as $\text{Cl}_{\text{incorporation}} = [3\text{ClTyr}] + 2 \times [\text{Cl}_2\text{Tyr}]$. The chlorination of tyrosine by a free lysine chloramine is much slower than by a lysine chloramine within the same peptide.

correspond to the M+H fragment of the peptide containing Tyr, 3ClTyr, and Cl₂Tyr, respectively. In negative ion mode, the MALDI showed three other peaks at 716.3, 750.3, and 784.3 m/z that correspond to the loss of four hydrogen atoms on each of these three analogues when the amine of lysine is oxidized to form a nitrile (**Appendix B**). HPLC was used to monitor the reaction of the peptide and HOCl over an hour (**Figure 8b**) and a rate constant k_1 of $2.4 \text{ M}^{-1}\text{s}^{-1}$ was determined by modeling as described above. Comparison of the chlorination kinetics for the tyrosine-containing peptide and amino acid mixture highlights the acceleration of tyrosine chlorination by a nearby chloramine (**Figure 8c**).

Discussion

The biomarker 3ClTyr is formed when HOCl chlorinates tyrosine. Active MPO, secreted by leukocytes in the innate immune response or chronic inflammation, synthesizes HOCl from a chloride ion and hydrogen peroxide. However, the reported loss of 3ClTyr to form an unknown product in the presence of HOCl calls into question the use of 3ClTyr as a biomarker of HOCl or active MPO.¹ Previous studies indicate that Cl₂Tyr is formed when tyrosine-containing proteins are exposed to HOCl suggesting that HOCl chlorinates 3ClTyr to form Cl₂Tyr. This report is the first to determine the kinetics of HOCl reacting with the side-chains of 3ClTyr and Cl₂Tyr.^{42, 43, 45}

Given the overlapping UV spectra of these compounds, an HPLC-UV approach was chosen to monitoring the reaction kinetics. The examined compounds and chlorination products were cleanly separated and easily quantitated. The standard curve for all compounds examined gave excellent correlation coefficients, $r^2 \geq 0.999$; the

standard error for measuring the concentrations of tyrosine analogues given these standard curves was 8 – 12%.

The kinetic rate constants reported in **Table 1** are 2- to 4-fold slower than those previously reported.^{31,48} We argue that this discrepancy is not due to the difference between the UV spectroscopy and UV-HPLC methods. The changes to the UV spectrum as HOCl reacts with AcTyr (**Figure 2**) are consistent with previous published descriptions. However, the UV spectra (**Figure 3**) of authentic AcTyr, Ac3ClTyr, and AcCl₂Tyr suggests, and the HPLC data confirms (**Figure 4**), that both Ac3ClTyr and AcCl₂Tyr are formed under the reported reaction conditions.³¹ The HPLC data (**Figure 5**) clearly shows that Ac3ClTyr formation precedes appearance of AcCl₂Tyr. However, Pattison and Davies assigned the UV spectral peaks at 240 and 300 nm to an intermediate compound between AcTyr and AcCl₂Tyr while the results reported here indicate that these spectral peaks are best assigned to AcCl₂Tyr. The chemical model (**Figure 6**) used to derive the rate constants (**Table 1**) reported here differs from that of Pattison and Davies.³¹ We have no reason to question the other rate constants reported by Pattison and Davies as the current criticism is limited to their proposed reaction scheme for AcTyr.^{31,48} Nonetheless, the 2- to 4-fold slower rate constants of tyrosine chlorination are reported here, despite their minor physiological importance relative to the competing reactions of HOCl *in vivo*.

Despite the relatively slow reaction between HOCl and protein-bound tyrosine, the observation of greater quantities of 3-chlorotyrosine in diseased tissues than normal tissues indicates that HOCl production *in vivo* is sufficient to chlorinate tyrosine residues in cellular proteins. Measurements *in vivo* observe 0 – 1000 μmol 3ClTyr per mole

tyrosine in various tissues and diseases.^{39, 55-61} The chlorination of specific proteins, such as apolipoprotein A2 from atherosclerotic plaques reaches levels of 7000 μmol 3ClTyr per mol tyrosine.⁴¹

Consideration of the known rate constants from *in vitro* experiments offers some insights into the meaning of *in vivo* 3ClTyr measurements. At the physiological 3ClTyr/Tyr ratio reported in the literature, the rate constants reported here predict only 1% of 3ClTyr would be chlorinated to form Cl₂Tyr assuming no other biologically relevant reactions are present. The competing reactions of HOCl with the sulfur containing amino acids cysteine and methionine in proteins and glutathione are rapid with rate constants faster than $1 \times 10^8 \text{ M}^{-1}\text{s}^{-1}$.^{31, 62} Therefore, the presence of 3ClTyr observed *in vivo* is usually interpreted to represent the lower limit of HOCl formation after the available anti-oxidant glutathione is consumed.^{31, 62} The *direct* chlorination of 3ClTyr to form Cl₂Tyr *in vivo*, given the rate constants reported here, is unlikely at 3ClTyr/Tyr ratios observed *in vivo*.

The reaction of HOCl with amines to form a chloramine, however, has emerged from *in vitro* studies as the most likely pathway to form protein-bound 3ClTyr.^{43, 44} Tyrosine residues in peptides and proteins near the N-terminal amine group or on lysine and histidine residues are preferentially chlorinated indicating that the formation of an intermediate chloramine accelerates tyrosine chlorination.^{43, 44, 47} Because the *in vivo* HOCl concentrations and quantities are not known, the physiological relevance of HOCl used during *in vitro* experiments is uncertain, particularly as these *in vitro* reactions also exclude glutathione. However, the quantity of Cl₂Tyr formed is informative when 3ClTyr formation, as a ratio to Tyr, is similar to that observed *in vivo*. Instead of Cl₂Tyr values

less than 1% as predicted above, *in vitro* experiments with histone proteins or BSA found approximately 10% Cl₂Tyr when 3ClTyr values were less than 7,000 μmol/mol of tyrosine, the current upper limit of 3ClTyr reported from *in vivo* samples.⁴¹⁻⁴³ Furthermore, for histone H3 and BSA the quantity of HOCl needed to produce these physiological quantities of 3ClTyr was less than the number of cysteine and/or methionine residues indicating that either the kinetics of HOCl reduction by these residues is less than expected, presumably due to burial by the protein structure, or that acceleration of tyrosine chlorination by first forming nearby chloramines is sufficiently fast to successfully compete with cysteine and methionine residues.

Chlorination of a peptide-bound tyrosine by a nearby lysine chloramine may be further favored because of this chloramines decreased reactivity with glutathione (**Figure 9**). Lysine chloramine reacts more slowly with glutathione (~300 M⁻¹s⁻¹) than HOCl or histidine chloramine, allowing lysine chloramine to persist longer in solution and facilitate chlorination of nearby tyrosine residues.^{31, 62} Additionally, while lysine chloramine can eventually undergo hydrolysis into an aldehyde or nitrile,⁶⁵ chlorination of a nearby tyrosine appears to be a more favorable reaction based on the absence of lysine modifications and prevalence of 3ClTyr in previous studies.^{42, 43}

The primary limitation of the chloramine rate constants reported in **Table 1** is that they are bimolecular and represent the restriction of more degrees of freedom during chlorination of tyrosine than would occur when a chloramine chlorinates a nearby tyrosine residue on the same polypeptide chain. Inclusion of a nearby lysine residue on the same peptide chain accelerated the rate of tyrosine chlorination by approximately 600-fold (**Figure 8**) and nearby histidine residues also appear to favor tyrosine

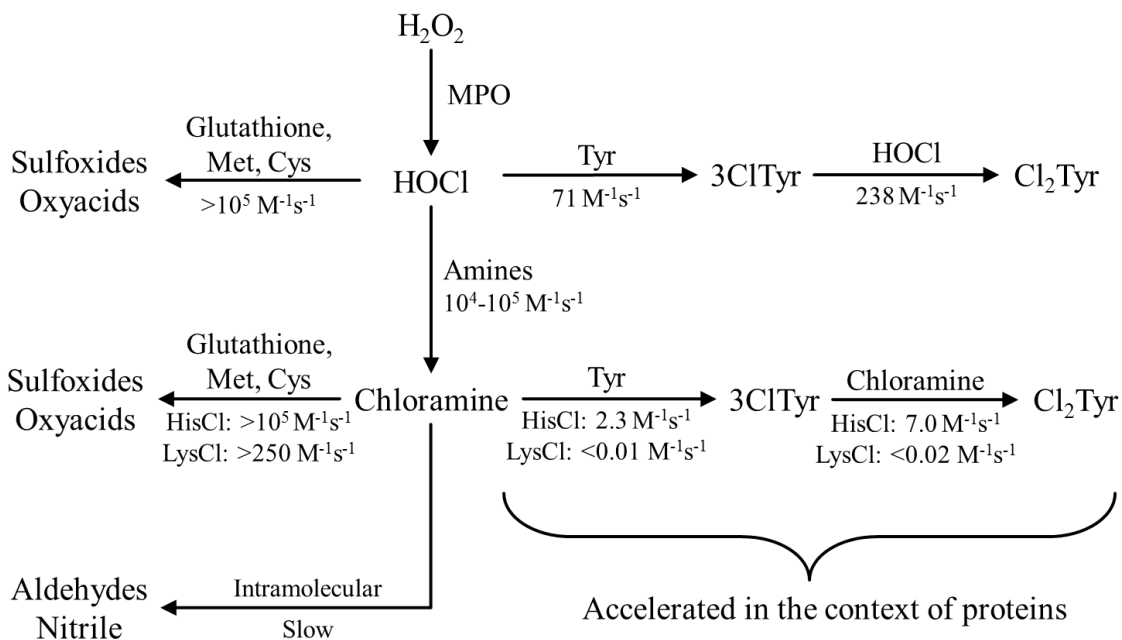


Figure 9: Summary of Reactions by HOCl that Compete with 3ClTyr Formation. All rate constants are for individual amino acid analogues. The rate constants for HOCl or chloramines reacting with sulfur containing amino acids or glutathione and primary amines reacting with HOCl are published elsewhere.^{31, 34} The remaining rate constants are from Table 1.

chlorination.^{43, 48, 66, 67} The maximal rate enhancement is likely higher than that observed here when a less flexible polypeptide backbone and an optimal position of the chloramine relative to the phenol ring are present, warranting further investigation.

The kinetics of AcTyr or Ac3ClTyr by HOCl is pH dependent (**Figure 7**) and phenolate is more rapidly chlorinated by HOCl as expected for an electrophilic aromatic substitution reaction. The phenolate form is approximately 25- to 400-fold more rapidly chlorinated than the phenol form of AcTyr; the uncertainty in this rate enhancement is because the data did not allow us to discriminate between hypochlorous acid reacting with the phenolate and the phenol reacting with hypochlorite. A possible explanation of the effect of neighboring histidine or lysine residues on the kinetics of tyrosine chlorination is that these basic residues lower the pK_a value of tyrosine, accelerating the reaction kinetics. However, the apparent rate enhancement of tyrosine in the context of a peptide can be over 500-fold, suggesting that this alternate explanation is not the major reason for selective chlorination of tyrosine residues near lysine or histidine. Furthermore, the pK_a value of the phenol group in the peptide was no different than that of AcTyr, eliminating this possible mechanism of enhanced kinetics in our model.

The equilibrium between HOCl and Cl₂, another chlorinating agent present at acidic pH values in the presence of chloride ions, could influence the *in vivo* kinetics of tyrosine chlorination. While chloride had no significant effect on tyrosine chlorination at the neutral pH values (**Figure 7**) found in blood and most human tissue, a significant increase in tyrosine chlorination kinetics is expected in the stomach given its acidic pH and high chloride concentration, as observed in the stomach of rats.⁶⁸ Modeling the effect of chloride concentration on tyrosine chlorination indicated that the rate enhancement

was approximately equal to the published rate of Cl_2 formation.⁵³ The actual rate of tyrosine chlorination by Cl_2 was not accessible by the experiments described here, but is expected to be approximately 100-fold faster given its kinetics with phenol.⁶⁹

Most reports that measure 3ClTyr from *in vivo* tissues did not also measure Cl_2 Tyr. However, other reports that measured both 3ClTyr and Cl_2 Tyr observed quantities of Cl_2 Tyr approaching the quantity of 3ClTyr observed.^{61, 64, 70} The nasal tissue of Fisher 344 rats exposed to chlorine gas resulted in equal quantities of 3ClTyr and Cl_2 Tyr;⁷⁰ this result could be due to the different mechanism, relative to HOCl, of tyrosine chlorination by Cl_2 .⁶⁹ Of more relevance to the *in vivo* kinetics of HOCl is the observation of Cl_2 Tyr in both bacterial and neutrophil proteins where up to one third of chlorinated tyrosine residues were Cl_2 Tyr.⁶⁴ The observation of 3ClTyr in the sputum of asthmatic subjects was not significantly different than that of normal controls, however, Cl_2 Tyr was significantly elevated.⁶¹ The chemical reaction and rate constants reported here indicate that the formation of 3ClTyr is limited by the formation of Cl_2 Tyr with exposure to significant quantities of HOCl. In control tissues with activated neutrophils, Cl_2 Tyr formation may be a better biomarker of disease processes.

The above predictions based on rate constants reported here indicate that formation of the free amino acid Cl_2 Tyr is not likely. However, the limited reports measuring protein-bound Cl_2 Tyr in biological tissue further suggest that the formation of protein-bound Cl_2 Tyr is more likely and could prove important in unraveling questions concerning physiological relevant levels of HOCl synthesis.

References

1. Whiteman, M., and Spencer, J. P. (2008) Loss of 3-chlorotyrosine by inflammatory oxidants: implications for the use of 3-chlorotyrosine as a bio-marker in vivo. *Biochem Biophys Res Commun*, 371, 50-53.
2. Pickup, J. C. (2004) Inflammation and activated innate immunity in the pathogenesis of type 2 diabetes. *Diabetes Care*, 27, 813-823.
3. Heneka, M. T., and O'Banion, M. K. (2007) Inflammatory processes in Alzheimer's disease. *Journal of Neuroimmunology*, 184, 69-91.
4. Moisse, K., and Strong, M. J. (2006) Innate immunity in amyotrophic lateral sclerosis. *Biochimica Et Biophysica Acta-Molecular Basis of Disease*, 1762, 1083-1093.
5. Nijhuis, M. M. O., van Keulen, J. K., Pasterkamp, G., Quax, P. H., and de Kleijn, D. P. V. (2007) Activation of the innate immune system in atherosclerotic disease. *Current Pharmaceutical Design*, 13, 983-994.
6. Coussens, L. M., and Werb, Z. (2002) Inflammation and cancer. *Nature*, 420, 860-867.
7. Roncucci, L., Mora, E., Mariani, F., Bursi, S., Pezzi, A., Rossi, G., Pedroni, M., Luppi, D., Santoro, L., Monni, S., Manenti, A., Bertani, A., Merighi, A., Benatti, P., Di Gregorio, C., and de Leon, M. P. (2008) Myeloperoxidase-positive cell infiltration in colorectal carcinogenesis as indicator of colorectal cancer risk. *Cancer Epidem Biomar*, 17, 2291-2297.
8. Babior, B. M. (2000) Phagocytes and oxidative stress. *Am J Med*, 109, 33-44.
9. Klebanoff, S. J. (2005) Myeloperoxidase: friend and foe. *J Leukocyte Biol*, 77, 598-625.
10. Pullar, J. M., Vissers, M. C., and Winterbourn, C. C. (2000) Living with a killer: the effects of hypochlorous acid on mammalian cells. *IUBMB Life*, 50, 259-266.
11. Weiss, S. J. (1989) Tissue destruction by neutrophils. *N Engl J Med*, 320, 365-376.
12. Martinez-Cayuela, M. (1995) Oxygen free radicals and human disease. *Biochimie*, 77, 147-161.
13. Dalle-Donne, I., Scaloni, A., Giustarini, D., Cavarra, E., Tell, G., Lungarella, G., Colombo, R., Rossi, R., and Milzani, A. (2005) Proteins as biomarkers of oxidative/nitrosative stress in diseases: the contribution of redox proteomics. *Mass Spectrom Rev*, 24, 55-99.

14. Daugherty, A., Dunn, J. L., Rateri, D. L., and Heinecke, J. W. (1994) Myeloperoxidase, a catalyst for lipoprotein oxidation, is expressed in human atherosclerotic lesions. *J Clin Invest*, 94, 437-444.
15. Sugiyama, S., Okada, Y., Sukhova, G. K., Virmani, R., Heinecke, J. W., and Libby, P. (2001) Macrophage myeloperoxidase regulation by granulocyte macrophage colony-stimulating factor in human atherosclerosis and implications in acute coronary syndromes. *American Journal of Pathology*, 158, 879-891.
16. Rainis, T., Maor, I., Lanir, A., Shnizer, S., and Lavy, A. (2007) Enhanced oxidative stress and leucocyte activation in neoplastic tissues of the colon. *Digest Dis Sci*, 52, 526-530.
17. Choi, D. K., Pennathur, S., Perier, C., Tieu, K., Teismann, P., Wu, D. C., Jackson-Lewis, V., Vila, M., Vonsattel, J. P., Heinecke, J. W., and Przedborski, S. (2005) Ablation of the inflammatory enzyme myeloperoxidase mitigates features of Parkinson's disease in mice. *Journal of Neuroscience*, 25, 6594-6600.
18. Green, P. S., Mendez, A. J., Jacob, J. S., Crowley, J. R., Growdon, W., Hyman, B. T., and Heinecke, J. W. (2004) Neuronal expression of myeloperoxidase is increased in Alzheimer's disease. *Journal of Neurochemistry*, 90, 724-733.
19. Nagra, R. M., Becher, B., Tourtellotte, W. W., Antel, J. P., Gold, D., Paladino, T., Smith, R. A., Nelson, J. R., and Reynolds, W. F. (1997) Immunohistochemical and genetic evidence of myeloperoxidase involvement in multiple sclerosis. *Journal of Neuroimmunology*, 78, 97-107.
20. King, C. C., Jefferson, M. M., and Thomas, E. L. (1997) Secretion and inactivation of myeloperoxidase by isolated neutrophils. *J Leukocyte Biol*, 61, 293-302.
21. Bradley, P. P., Christensen, R. D., and Rothstein, G. (1982) Cellular and Extracellular Myeloperoxidase in Pyogenic Inflammation. *Blood*, 60, 618-622.
22. Edwards, S. W., Hughes, V., Barlow, J., and Bucknall, R. (1988) Immunological Detection of Myeloperoxidase in Synovial-Fluid from Patients with Rheumatoid-Arthritis. *Biochemical Journal*, 250, 81-85.
23. Dalle-Donne, I., Rossi, R., Colombo, R., Giustarini, D., and Milzani, A. (2006) Biomarkers of oxidative damage in human disease. *Clin Chem*, 52, 601-623.
24. Atkinson, A. J., Colburn, W. A., DeGruttola, V. G., DeMets, D. L., Downing, G. J., Hoth, D. F., Oates, J. A., Peck, C. C., Schooley, R. T., Spilker, B. A., Woodcock, J., Zeger, S. L., and Grp, B. D. W. (2001) Biomarkers and surrogate endpoints: Preferred definitions and conceptual framework. *Clinical Pharmacology & Therapeutics*, 69, 89-95.

25. Winterbourn, C. C., and Kettle, A. J. (2000) Biomarkers of myeloperoxidase-derived hypochlorous acid. *Free Radic Biol Med*, 29, 403-409.
26. Whiteman, M., Jenner, A., and Halliwell, B. (1997) Hypochlorous acid-induced base modifications in isolated calf thymus DNA. *Chem Res Toxicol*, 10, 1240-1246.
27. Badouard, C., Masuda, M., Nishino, H., Cadet, J., Favier, A., and Ravanat, J. L. (2005) Detection of chlorinated DNA and RNA nucleosides by HPLC coupled to tandem mass spectrometry as potential biomarkers of inflammation. *J Chromatogr B Analyt Technol Biomed Life Sci*, 827, 26-31.
28. Kreuzer, D. A., and Essigmann, J. M. (1998) Oxidized, deaminated cytosines are a source of C → T transitions in vivo. *P Natl Acad Sci USA*, 95, 3578-3582.
29. Theruvathu, J. A., Kim, C. H., Rogstad, D. K., Neidigh, J. W., and Sowers, L. C. (2009) Base Pairing Configuration and Stability of an Oligonucleotide Duplex Containing a 5-Chlorouracil-Adenine Base Pair. *Biochemistry*, 48, 7539-7546.
30. Valinluck, V., Liu, P., Kang, J. I., Jr., Burdzy, A., and Sowers, L. C. (2005) 5-halogenated pyrimidine lesions within a CpG sequence context mimic 5-methylcytosine by enhancing the binding of the methyl-CpG-binding domain of methyl-CpG-binding protein 2 (MeCP2). *Nucleic Acids Res*, 33, 3057-3064.
31. Pattison, D. I., and Davies, M. J. (2001) Absolute rate constants for the reaction of hypochlorous acid with protein side chains and peptide bonds. *Chem Res Toxicol*, 14, 1453-1464.
32. Pattison, D. I., Hawkins, C. L., and Davies, M. J. (2003) Hypochlorous acid-mediated oxidation of lipid components and antioxidants present in low-density lipoproteins: absolute rate constants, product analysis, and computational modeling. *Chem Res Toxicol*, 16, 439-449.
33. Hawkins, C. L., Pattison, D. I., and Davies, M. J. (2002) Reaction of protein chloramines with DNA and nucleosides: evidence for the formation of radicals, protein-DNA cross-links and DNA fragmentation. *Biochem J*, 365, 605-615.
34. Prutz, W. A. (1996) Hypochlorous acid interactions with thiols, nucleotides, DNA, and other biological substrates. *Arch Biochem Biophys*, 332, 110-120.
35. Hawkins, C. L., Pattison, D. I., and Davies, M. J. (2003) Hypochlorite-induced oxidation of amino acids, peptides and proteins. *Amino Acids*, 25, 259-274.
36. Malle, E., Hazell, L., Stocker, R., Sattler, W., Esterbauer, H., and Waeg, G. (1995) Immunological Detection and Measurement of Hypochlorite-Modified Ldl with Specific Monoclonal-Antibodies. *Arterioscl Throm Vas*, 15, 982-989.

37. Malle, E., Waeg, G., Schreiber, R., Grone, E. F., Sattler, W. S., and Grone, H. J. (2000) Immunohistochemical evidence for the myeloperoxidase/H₂O₂/halide system in human atherosclerotic lesions - Colocalization of myeloperoxidase and hypochlorite-modified proteins. *European Journal of Biochemistry*, 267, 4495-4503.
38. Hazen, S. L., Crowley, J. R., Mueller, D. M., and Heinecke, J. W. (1997) Mass spectrometric quantification of 3-chlorotyrosine in human tissues with attomole sensitivity: a sensitive and specific marker for myeloperoxidase-catalyzed chlorination at sites of inflammation. *Free Radic Biol Med*, 23, 909-916.
39. Buss, I. H., Senthilmohan, R., Darlow, B. A., Mogridge, N., Kettle, A. J., and Winterbourn, C. C. (2003) 3-Chlorotyrosine as a marker of protein damage by myeloperoxidase in tracheal aspirates from preterm infants: association with adverse respiratory outcome. *Pediatr Res*, 53, 455-462.
40. Cheng, M. L., Chen, C. M., Gu, P. W., Ho, H. Y., and Chiu, D. T. (2008) Elevated levels of myeloperoxidase, white blood cell count and 3-chlorotyrosine in Taiwanese patients with acute myocardial infarction. *Clin Biochem*, 41, 554-560.
41. Zheng, L., Nukuna, B., Brennan, M. L., Sun, M., Goormastic, M., Settle, M., Schmitt, D., Fu, X., Thomson, L., Fox, P. L., Ischiropoulos, H., Smith, J. D., Kinter, M., and Hazen, S. L. (2004) Apolipoprotein A-I is a selective target for myeloperoxidase-catalyzed oxidation and functional impairment in subjects with cardiovascular disease. *J Clin Invest*, 114, 529-541.
42. Chapman, A. L., Senthilmohan, R., Winterbourn, C. C., and Kettle, A. J. (2000) Comparison of mono- and dichlorinated tyrosines with carbonyls for detection of hypochlorous acid modified proteins. *Arch Biochem Biophys*, 377, 95-100.
43. Kang, J. I., Jr., and Neidigh, J. W. (2008) Hypochlorous acid damages histone proteins forming 3-chlorotyrosine and 3,5-dichlorotyrosine. *Chem Res Toxicol*, 21, 1028-1038.
44. Bergt, C., Fu, X., Huq, N. P., Kao, J., and Heinecke, J. W. (2004) Lysine residues direct the chlorination of tyrosines in YXXK motifs of apolipoprotein A-I when hypochlorous acid oxidizes high density lipoprotein. *J Biol Chem*, 279, 7856-7866.
45. Fu, S., Wang, H., Davies, M., and Dean, R. (2000) Reactions of hypochlorous acid with tyrosine and peptidyl-tyrosyl residues give dichlorinated and aldehydic products in addition to 3-chlorotyrosine. *J Biol Chem*, 275, 10851-10858.
46. Drabik, G., and Naskalski, J. W. (2001) Chlorination of N-acetyltyrosine with HOCl, chloramines, and myeloperoxidase-hydrogen peroxide-chloride system. *Acta Biochimica Polonica*, 48, 271-275.

47. Domigan, N. M., Charlton, T. S., Duncan, M. W., Winterbourn, C. C., and Kettle, A. J. (1995) Chlorination of tyrosyl residues in peptides by myeloperoxidase and human neutrophils. *J Biol Chem*, 270, 16542-16548.
48. Pattison, D. I., and Davies, M. J. (2005) Kinetic analysis of the role of histidine chloramines in hypochlorous acid mediated protein oxidation. *Biochemistry*, 44, 7378-7387.
49. Hunt, S. (1984) Halogenated tyrosine derivatives in invertebrate scleroproteins: isolation and identification. *Methods Enzymol*, 107, 413-438.
50. Allevi, P., Olivero, P., and Anastasia, M. (2004) Controlled synthesis of labelled 3-L-chlorotyrosine-[ring-C-13(6)] and of 3,5-L-dichlorotyrosine-[ring-C-13(6)]. *J Labelled Compd Rad*, 47, 935-945.
51. Morris, J. C. (1966) Acid Ionization Constant of HOCl from 5 to 35 Degrees. *Journal of Physical Chemistry*, 70, 3798-&.
52. Motulsky, H., and Christopoulos, A. (2005) *Fitting Models to Biological Data Using Linear and Nonlinear Regression*, pp 109 - 117, GraphPad Software, San Diego, CA.
53. Wang, T. X., and Margerum, D. W. (1994) Kinetics of Reversible Chlorine Hydrolysis - Temperature-Dependence and General Acid Base-Assisted Mechanisms. *Inorganic Chemistry*, 33, 1050-1055.
54. Pattison, D. I., and Davies, M. J. (2006) Evidence for rapid inter- and intramolecular chlorine transfer reactions of histamine and carnosine chloramines: implications for the prevention of hypochlorous-acid-mediated damage. *Biochemistry*, 45, 8152-8162.
55. Bergt, C., Pennathur, S., Fu, X., Byun, J., O'Brien, K., McDonald, T. O., Singh, P., Anantharamaiah, G. M., Chait, A., Brunzell, J., Geary, R. L., Oram, J. F., and Heinecke, J. W. (2004) The myeloperoxidase product hypochlorous acid oxidizes HDL in the human artery wall and impairs ABCA1-dependent cholesterol transport. *Proc Natl Acad Sci U S A*, 101, 13032-13037.
56. Citardi, M. J., Song, W., Batra, P. S., Lanza, D. C., and Hazen, S. L. (2006) Characterization of oxidative pathways in chronic rhinosinusitis and sinonasal polyposis. *Am J Rhinol*, 20, 353-359.
57. Hazen, S. L., and Heinecke, J. W. (1997) 3-Chlorotyrosine, a specific marker of myeloperoxidase-catalyzed oxidation, is markedly elevated in low density lipoprotein isolated from human atherosclerotic intima. *J Clin Invest*, 99, 2075-2081.
58. Himmelfarb, J., McMenamin, M. E., Loseto, G., and Heinecke, J. W. (2001) Myeloperoxidase-catalyzed 3-chlorotyrosine formation in dialysis patients. *Free Radic Biol Med*, 31, 1163-1169.

59. Mita, H., Higashi, N., Taniguchi, M., Higashi, A., Kawagishi, Y., and Akiyama, K. (2004) Urinary 3-bromotyrosine and 3-chlorotyrosine concentrations in asthmatic patients: lack of increase in 3-bromotyrosine concentration in urine and plasma proteins in aspirin-induced asthma after intravenous aspirin challenge. *Clin Exp Allergy*, 34, 931-938.
60. Shao, B. H., Oda, M. N., Oram, J. F., and Heinecke, J. W. (2010) Myeloperoxidase: An Oxidative Pathway for Generating Dysfunctional High-Density Lipoprotein. *Chemical Research in Toxicology*, 23, 447-454.
61. Aldridge, R. E., Chan, T., Van Dalen, C. J., Senthilmohan, R., Winn, M., Venge, P., Town, G. I., and Kettle, A. J. (2002) Eosinophil peroxidase produces hypobromous acid in the airways of stable asthmatics. *Free Radical Bio Med*, 33, 847-856.
62. Peskin, A. V., and Winterbourn, C. C. (2001) Kinetics of the reactions of hypochlorous [7]acid and amino acid chloramines with thiols, methionine, and ascorbate. *Free Radic Biol Med*, 30, 572-579.
63. Pastore, A., Federici, G., Bertini, E., and Piemonte, F. (2003) Analysis of glutathione: implication in redox and detoxification. *Clinica Chimica Acta*, 333, 19-39.
64. Chapman, A. L., Hampton, M. B., Senthilmohan, R., Winterbourn, C. C., and Kettle, A. J. (2002) Chlorination of bacterial and neutrophil proteins during phagocytosis and killing of *Staphylococcus aureus*. *J Biol Chem*, 277, 9757-9762.
65. Joo, S. H., and Mitch, W. A. (2007) Nitrile, aldehyde, and halonitroalkane formation during chlorination/chloramination of primary amines. *Environ Sci Technol*, 41, 1288-1296.
66. Nightingale, Z. D., Lancha, A. H., Jr., Handelman, S. K., Dolnikowski, G. G., Busse, S. C., Dratz, E. A., Blumberg, J. B., and Handelman, G. J. (2000) Relative reactivity of lysine and other peptide-bound amino acids to oxidation by hypochlorite. *Free Radic Biol Med*, 29, 425-433.
67. Pattison, D. I., Hawkins, C. L., and Davies, M. J. (2007) Hypochlorous acid-mediated protein oxidation: How important are chloramine transfer reactions and protein tertiary Structure? *Biochemistry*, 46, 9853-9864.
68. Nickelsen, M. G., Nweke, A., Scully, F. E., Ringhand, H. P. (1992) Reactions of aqueous chlorine in vitro in stomach fluid from the rat: chlorination of tyrosine. *Chem Res Toxicol*, 4, 94-101.
69. Grimley, E., and Gordon, G. (1973) Kinetics and Mechanism of Reaction between Chlorine and Phenol in Acidic Aqueous-Solution. *Journal of Physical Chemistry*, 77, 973-978.

70. Sochaski, M. A., Jarabek, A. M., Murphy, J., and Andersen, M. E. (2008) 3-chlorotyrosine and 3,5-dichlorotyrosine as biomarkers of respiratory tract exposure to chlorine gas. *J Anal Toxicol*, 32, 99-105.

CHAPTER THREE
KINETICS OF 3-NITROTYROSINE CHLORINATION BY HYPOCHLOROUS
ACID AND CHLORAMINES

Matthew P. Curtis, Jonathan W. Neidigh

Department of Basic Sciences, Loma Linda University School of Medicine

Loma Linda, CA 92350

Adapted from Curtis, M.P., and Neidigh, J.W. (2014). Free Radical Res. 48: p. 1355-
1362.

Abstract

The markers 3-nitrotyrosine and 3-chlorotyrosine are measured as surrogates for reactive nitrogen species and hypochlorous acid, respectively, which are both elevated in inflamed tissues of humans. However, a previous study¹ observed that 3-nitrotyrosine is lost when exposed to hypochlorous acid suggesting that 3-nitrotyrosine underestimates the reactive nitrogen species present in diseased tissues when 3-chlorotyrosine is also present. This study evaluates the significance of this qualitative finding by measuring the kinetics of 3-nitrotyrosine loss upon reaction with hypochlorous acid. The results demonstrate that 3-nitrotyrosine is chlorinated by hypochlorous acid or chloramines to form 3-chloro-5-nitrotyrosine. As 3-nitrotyrosine from *in vivo* samples is usually found within proteins, as opposed to the free amino acid, we also examined the reaction of 3-nitrotyrosine loss in the context of peptides. The chlorination of 3-nitrotyrosine in peptides was observed to occur up to 700 fold faster than control reactions using equivalent amino acid mixtures and depended on the peptide sequence. The chlorination in peptides whereby the rapid intermolecular formation of a peptide chloramine is followed by a slower intramolecular chlorination of 3-nitrotyrosine is supported by the observed first order kinetics of chlorination during the rate limiting intramolecular reaction. These results further advance our understanding of the chloramine-dependence of tyrosine chlorination in peptides improving the ability to predict likely damage sites in proteins.

Introduction

Reactive chemicals are implicated in the pathology of human diseases associated with aberrant or chronic inflammation including cancer, neurodegenerative diseases, and cardiovascular disease.²⁻⁵ The innate immune cells recruited to inflamed tissues by cytokines express enzymes that catalyze the synthesis of these reactive chemicals.⁶⁻¹¹ Myeloperoxidase catalyzes the oxidation of chloride ions by hydrogen peroxide to form hypochlorous acid (HOCl) that damages biological molecules including tyrosine free in solution and tyrosine residues in proteins to form 3-chlorotyrosine (3ClTyr).^{12, 13} Reactive nitrogen species, such as peroxynitrite and nitrogen dioxide formed when nitric oxide is oxidized, damage biological molecules such as free or protein-bound tyrosine to produce 3-nitrotyrosine (NO₂Tyr).⁵ The markers NO₂Tyr and 3ClTyr are measured as surrogates, respectively, of reactive nitrogen species and HOCl formed *in vivo* because these tyrosine damage products are chemically stable and readily measured with existing analytical methods.¹⁴⁻¹⁷ One study, however, demonstrated *in vitro* that NO₂Tyr is lost in the presence of HOCl suggesting that the observed NO₂Tyr underestimates the levels of reactive nitrogen species in tissues that also produce HOCl.¹

The coincident formation of reactive halogen and reactive nitrogen species occurs when the enzymes myeloperoxidase and nitric oxide synthase are both present. Myeloperoxidase can consume nitric oxide in the presence of hydrogen peroxide and generate reactive nitrogen species capable of nitrating tyrosine residues to form NO₂Tyr.^{18, 19} Resting human neutrophils isolated from peripheral blood do not normally express inducible nitric oxide synthase (iNOS).⁷ However, activated neutrophils exposed to cytokines can express iNOS, produce nitric oxide, and increase the level of reactive

nitrogen species suggesting that recruitment of neutrophils during inflammation can increase both tyrosine nitration and chlorination. Some populations of tissue macrophages, notably those found in atherosclerotic plaques and the brain, contain both iNOS and myeloperoxidase.⁷ The observation of both 3ClTyr and NO₂Tyr in diseased tissues of patients with atherosclerosis, cardiovascular disease, or neurodegeneration confirms the presence of active MPO in tissues with reactive nitrogen species.^{11, 20, 21}

The kinetics of NO₂Tyr reacting with HOCl or HOCl-derived chloramines is important for estimating the loss of the marker NO₂Tyr *in vivo* when both reactive nitrogen species and active myeloperoxidase are present. The kinetics reported here include the direct reaction of HOCl or chloramines with NO₂Tyr and the reaction of HOCl to form a peptide-bound chloramine followed by indirect chlorination of a nearby NO₂Tyr residue. The product of NO₂Tyr chlorination, 3-chloro-5-nitrotyrosine (ClNO₂Tyr), is also reported. Comparison of the intramolecular and intermolecular chlorination kinetics of NO₂Tyr by chloramines indicates that the indirect chlorination of tyrosine residues is accelerated relative to the otherwise slow intermolecular rates for free amino acids. The relevance of these results to the chlorination of tyrosine residues to form the biomarker 3ClTyr is discussed.

Experimental Procedures

Materials

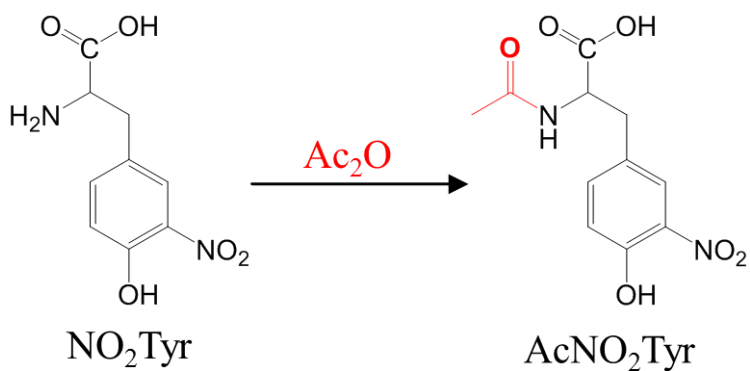
N-Acetyl-L-tyrosine (AcTyr), N- α -acetyl-L-lysine (AcLys), and N-acetyl-L-histidine (AcHis) were purchased from Novabiochem (San Diego, CA). Fmoc-amide resin was purchased from Applied Biosystems, Inc. (Foster City, CA). Fmoc-OSu,

FMOC-Lys(BOC)-OH, FMOC-His(Trt)-OH, and all other FMOC amino acids were purchased from Advanced ChemTech (Louisville, KY), with the exception of FMOC-Tyr(NO₂)-OH which was synthesized as described below. All other laboratory chemicals were purchased from Sigma-Aldrich (St. Louis, MO).

Synthesis of N-acetyl-3-nitrotyrosine

3-Nitro-L-tyrosine was acetylated with excess acetic anhydride in acetone at room temperature (**Figure 1**). After reacting overnight, the product, N-acetyl-3-nitrotyrosine (AcNO₂Tyr), was formed and found soluble in acetone. The acetone was evaporated by use of a rotary evaporator and any remaining acetic anhydride was hydrolyzed by the addition of water. The solution was added to a SupelClean, LC-18 packing, solid phase extraction (SPE) column (Supelco, Bellefonte, PA). The column was washed with 0.1% trifluoroacetic acid (TFA) and subsequent washes were composed of increasing concentrations of methanol (5% increments) in 0.1% TFA. Aliquots were analyzed by analytic HPLC to determine the purity and fractions > 98% pure were combined and lyophilized. The compound gave the expected UV/vis maximums at 279 nm and 360 nm.²² The ¹H-NMR spectra is consistent with AcNO₂Tyr. ¹H-NMR (500 MHz, DMSO): 12.72 (s, 1H, -CO₂H), 10.79 (s, 1H, -OH), 8.18 (d, *J* = 8.1 Hz, 1H, NH), 7.74 (d, *J* = 2.0 Hz, 1H, H2), 7.41 (dd, *J* = 2.0, 8.5 Hz, 1H, H6), 7.05 (d, *J* = 8.5 Hz, 1H, H5), 4.38 (m, 1H, H α), 3.01 (dd, *J* = 4.7, 13.9 Hz, 1H, H β), 2.80 (dd, *J* = 9.4, 13.9 Hz, H β), 1.78 (s, 3H, CH₃).

A. Synthesis of Ac3ClTyr



B. Synthesis of AcCl₂Tyr

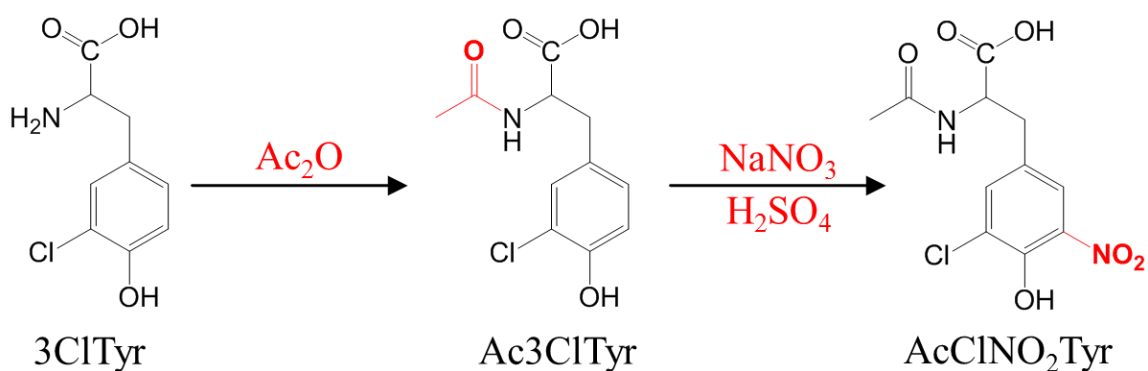


Figure 1: Synthesis of AcNO₂Tyr and AcClNO₂Tyr. AcNO₂ClTyr was synthesized by acetylation of NO₂Tyr with excess acetic anhydride (Ac₂O) (A). AcClNO₂Tyr was synthesized by acetylation of 3ClTyr with subsequent nitration by excess sodium nitrate in sulfuric acid (B).

Synthesis of N-acetyl-3-chloro-5-nitrotyrosine

3-Chloro-L-tyrosine (3ClTyr) was acetylated as described previously. The crude product, N,O-diacetyl-3-chlorotyrosine, was produced after an overnight reaction and is soluble in acetone. The acetone was evaporated and the crude compound was then dissolved in water. Excess sodium nitrate (approximately 3-fold) was added, the solution was placed on ice, and then concentrated sulfuric acid was added dropwise to hydrolyze the phenol acetate ester and nitrate the phenol giving N-acetyl-3-chloro-5-nitrotyrosine (AcClNO₂Tyr) (**Figure 1**). The solution was allowed to react for two hours before being purified by SPE as described above. Analytical HPLC showed the final purity was > 98%. The UV/vis spectrum shows maximums at 285 nm and 358 nm under acidic conditions. The ¹H-NMR is consistent with AcClNO₂Tyr. ¹H-NMR (500 MHz, DMSO): 12.77 (s, 1H, -CO₂H), 10.91 (s, 1H, -OH), 8.21 (d, *J*=8.3 Hz, 1H, NH), 7.79 (d, *J* = 2.0 Hz, 1H, H6), 7.70 (d, *J* = 2.0 Hz, 1H, H2), 4.43 (m, 1H, H α), 3.05 (dd, *J* = 4.8, 13.8 Hz, 1H, H β), 2.83 (dd, *J* = 9.7, 13.8 Hz, 1H, H β), 1.80 (s, 3H, CH₃).

Synthesis of N-FMOC-3-nitrotyrosine

An FMOC protecting group was added to the N-terminus of NO₂Tyr by reacting with equimolar FMOC-OSu and 3-fold excess sodium bicarbonate in a 50:50 mixture of water and acetone. After stirring overnight at room temperature, the aqueous layer was extracted four times with diethyl ether. The combined diethyl ether solution was back-extracted twice with a 5% sodium bicarbonate solution. The combined aqueous layers were acidified by adding concentrated HCl until precipitate formed. The product was extracted with ethyl acetate twice, combined, and dried using anhydrous magnesium

sulfate. Finally, the solvent was removed by rotary evaporation, leaving a golden powder for use in peptide synthesis.

Peptide Synthesis and Purification

Peptides containing histidine or lysine residues in close proximity to the NO₂Tyr residue were synthesized on an ABI model 433A peptide synthesizer using fast Fmoc chemistry. Following synthesis, the N-terminus was acetylated using acetic anhydride. The protecting groups and resin support were cleaved from the peptides using a mixture of TFA/phenol/water/triisopropylsilane (88:5:5:2). The resin was removed by filtration, the cleavage reaction was concentrated by rotary evaporation, and then the peptide was precipitated by adding cold diethyl ether to the cleavage mixture. The ether was removed following centrifugation to pellet the precipitated peptide. After washing the crude peptide with cold diethyl ether three times, the peptides were purified by reverse phase HPLC using a C18 column (Varian Dynamax, 250 mm x 21.4 mm, 300 Å, 5 μM) with a gradient of 20 - 60% mobile phase B (acetonitrile with 0.085% TFA) where mobile phase A contained aqueous 0.1% TFA. The sequence of the purified peptides was confirmed by MS/MS using a ThermoFinnigan LCQ Deca XP mass spectrometer, and a purity of > 95% was verified by analytical HPLC.

Methods

The purchased sodium hypochlorite stock was stored at 4 °C. The pK_a of HOCl is 7.5 resulting in almost equal concentrations of hypochlorous acid and its conjugate base, hypochlorite, at physiological pH. The term “hypochlorous acid” is thus used to refer to

both the acid and its conjugate base. The concentration of the sodium hypochlorite stock was determined daily using the absorbance at 290 nm ($\epsilon_{290\text{ nm}} = 350\text{ M}^{-1}\text{cm}^{-1}$) for a fresh dilution of the stock into 0.1 M NaOH.²³ Dilutions of HOCl stock were then made into 20 - 200 mM phosphate buffer. The stock concentrations of NO₂Tyr or AcClNO₂Tyr containing chemicals were determined following dilution into 0.1 M HCl and using UV/vis spectroscopy with molar absorptivity values of $\epsilon_{360\text{ nm}} = 2790\text{ M}^{-1}\text{cm}^{-1}$ and $\epsilon_{358\text{ nm}} = 2496\text{ M}^{-1}\text{cm}^{-1}$, respectively. The molar absorptivity value of ClNO₂Tyr was determined as a ratio of the published value for NO₂Tyr by mixing AcClNO₂Tyr and AcNO₂Tyr stock solutions with known UV spectra, vacuum centrifuging to remove water, dissolving in deuterated DMSO, collecting a 1D NMR spectrum, and calculating the ratio of both compounds based on pairs of integrated peaks corresponding to the same resonance.²²

Reactions of AcNO₂Tyr with HOCl or Chloramines

All reactions contained 200 μM HOCl, 400 – 1000 μM AcNO₂Tyr, and 100 mM phosphate buffer at the indicated pH. For reactions with lysine or histidine chloramines, five-fold excess AcLys or AcHis was added to the AcNO₂Tyr solution before the addition of HOCl. Previous studies pre-formed the chloramine by addition of HOCl to AcHis,²³ but when comparing techniques, there was no significant difference in ClNO₂Tyr product formation. Reactants were mixed in 1.5 mL glass vials in an aluminum block maintained at 37 °C with stir bars in the reaction vessels. All reactions with HOCl or chloramines were quenched with 10-fold excess methionine or cysteine, respectively, at time points ranging between 5 seconds and 2 hr.

UV/Vis Spectroscopy of AcClNO₂Tyr Chlorination by HOCl

The UV-spectra of AcClNO₂Tyr reacting with HOCl was measured on a Varian (Palo Alto, CA) Cary 100 Bio UV/vis spectrophotometer in a 1-cm micro quartz cell. AcClNO₂Tyr (185 μM) was reacted with 720 μM HOCl at 37 °C and the spectra between 350 and 550 nm were measured every 24 seconds.

Reaction of Peptides with HOCl

HOCl was reacted with excess peptide at 20 – 240 μM peptide and 10 - 120 μM HOCl in 10 mM phosphate buffer at the indicated pH. Reactants were rapidly mixed in a 1.5 mL glass vials in an aluminum block at 37 °C and quenched with 10-fold excess of cysteine at time points between 5 seconds and 12 hr.

HPLC Quantitation of Reaction Products

The concentration of products and reactants in kinetic samples were measured using a ThermoFinnigan (Waltham, MA) Surveyor HPLC system with a MS Pump, Autosampler, and PDA detector (200-600 nm). Standard curves were generated using stocks (> 98% pure) of AcNO₂Tyr and AcClNO₂Tyr ($r^2 > 0.999$). Separation of each analyte was accomplished using a Restek Ultra IBD column (C18, 3 μm, 150 x 2.1 mm). The initial solvent mix was 95% mobile phase A (0.1% TFA in water) and 5% mobile phase B (0.085% TFA in acetonitrile) for 5 min followed by a linear gradient to 50% mobile phase B over 20 min at a flow rate of 100 μL/min. The gradient stayed constant for 2.5 min followed by a linear decrease to 5% B in 2.5 min. The limit of detection (S/N > 3) was ≈ 0.1 μM while the limit of quantitation was approximately 120 μM for each

analyte. Kinetics samples were diluted as necessary to achieve a final concentration of AcNO₂Tyr and AcClNO₂Tyr less than the limit of quantitation. AcNO₂Tyr and AcClNO₂Tyr were quantitated at 360 nm. The Qual browser module of Xcalibur, ver. 1.3 (Thermo-Finnigan, Ontario, Canada) was used to analyze the HPLC chromatogram. Standard curves using AcNO₂Tyr and AcClNO₂Tyr were obtained regularly to ensure accuracy of measured concentrations.

Determination of Initial Reaction Rate and Reaction Order

The lysine-containing peptides were reacted with HOCl and quenched with excess cysteine at 37 °C in 10 mM phosphate buffer at pH 7.4. Four or five time points were chosen in which the product formation was less than 20% of the initial HOCl concentration. The reported initial reaction rate of NO₂Tyr chlorination, V_0 , was determined as the slope of product formation with respect to time that is by a linear line. The V_0 of 12-15 reactions with various initial concentrations of peptide and HOCl were used to solve for the reaction order using the equation $V_0 = k * [\text{Peptide}]_0^A * [\text{Chloramine}]_0^B$, where A and B are the rate order of peptide and chloramine, respectively. Because HOCl reacts with lysine forming a chloramine significantly faster than any measurable formation of ClNO₂Tyr, the initial concentration of chloramine peptide is equivalent to the initial concentration of HOCl.²⁵

Analysis of Kinetics Data and Determination of Rate Constants

Microsoft Excel was used to analyze all kinetic data using a model comparison method.²⁶ A time interval of 0.1 seconds was used to numerically model the differential

equations. The chemical models for chlorination of NO₂Tyr by HOCl or chloramines are presented in the Results section. The sum of the squared differences (SSD) was calculated between the experimental and modeled concentrations for time points in a kinetics experiment. The Solver tool in Excel was used to determine the optimized second order rate constants that minimized the SSD giving SSD_{opt}. The error in each rate constant was estimated by determining the rate constant that gave SSD = SSD_{opt}*(F(P/(N-P))+1) where F is the critical value of the F distribution, P is the number of model parameters, and N is the number of data points. We chose a value of F corresponding to the 95% confidence level. The rate constant values are reported as middle value ± ½*range; the middle value was calculated from the high and low SSD values that defined the range of certainty (95% confidence level) and were within 1% of the optimized value in all cases.

Results

HOCl Reacts with NO₂Tyr to Form ClNO₂Tyr

The published chlorination of 3-substituted tyrosine analogues by HOCl suggested that the loss of 3-nitrotyrosine observed previously resulted in the formation of 3-chloro-5-nitrotyrosine.^{1,27} To avoid the competing reaction of HOCl with the amino group of 3-nitrotyrosine, the acetylated analogues of NO₂Tyr and ClNO₂Tyr were synthesized.²⁸ The ¹H-NMR and UV/vis spectra were consistent with the expected structure and HPLC indicated that the purified compounds were > 98% pure. The pK_a values of AcNO₂Tyr and AcClNO₂Tyr were determined by UV/vis spectroscopy to be

7.1 ± 1 and 5.4 ± 1 , respectively (**Appendix D**). The pK_a of AcNO₂Tyr is comparable to the previously published pK_a value of NO₂Tyr (7.2-7.5).²⁹

The reaction of AcNO₂Tyr with HOCl to form AcClNO₂Tyr was monitored by HPLC. All reactions were initiated by adding HOCl in concentrated buffer (200 mM, pH of 7.4) to equal volumes of the AcNO₂Tyr in purified water with and without excess AcHis or AcLys present. The reactions were stopped by adding a minimum 10-fold excess methionine or cysteine which rapidly reacts with any remaining HOCl or chloramine, respectively.^{24, 25, 30} **Figure 2** shows the formation of AcClNO₂Tyr after a 30-second reaction of AcNO₂Tyr with HOCl. The observed product peak had the same retention time and UV spectra as observed for the authentic standard of AcClNO₂Tyr.

We monitored the reactions between AcNO₂Tyr and HOCl, N-acetylhistidine chloramine (AcHisCl), or N- α -acetyllysine chloramine (AcLysCl) at pH 7.4 and 37 °C between 5 seconds and 120 min. AcNO₂Tyr at concentrations of approximately 500, 750, and 1000 μ M were reacted with 200 μ M HOCl both in the presence and absence of excess AcHis or AcLys. The reaction of 750 μ M AcNO₂Tyr with 200 μ M HOCl (**Figure 3a**) or AcHisCl (**Figure 3b**) results in AcClNO₂Tyr production. The reaction with AcLysCl was too slow to produce any measureable amount of AcClNO₂Tyr after two hours but product was seen the next day (data not shown). In all cases, the total amount of AcClNO₂Tyr produced was less than the initial amount of HOCl, suggesting that HOCl further reacts with AcClNO₂Tyr to form compounds without UV absorbance at wavelengths longer than 200 nm.²⁷ Due to this apparent reaction, only the early time points where the AcClNO₂Tyr concentration was less than 30% of the initial HOCl concentration were modeled to calculate the rate constants. One possible explanation as

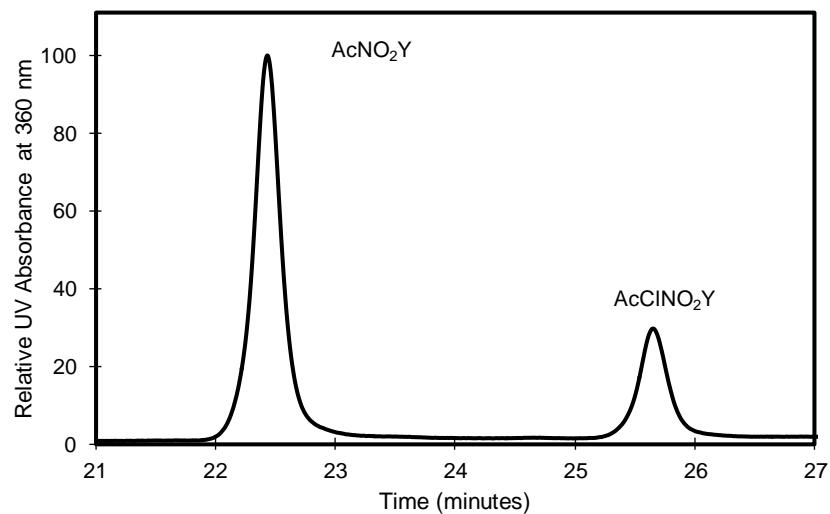
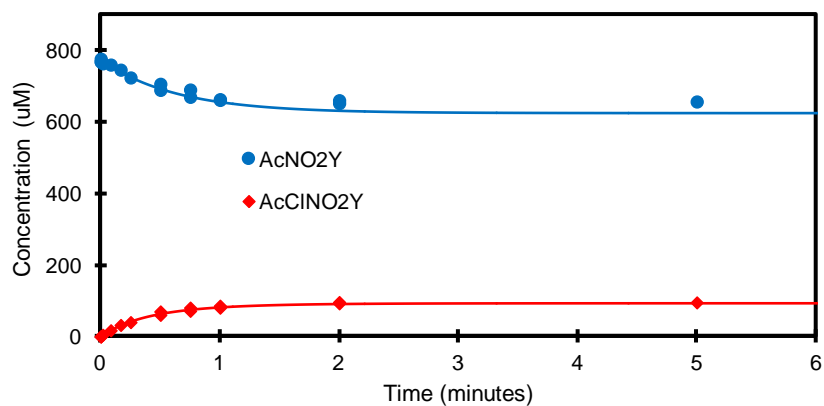


Figure 2: Separation and Quantitation of AcNO₂Tyr and AcClNO₂Tyr by HPLC. AcClNO₂Tyr is formed after 500 μ M AcNO₂Tyr is reacted with 200 μ M HOCl at 37 $^{\circ}$ C, pH 7.4. The reaction was stopped by the addition of excess methionine after 30 s. The peaks at 22.8 and 25.7 min have identical UV spectra and retention times as authentic standards of AcNO₂Tyr and AcClNO₂Tyr, respectively.

A. AcNO₂Tyr + HOCl



B. AcNO₂Tyr + AcHisCl

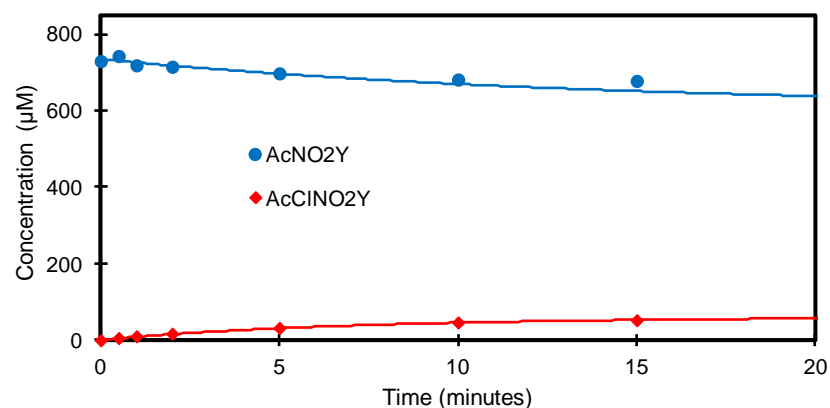


Figure 3: Kinetics of AcNO₂Tyr Chlorination by HOCl or AcHisCl. (A) 780 µM AcNO₂Tyr or (B) 730 µM AcNO₂Tyr with 1000 µM AcHis were reacted with 200 µM HOCl at 37 °C for the indicated time; the reaction was stopped with excess methionine, and the products were quantitated by UV-detected HPLC. The solid lines in each panel represent the modeled reaction progress with optimized rate constants. The rate constant k_1 for AcNO₂Tyr reacting with HOCl in panel A is 24.5 M⁻¹s⁻¹. The rate constant k_1 for AcNO₂Tyr reacting with AcHisCl in panel B is 1.0 M⁻¹s⁻¹. Similar experiments were done for AcLysCl but no product was measured after two hours of reaction.

to the loss of chlorinating potential is the degradation and loss of AcHisCl as previously reported.³⁰ However, even tripling the reported rate of AcHisCl degradation and incorporating that into our model, we saw no significant change in our rate constant or the available amount of AcHisCl during the earlier time points. The complete set of data for AcNO₂Tyr reacting with HOCl or AcHisCl was modeled to obtain a single set of rate constants, summarized in **Table 1**.

HOCl Reacts with AcClNO₂Tyr to Form Unknown Products

We investigated the reaction of AcClNO₂Tyr with HOCl by HPLC and UV/vis. No product peaks were identified by UV-HPLC and the measured loss of AcClNO₂Tyr was less than the initial HOCl introduced. This would seem to indicate that an unknown product with no significant UV/vis chromophore forms and that it reacts more readily with HOCl than AcClNO₂Tyr. We followed the loss of AcClNO₂Tyr in the presence of HOCl by UV/vis at 37 °C, pH 7.4 (**Figure 4**). The rate of loss of AcClNO₂Tyr decreases as the reaction progresses, indicative of the unknown products being able to successfully compete with AcClNO₂Tyr for reaction with HOCl. It takes approximately 6-fold excess HOCl to completely degrade AcClNO₂Tyr (data not shown). Possible products could be chlorinated ketones and chloroform, as seen when phenol analogues are reacted with excess HOCl,³¹ but as the focus of this report is the physiological significance of NO₂Tyr loss, we did not identify the unknown products or reaction kinetics when ClNO₂Tyr reacts with HOCl.

Table 1: Rate Constants for Chlorination of Tyrosine, 3ClTyr, and NO₂Tyr.^a

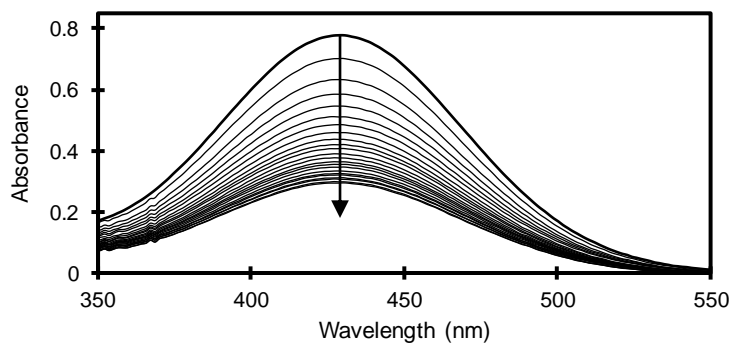
Chlorinating Species	AcTyr^b (M⁻¹s⁻¹)	Ac3ClTyr^b (M⁻¹s⁻¹)	AcNO₂Tyr (M⁻¹s⁻¹)
HOCl	71 ± 8	238 ± 27	24.5 ± 1.2
HisCl	3.0 ± 0.3	10.4 ± 1.0	1.1 ± 0.2
LysCl	0.004 ± 0.003	0.008 ± 0.002	ND ^c

^aReactions were performed at 37 °C, pH 7.4 in 100 mM phosphate buffer.

^bRate constants were reported previously in reference 27.

^cNo significant amount of product was detected after two hours of reaction.

A. UV/vis Spectrum of AcCINO₂Tyr + HOCl



B. Consumption of AcCINO₂Tyr by HOCl

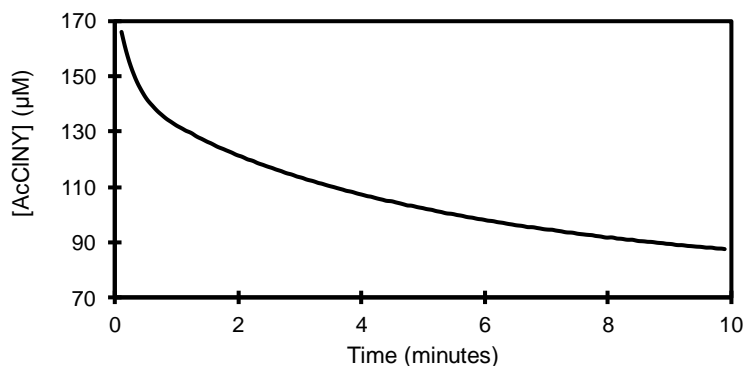


Figure 4: UV/Vis Analysis of AcCINO₂Tyr Reacting with HOCl. (A) UV spectrum of 185 μM AcCINO₂Tyr reacting with 720 μM HOCl at 37 °C, pH 7.4. The initial spectrum is shown as a bold line while the arrow shows the changes in the spectra collected every subsequent 24 s. (B) The consumption of 185 μM AcCINO₂Tyr by 720 μM HOCl at 37 °C, pH 7.4. The concentration of AcCINO₂Tyr was based on the absorbance at 430 nm and a molar absorptivity value of $\epsilon_{430} = 4205 \text{ M}^{-1}\text{cm}^{-1}$. The change in the rate of AcCINO₂Tyr degradation indicates multiple reactions going on, likely between HOCl and the product of AcCINO₂Tyr chlorination. It takes approximately six-fold excess HOCl to completely degrade AcCINO₂Tyr (data not shown).

Rate of NO₂Tyr Chlorination by HOCl Increases in Peptides

Previous studies indicate that chlorination of tyrosine residues in polypeptides is facilitated by nearby histidine or lysine residues.^{24, 27, 32} We reacted the synthetic peptide, Ac-HGNY(NO₂)AE-NH₂, with a 0.5-fold concentration of HOCl and followed product formation by HPLC as shown in **Figure 5**. An amino acid mixture of N-acetyl amino acids that match the residue composition of the peptide Ac-HGNY(NO₂)AE-NH₂ was also reacted with 0.5-fold concentration of HOCl as a control reaction (**Figure 5**). The reactions were quenched with excess cysteine at various time points and the peptide reactants and products were quantitated by HPLC. The production of ClNO₂Tyr in the peptide was approximately 700-fold faster than in the amino acid mixture at the concentrations and reaction conditions examined.

NO₂Tyr Chlorination by HOCl in Peptides is a First Order Reaction

To probe the mechanism whereby neighboring lysine or histidine residues facilitate NO₂Tyr chlorination, we varied the peptide and HOCl concentrations to determine the order of the reaction kinetics. The initial reaction kinetics were measured to minimize the effect of ClNO₂Tyr reacting with HOCl or chloramines. Initial experiments found that the reaction kinetics were independent of the initial peptide concentration and changed only with the amount of HOCl. The reaction kinetics shown in **Figure 6** indicate that the kinetics are first order with respect to chloramine-containing peptide concentration which is equivalent to the amount of HOCl. Given the rapid reaction of HOCl with a peptide amine that is complete within 1 second, the reaction is first order with respect to chloramine concentration provided the peptide is present in excess. The rate constants of

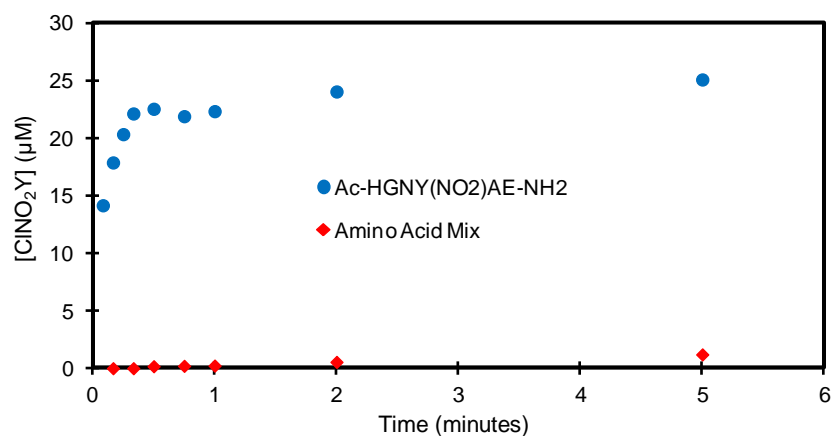
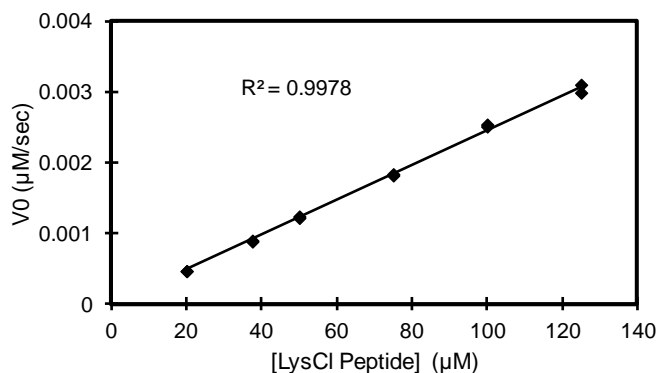


Figure 5: Acceleration of NO₂Tyr Chlorination by His Chloramine in a Peptide. 75 µM Ac-HGNY(NO₂)AE-NH₂ or an analogous amino acid mixture were reacted with 37.5 µM HOCl at 37 °C for the indicated times; the reaction was stopped with excess cysteine and the products were quantitated by UV-detected HPLC. At the concentrations indicated here, the rate of NO₂Tyr chlorination in the peptide is approximately 700-fold faster than in the analogous amino acid mixture.

A. Intramolecular – First Order



B. Intramolecular - Second Order

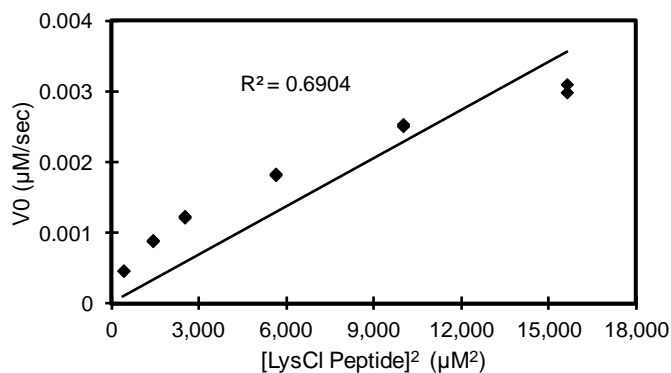


Figure 6: Determining the Rate Order of NO_2Tyr Chlorination by Chloramines within a Peptide. Excess Ac-KGNY(NO_2)AE- NH_2 was reacted with HOCl at 37 °C, pH 7.4. The initial reaction rate was determined by using HPLC to measure the formation of Cl NO_2Tyr at early time points where less than 20% of the reactant peptide was consumed. Samples were quenched with excess cysteine before HPLC. The initial reaction rate was calculated by linearly fitting the early time points. Because the reaction of Lys with HOCl is significantly faster than the chlorination of NO_2Tyr , it was assumed that the concentration of peptide containing lysine chloramine was equal to the amount of HOCl added. The initial reaction rate was plotted to (A) the concentration of Ac-K(Cl)GNY(NO_2)AE- NH_2 to model a first-order reaction and to (B) the square of the concentration of this peptide to model a second-order reaction. The linearity of the first-order fit indicates that NO_2Tyr is chlorinated through an intramolecular reaction with the lysine chloramine.

NO₂Tyr chlorination by chloramine intermediates in the peptides we synthesized in this study are summarized in **Table 2**.

Discussion

Reactive nitrogen species (RNS) chemically damage tyrosine residues to form 3-nitrotyrosine (NO₂Tyr), a surrogate marker used to investigate the role of RNS in human diseases. However, Whiteman and Halliwell reported that NO₂Tyr disappears when exposed to HOCl suggesting that observed NO₂Tyr underestimates the role of RNS in tissues when chlorinating species are also present.¹ That study did not report the resulting product when NO₂Tyr reacts with HOCl, but subsequent studies on the reaction of HOCl with 3ClTyr to form Cl₂Tyr suggested that the expected product should be ClNO₂Tyr.^{27, 33-35} This expectation is now confirmed since reaction of AcNO₂Tyr with HOCl forms a new product that has the same HPLC retention time and UV-spectra as authentic AcClNO₂Tyr (**Figure 2**).

The extent of NO₂Tyr loss depends on the quantity of HOCl produced and the kinetics of NO₂Tyr chlorination. The kinetics of AcNO₂Tyr reacting with HOCl or chloramines were accurately determined by HPLC (**Figure 3**) and are reported in **Table 1**. While the kinetics of 3ClTyr reacting with HOCl or a histidine chloramine are approximately three times faster than tyrosine chlorination, the kinetics of NO₂Tyr chlorination are three times slower. The 3-nitro groups on chlorination kinetics is consistent with an electrophilic aromatic substitution reaction where the kinetics of chlorination are slower due to the electron withdrawing groups deactivating the aromatic ring. The kinetics of chlorination is affected by pH with maximum rates at pH values of

Table 2: Rate Constants for Chlorination of Tyr and NO₂Tyr within a Peptide^a

Peptide Sequence	Rate Constant (s ⁻¹)	pK _a
Ac-HGN-Y(NO ₂)-AE-NH ₂	2.60 ± 0.53 x 10 ⁻²	6.9 ± 0.1
Ac-KGN-Y(NO ₂)-AE-NH ₂	2.54 ± 0.03 x 10 ⁻⁵	6.9 ± 0.1
Ac-KGN-Y-AE-NH ₂	2.38 ± 0.07 x 10 ⁻⁴	9.8 ± 0.1

^aReactions were performed at 37 °C, pH 7.4 in 10 mM phosphate buffer.

7.4 and 8.0 for NO₂Tyr (**Appendix E**) and 3ClTyr, respectively.²⁷ The faster kinetics of chlorination at these pH values is consistent with an electrophilic aromatic substitution reaction where a phenolate is more reactive than a phenol.

As observed with Cl₂Tyr,²⁷ ClNO₂Tyr also reacts with HOCl to form multiple compounds without a UV spectrum as shown in **Figure 4**. The reaction of ClNO₂Tyr with chlorinating compounds to form compounds with no UV absorption explains the apparent loss of tyrosine analogues observed by UV-detected HPLC at longer reaction times and/or higher ratios of chlorinating agent relative to tyrosine analogue. The reported kinetics rates used excess NO₂Tyr and were calculated using earlier reaction times where the loss of ClNO₂Tyr was not observed.

Measurements of 3ClTyr or NO₂Tyr from biological tissues usually measure these surrogate markers in the context of proteins instead of the free amino acid. The observation that tyrosine residues with a nearby histidine or lysine residues are preferentially chlorinated is better explained by the intramolecular reaction with a nearby chloramine than the direct intermolecular chlorination by HOCl to form a protein-bound 3ClTyr.^{24, 27, 33, 35, 36} The fast reaction of HOCl with protein amines ($\sim 10^5 \text{ M}^{-1}\text{s}^{-1}$) better competes with the antioxidant glutathione ($\sim 10^8 \text{ M}^{-1}\text{s}^{-1}$) than the direct chlorination of tyrosine analogues ($\sim 10^2 \text{ M}^{-1}\text{s}^{-1}$) and explains the preferential chlorination of some protein-bound tyrosine residues, provided the intramolecular kinetics are sufficiently fast.^{25, 32}

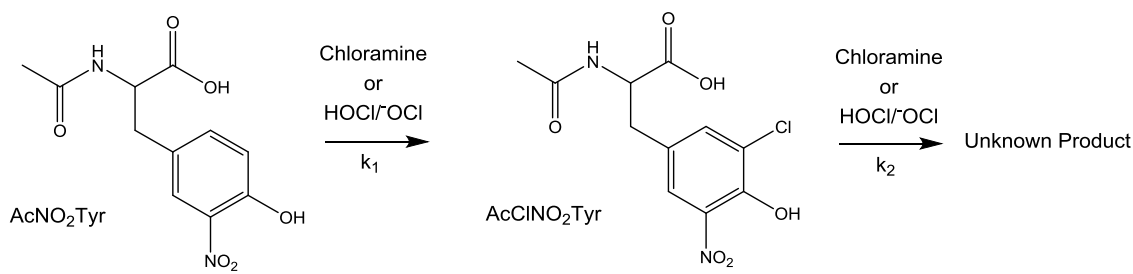
The rates of tyrosine, 3ClTyr, or NO₂Tyr chlorination by a histidine chloramine in **Table 1** are 24-fold slower than the reaction with HOCl. However, the rate of NO₂Tyr chlorination by HOCl is 700-fold faster in the peptide Ac-HGNY(NO₂)AE-NH₂ than an

equivalent amino acid mix containing AcNO₂Tyr and Ac-His (**Figure 5**). We argue that this increased rate of chlorination is due to the reduced degrees of freedom and close proximity maintained between the histidine chloramine and the NO₂Tyr residues in the peptide context. The rapid intermolecular reaction of HOCl with a polypeptide amine to form a chloramine followed by the slower intramolecular chlorination of a nearby tyrosine analogue predicts that the kinetics of peptide tyrosine chlorination will follow first order kinetics. To our knowledge, this study is the first to demonstrate that the kinetics of tyrosine chlorination in a peptide with nearby amine follows first order kinetics (**Figure 6**).

The second order kinetics of AcTyr or N-acetyl-3chlorotyrosine (Ac3ClTyr) chlorination by lysine chloramines is approximately 1000 times slower than chlorination by histidine chloramines.²⁷ Likewise, the first order kinetics of NO₂Tyr chlorination in a peptide by a lysine chloramine is 1000 times slower than a histidine chloramine (**Table 2**). **Figure 7** shows the intermolecular and intramolecular reaction schemes used in this report to extract first and second order rate constants. It should be noted that AcHisCl and, to a lesser extent, AcLysCl naturally decompose,^{30, 37} but this rate was not incorporated into our model since it had no significant effect at the concentrations and time points used in this study.

Given the slow intermolecular kinetics of NO₂Tyr chlorination, the loss of NO₂Tyr in proteins due to HOCl likely requires a nearby lysine or histidine residue. For example, Tyr¹⁹² of apolipoprotein A-1 can be nitrated or chlorinated suggesting that measurements of Tyr¹⁹² nitration will underestimate RNS when HOCl is present.³⁸ However, selective tyrosine nitration is reported to have different sequence requirements

A. Intermolecular Scheme



B. Intramolecular Scheme

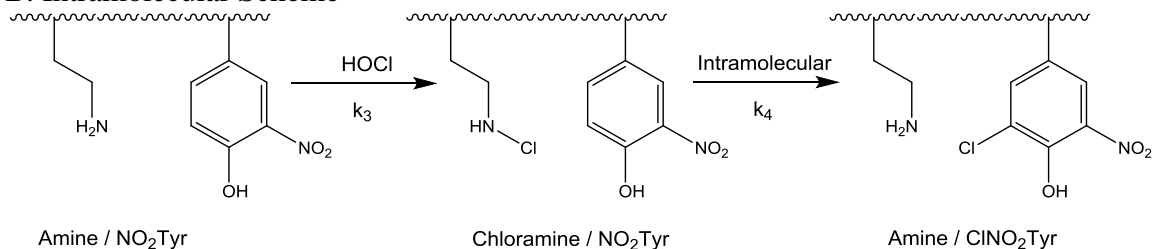


Figure 7: Kinetics Schemes for the Chlorination of NO₂Tyr by HOCl. (A) HOCl converts AcNO₂Tyr to AcClNO₂Tyr which is consumed when exposed to HOCl or chloramines to form unknown products. (B) When NO₂Tyr is on a peptide containing a nearby lysine or histidine, the amine is first rapidly chlorinated by HOCl in an intermolecular reaction. The rate of chloramine formation by HOCl, k_3 , is much greater than the direct chlorination of NO₂Tyr by HOCl, k_1 . The peptide chloramine then chlorinates NO₂Tyr in an intramolecular reaction to form ClNO₂Tyr.

than selective tyrosine chlorination suggesting that loss of NO₂Tyr in the presence to HOCl will depend on the specific tyrosine residue examined.³⁹⁻⁴² It should be acknowledged that with the low rate of NO₂Tyr chlorination by HOCl, it is unlikely that the product, ClNO₂Tyr, would be important physiologically. Of greater concern is the loss of 3ClTyr in the presence of HOCl, since the same sequence characteristics, a nearby histidine or lysine, favor tyrosine chlorination as well as 3ClTyr chlorination to Cl₂Tyr. While most studies only measure 3ClTyr, some reports that measure 3ClTyr and Cl₂Tyr find significant quantities of both chlorination products when the quantity of 3ClTyr is consistent with the quantities observed *in vivo* indicating that published 3ClTyr levels and may underestimate the extent of HOCl production.^{27, 34, 35, 43, 44} Future measurements of 3ClTyr should also include Cl₂Tyr in order to better estimate the extent of HOCl production *in vivo*.

References

1. Whiteman, M., and Halliwell, B. (1999) Loss of 3-nitrotyrosine on exposure to hypochlorous acid: Implications for the use of 3-nitrotyrosine as a bio-marker in vivo. *Biochem Bioph Res Co*, 258, 168-172.
2. Ohshima, H., Tatemichi, M., and Sawa, T. (2003) Chemical basis of inflammation-induced carcinogenesis. *Arch Biochem Biophys*, 417, 3-11.
3. Sayre, L. M., Perry, G., and Smith, M. A. (2008) Oxidative stress and neurotoxicity. *Chem Res Toxicol*, 21, 172-188.
4. Stocker, R., and Keaney, J. F. (2004) Role of oxidative modifications in atherosclerosis. *Physiol Rev*, 84, 1381-1478.
5. Dedon, P. C., and Tannenbaum, S. R. (2004) Reactive nitrogen species in the chemical biology of inflammation. *Arch Biochem Biophys*, 423, 12-22.
6. Cedergren, J., Follin, P., Forslund, T., Lindmark, M., Sungqvist, T., and Skogh, T. (2003) Inducible nitric oxide synthase (NOS II) is constitutive in human neutrophils. *Apmis*, 111, 963-968.
7. Evans, T. J., Buttery, L. D. K., Carpenter, A., Springall, D. R., Polak, J. M., and Cohen, J. (1996) Cytokine-treated human neutrophils contain inducible nitric oxide synthase that produces nitration of ingested bacteria. *P Natl Acad Sci USA*, 93, 9553-9558.
8. Sugiyama, S., Okada, Y., Sukhova, G. K., Virmani, R., Heinecke, J. W., and Libby, P. (2001) Macrophage myeloperoxidase regulation by granulocyte macrophage colony-stimulating factor in human atherosclerosis and implications in acute coronary syndromes. *Am J Pathol*, 158, 879-891.
9. Paquet, P., De Groote, D., and Pierard, G. E. (2010) Functionally Active Macrophage-Derived Myeloperoxidase in the Skin of Drug-Induced Toxic Epidermal Necrolysis. *Dermatology*, 220, 201-207.
10. Sugiyama, S., Kugiyama, K., Aikawa, M., Nakamura, S., Ogawa, H., and Libby, P. (2004) Hypochlorous acid, a macrophage product, induces endothelial apoptosis and tissue factor expression - Involvement of myeloperoxidase-mediated oxidant in plaque erosion and thrombogenesis. *Arterioscl Throm Vas*, 24, 1309-1314.
11. Green, P. S., Mendez, A. J., Jacob, J. S., Crowley, J. R., Growdon, W., Hyman, B. T., and Heinecke, J. W. (2004) Neuronal expression of myeloperoxidase is increased in Alzheimer's disease. *J Neurochem*, 90, 724-733.
12. Klebanoff, S. J. (2005) Myeloperoxidase: friend and foe. *J Leukocyte Biol*, 77, 598-625.

13. Hawkins, C. L., Pattison, D. I., and Davies, M. J. (2003) Hypochlorite-induced oxidation of amino acids, peptides and proteins. *Amino Acids*, 25, 259-274.
14. Gaut, J. P., Byun, J., Tran, H. D., and Heinecke, J. W. (2002) Artifact-free quantification of free 3-chlorotyrosine, 3-bromotyrosine, and 3-nitrotyrosine in human plasma by electron capture-negative chemical ionization gas chromatography mass spectrometry and liquid chromatography-electrospray ionization tandem mass spectrometry. *Anal Biochem*, 300, 252-259.
15. Winterbourn, C. C., and Kettle, A. J. (2000) Biomarkers of myeloperoxidase-derived hypochlorous acid. *Free Radical Bio Med*, 29, 403-409.
16. Dalle-Donne, I., Rossi, R., Colombo, R., Giustarini, D., and Milzani, A. (2006) Biomarkers of oxidative damage in human disease. *Clin Chem*, 52, 601-623.
17. Radi, R. (2004) Nitric oxide, oxidants, and protein tyrosine nitration. *P Natl Acad Sci USA*, 101, 4003-4008.
18. Abu-Soud, H. M., and Hazen, S. L. (2000) Nitric oxide is a physiological substrate for mammalian peroxidases. *J Biol Chem*, 275, 37524-37532.
19. Eiserich, J. P., Hristova, M., Cross, C. E., Jones, A. D., Freeman, B. A., Halliwell, B., and van der Vliet, A. (1998) Formation of nitric oxide derived inflammatory oxidants by myeloperoxidase in neutrophils. *Nature*, 391, 393-397.
20. Zheng, L. M., Nukuna, B., Brennan, M. L., Sun, M. J., Goormastic, M., Settle, M., Schmitt, D., Fu, X. M., Thomson, L., Fox, P. L., Ischiropoulos, H., Smith, J. D., Kinter, M., and Hazen, S. L. (2004) Apolipoprotein A-I is a selective target for myeloperoxidase-catalyzed oxidation and functional impairment in subjects with cardiovascular disease. *J Clin Invest*, 114, 529-541.
21. Hensley, K., Maitt, M. L., Yu, Z. Q., Sang, H., Markesbery, W. R., and Floyd, R. A. (1998) Electrochemical analysis of protein nitrotyrosine and dityrosine in the Alzheimer brain indicates region-specific accumulation. *J Neurosci*, 18, 8126-8132.
22. Riordan, J. F., Sokolovs, M., and Vallee, B. L. (1967) Environmentally Sensitive Tyrosyl Residues . Nitration with Tetranitromethane. *Biochemistry-U.S.*, 6, 358-&.
23. Morris, J. C. (1966) Acid Ionization Constant of Hoel from 5 to 35 Degrees. *J Phys Chem-U.S.*, 70, 3798-&.
24. Pattison, D. I., and Davies, M. J. (2005) Kinetic analysis of the role of histidine chloramines in hypochlorous acid mediated protein oxidation. *Biochemistry-U.S.*, 44, 7378-7387.

25. Pattison, D. I., and Davies, M. J. (2001) Absolute rate constants for the reaction of hypochlorous acid with protein side chains and peptide bonds. *Chem Res Toxicol*, 14, 1453-1464.
26. Motulsky, H., and Christopoulos, A. (2003) Generating confidence intervals via model comparison, In *Fitting Models to Biological Data using Linear and Nonlinear Regression. A Practical guide to curve fitting.* pp 109 - 117, GraphPad Software, Inc.
27. Curtis, M. P., Hicks, A. J., and Neidigh, J. W. (2011) Kinetics of 3-Chlorotyrosine Formation and Loss due to Hypochlorous Acid and Chloramines. *Chem Res Toxicol*, 24, 418-428.
28. Fu, S. L., Wang, H. J., Davies, M., and Dean, R. (2000) Reactions of hypochlorous acid with tyrosine and peptidyl-tyrosyl residues give dichlorinated and aldehydic products in addition to 3-chlorotyrosine. *J Biol Chem*, 275, 10851-10858.
29. Creighton, T. E. (1993). *Proteins: Structures and Molecular Properties.* (Second Edition). New York: W. H. Freeman & Co.
30. Hazen, S. L., Hsu, F. F., and Heinecke, J. W. (1998) Human neutrophils employ myeloperoxidase to convert alpha-amino acids to a battery of reactive aldehydes: a pathway for aldehyde generation at sites of inflammation. *Biochemistry*, 37, 6864-6873.
31. Gallard H., and von Gunten, U. (2002) Chlorination of Phenols: Kinetics and Formation of Chloroform. *Environ Sci Technol*, 36, 884-890.
32. Peskin, A. V., and Winterbourn, C. C. (2001) Kinetics of the reactions of hypochlorous acid and amino acid chloramines with thiols, methionine, and ascorbate. *Free Radical Bio Med*, 30, 572-579.
33. Bergt, C., Fu, X. Y., Huq, N. P., Kao, J., and Heinecke, J. W. (2004) Lysine residues direct the chlorination of tyrosines in YXXK motifs of apolipoprotein A-I when hypochlorous acid oxidizes high density lipoprotein. *J Biol Chem*, 279, 7856-7866.
34. Chapman, A. L. P., Senthilmohan, R., Winterbourn, C. C., and Kettle, A. J. (2000) Comparison of mono- and dichlorinated tyrosines with carbonyls for detection of hypochlorous acid modified proteins. *Arch Biochem Biophys*, 377, 95-100.
35. Kang, J. I., and Neidigh, J. W. (2008) Hypochlorous acid damages histone proteins forming 3-chlorotyrosine and 3,5-dichlorotyrosine. *Chem Res Toxicol*, 21, 1028-1038.
36. Domigan, N. M., Charlton, T. S., Duncan, M. W., Winterbourn, C. C., and Kettle, A. J. (1995) Chlorination of Tyrosyl Residues in Peptides by Myeloperoxidase and Human Neutrophils. *J Biol Chem*, 270, 16542-16548.

37. Pattison, D. I., Hawkins, C. L., Davies, M. J. (2007) Hypochlorous acid-mediated protein oxidation: how important are chloramine transfer reactions and protein tertiary structure? *Biochemistry*, 46, 9853-9864.
38. Shao, B. H., Bergt, C., Fu, X. Y., Green, P., Voss, J. C., Oda, M. N., Oram, J. F., and Heinecke, J. W. (2005) Tyrosine 192 in apolipoprotein A-I is the major site of nitration and chlorination by myeloperoxidase, but only chlorination markedly impairs ABCA1-dependent cholesterol transport. *J Biol Chem*, 280, 5983-5993.
39. Gunaydin, H., and Houk, K. N. (2009) Mechanisms of Peroxynitrite-Mediated Nitration of Tyrosine. *Chem Res Toxicol*, 22, 894-898.
40. Jiao, K. S., Mandapati, S., Skipper, P. L., Tannenbaum, S. R., and Wishnok, J. S. (2001) Site-selective nitration of tyrosine in human serum albumin by peroxynitrite. *Anal Biochem*, 293, 43-52.
41. Radi, R. (2013) Protein Tyrosine Nitration: Biochemical Mechanisms and Structural Basis of Functional Effects. *Accounts Chem Res*, 46, 550-559.
42. Souza, J. M., Daikhin, E., Yudkoff, M., Raman, C. S., and Ischiropoulos, H. (1999) Factors determining the selectivity of protein tyrosine nitration. *Arch Biochem Biophys*, 371, 169-178.
43. Saude, E. J., Lacy, P., Musat-Marcu, S., Mayes, D. C., Bagu, J., Man, S. F. P., Sykes, B. D., and Moqbel, R. (2004) NMR analysis of neutrophil samples from patients with activation in sputum cystic fibrosis. *Magnet Reson Med*, 52, 807-814.
44. Sochaski, M. A., Jarabek, A. M., Murphy, J., and Andersen, M. E. (2008) 3-chlorotyrosine and 3,5-dichlorotyrosine as biomarkers of respiratory tract exposure to chlorine gas. *J Anal Toxicol*, 32, 99-105.

CHAPTER FOUR
EFFECT OF PRIMARY AND SECONDARY STRUCTURE ON THE RATE OF
TYROSINE CHLORINATION BY HYPOCHLOROUS ACID

Matthew P. Curtis, Jonathan W. Neidigh

Department of Basic Sciences, Loma Linda University School of Medicine

Loma Linda, CA 92350

Abstract

The molecule 3-chlorotyrosine (3ClTyr), formed when hypochlorous acid (HOCl) chlorinates tyrosine, is a biomarker of inflammation. HOCl can also chlorinate histidine or lysine side-chains creating chloramines. It has been postulated previously that 3ClTyr formation *in vivo* is predominantly through chloramine intermediates, as evidenced by the increased incidence of chlorination of tyrosine residues that are nearby histidine or lysine residues in a protein. While previous studies have shown how yields of 3ClTyr change depending on the positioning of lysine with respect to tyrosine in a peptide, they have failed to measure the change in the rate of chlorination. In this study, we use linear peptide sequences containing 3-nitrotyrosine (NO₂Tyr) and lysine at different positions to explore the effect this has on the rate of chlorination of the tyrosine analogue. We also synthesized and characterized a cyclic ten-residue peptide designed to structurally constrain tyrosine and lysine residues nearby in space to better facilitate chlorination. In simple linear peptides, the rate of chlorination changes based on the position of lysine to tyrosine such that $K_xY > KY > K_{xx}Y > K_{xxx}Y$, where x represents a residue that is unreactive with HOCl. The rate of chlorination is further increased if the secondary structure constricts lysine and tyrosine nearby in space, as determined in the gramicidin S analogue cyclo-P(OH)TKL^DFP(OH)TYL^DF. The intramolecular rate constants of tyrosine chlorination for all synthesized peptides are reported and the results discussed in relation to previous literature.

Introduction

Hypochlorous acid (HOCl) is the primary reactive oxygen species (ROS) produced by activated neutrophils at sites of inflammation. Phagocytic leukocytes, including neutrophils, monocytes, and macrophages, all generate reactive oxygen and chlorine species to kill invading microorganisms or in the clearance of damaged tissue.^{1, 2} In humans, the production of HOCl is unique to the activity of the enzyme myeloperoxidase (MPO) which utilizes hydrogen peroxide (H₂O₂) and chloride ions to generate this reactive species.³

While the generation of HOCl is typically confined to vesicles containing engulfed bacteria,^{4, 5} reactive species produced by phagocytes can also cause damage to host tissues.^{3, 6} For example, neutrophils can actively secrete MPO into the extracellular environment and disruption in enzyme trafficking can result in production of superoxide and H₂O₂ outside the cell.⁷⁻¹¹ It is thought that the generation of reactive species in chronically inflamed tissue contributes to the pathogenesis of several diseases, including the formation of atherosclerotic plaques,¹²⁻¹⁴ neurodegenerative diseases,¹⁵⁻¹⁸ arthritis,^{19, 20} and certain cancers.²¹⁻²⁴

The high reactivity of HOCl means that it only exists transiently *in vivo*. To determine the extent of HOCl production we must use more stable markers, typically the byproducts of HOCl reacting with the bases of DNA or the amino acids of proteins. While HOCl reacts with DNA bases to form hydroxylated or chlorinated uracil and cytosine,²⁵⁻²⁷ damaged DNA bases can be readily repaired. The reaction with the amine groups of histidine or lysine side-chains to form chloramines is rapid,^{28, 29} but these chloramines can react further and chlorinate other compounds.²⁹⁻³¹ The chlorination of

tyrosine, however, forms stable and unique products 3-chlorotyrosine (3ClTyr) and 3,5-dichlorotyrosine (Cl₂Tyr).³²⁻³⁴ These two markers have been measured from *in vivo* samples including in asthmatic sputum and in cultures in which *staphylococcus aureus* is phagocytized by neutrophils.^{35,36}

The direct chlorination of tyrosine residues by HOCl or HOCl-induced chloramines is slow.³⁷ This contradicts studies that show greater yields of 3ClTyr and Cl₂Tyr at tyrosine residues that are near histidine or lysine residues within proteins, particularly those that are in a KxxY sequence motif, where x is a residue that is unreactive with HOCl.^{33,38} The mechanism of 3ClTyr formation proposed by others^{38,39} and determined in our previous studies^{37,40} is by the intramolecular reaction between a lysine or histidine chloramine and a nearby tyrosine. While the effect of the spacing between lysine and tyrosine residues on the yield of 3ClTyr has been explored previously, there have been no studies examining how this changes the rate of chlorination and comparing this rate to competing reactions with HOCl.

In this study, we synthesized several peptides containing histidine or lysine with a varying number of residues between them and a 3-nitrotyrosine (NO₂Tyr) residue. NO₂Tyr was chosen because it has a slower rate of reaction with HOCl or chloramines than unmodified tyrosine yet undergoes the same mechanism of chlorination, making the formation of chlorinated product easier to follow.⁴⁰ These peptides were reacted with HOCl and the rate of chlorination were measured to determine the effect the primary structure had on tyrosine chlorination. Additionally, a cyclic peptide with a beta-sheet motif was designed and synthesized to position a lysine and tyrosine residue in constrained positions close in space in hopes of increasing the rate of chlorination. This

secondary structure of this peptide was characterized by circular dichroism (CD) spectroscopy and the rate of chlorination by HOCl was determined. The kinetics of chlorination of these peptides further support the role of chloramines in the formation of 3ClTyr and Cl₂Tyr within peptides and should allow future researchers greater ability to predict the likelihood of tyrosine chlorination and better determine the degree of MPO activity in chronically inflamed tissue.

Experimental Procedures

Materials

N-Acetyl-L-tyrosine (AcTyr), N- α -acetyl-L-lysine (AcLys), and N-acetyl-L-histidine (AcHis) were purchased from Novabiochem (San Diego, CA). Fmoc-amide resin was purchased from Applied Biosystems, Inc. (Foster City, CA). Fmoc-OSu, Fmoc-Lys(Boc)-OH, Fmoc-His(Trt)-OH, and all other Fmoc amino acids were purchased from Advanced ChemTech (Louisville, KY), with the exception of Fmoc-Tyr(NO₂)-OH which was synthesized as described below. All other laboratory chemicals including 3-chloro-L-tyrosine, 3-nitro-L-tyrosine, L-methionine, sodium hypochlorite, N-acetylglycine, N-acetyl-L-alanine, and N-acetyl-L-glutamic acid were purchased from Sigma-Aldrich (St. Louis, MO). Synthesis of N-Fmoc-3-nitrotyrosine was performed as described in Chapter 3.

Linear Peptide Synthesis and Purification

Linear peptides containing lysine residues in varying proximity to the NO₂Tyr residue were synthesized on an ABI model 433A peptide synthesizer using fast Fmoc

chemistry. Following synthesis, the N-terminus was acetylated using acetic anhydride. The protecting groups and resin support were cleaved from the peptides using a mixture of TFA/phenol/water/triisopropylsilane (88:5:5:2). The resin was removed by filtration, the cleavage reaction was concentrated by rotary evaporation, and then the peptide was precipitated by adding cold diethyl ether to the cleavage mixture. The ether was removed following centrifugation to pellet the precipitated peptide. After washing the crude peptide with cold diethyl ether three times, the peptides were purified by reverse phase HPLC using a C18 column (Varian Dynamax, 250 mm x 21.4 mm, 300 Å, 5 µM) with a gradient of 20 - 60% mobile phase B (acetonitrile with 0.085% TFA) where mobile phase A contained aqueous 0.1% TFA. The sequence of the purified peptides was confirmed by MS/MS using a ThermoFinnigan LCQ Deca XP mass spectrometer, and a purity of > 95% was verified by analytical HPLC.

Synthesis of ^DPhe-chlorotrityl Resin

1 g of 2-chlorotrityl chloride resin was washed in dichloromethane (DCM) and the resin was filtered. 2 mmol of Fmoc-^DPhe-OH and 5 mmol of N,N-diisopropylethylamine (DIPEA) were dissolved in DCM and added to the resin. The resin was washed twice with dimethylformamide (DMF) and a mixture of DCM/methanol/DIPEA (80:15:5) was added to the resin for 10 min twice. The resin was then washed with DMF three times then suspended in 25% piperidine in DMF while being shaken for twenty minutes. The resin was washed again in DMF six times, isopropanol three times, and hexane four times. The final product was dried by suction and stored at 4 °C until use for peptide synthesis.

Cyclic Peptide Synthesis and Purification

The cyclic, 10-residue peptide cyclo-P(OH)TKL^DFP(OH)TYL^DF (**Figure 1**) was based on gramicidin S, another cyclic peptide that mimics a beta-pleated sheet motif.⁴¹ The linear, protected peptide was synthesized on ^DPhe-chlorotrityl resin using fast Fmoc chemistry and an ABI peptide synthesizer as described above. Beginning with a ^DPhe-chlorotrityl resin has been shown to result in the highest yield of the final cyclized product.⁴⁴ The chlorotrityl resin was selectively removed while keeping the side-chain protecting groups intact by suspending the resin in 2,2,2-trifluoroethanol and DCM (2:8) for 45 minutes at room temperature and filtering off the resin. The filtrate was concentrated by rotary evaporation and the peptide was precipitated by the addition of hexane and ether. The peptide was then centrifuged and the pellet was washed twice with ether, leaving a linear, side-chain protected peptide, NH₂-P(OH)TKL^DFP(OH)TYL^DF-OH.

Approximately 100 mg of the crude, protected, linear peptide was diluted heavily in 200 mL of DCM in order to favor intramolecular cyclization over intermolecular polymerization.⁴⁴ Cyclization was initiated by the addition of HBTU, HoBt hydrate, and DIPEA to a final concentration of 1 mM, 1 mM, and 2 mM respectively. The reaction was conducted at room temperature overnight and concentrated by rotary evaporation. Following cyclization, the side-chain protecting groups were cleaved by reacting with TFA/phenol/water/triisopropylsilane (88:5:5:2) for two hours followed by washing with diethyl ether. The crude, cyclic peptide was purified by HPLC and the sequence was confirmed by MS/MS as described above. Fragmentation of the cyclic peptide by MS/MS

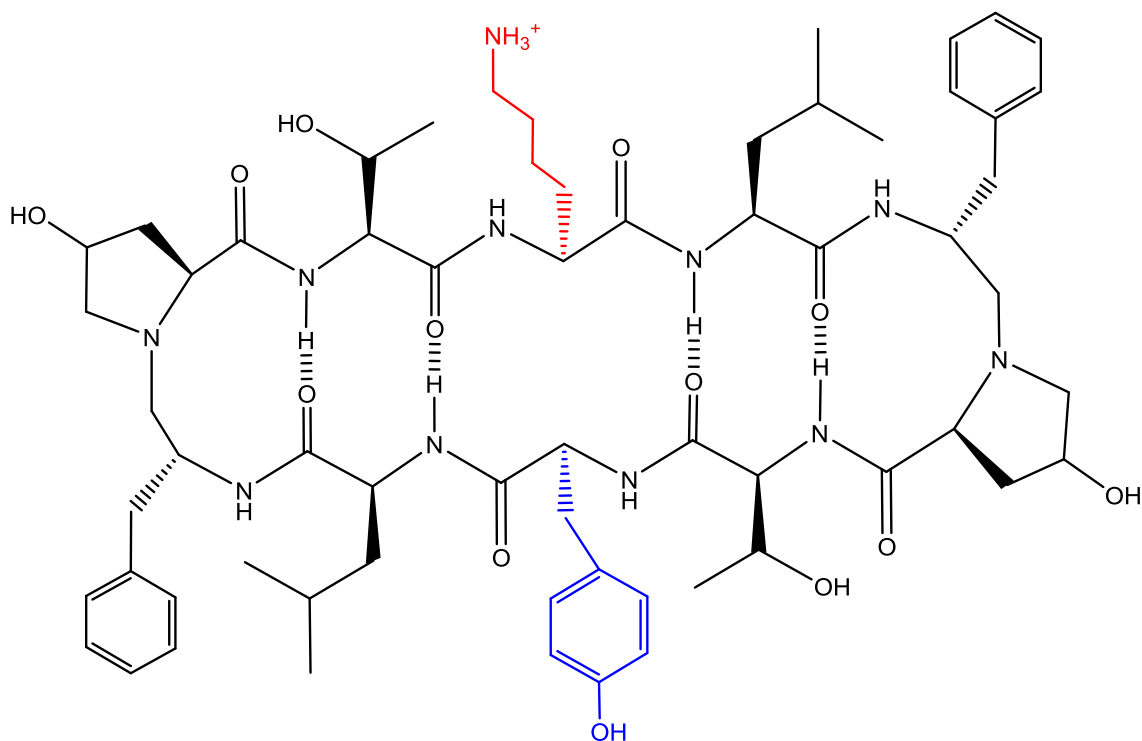


Figure 1: Structure of cyclo-P(OH)TKL^DFP(OH)TYL^DF. This structure was based on the cyclic decapeptide gramicidin S, which is a known beta-sheet analogue. ^DPhe-Pro bonds induce II' beta-turns and hydrogen bonds between anti-parallel strands further stabilize the structure.^{42, 43} When this ten-residue peptide is cyclized, the side-chains of lysine (red) and tyrosine (blue) are on the same surface of the ring structure.

showed unique peptides confirming the cyclization occurred between the N-terminal hydroxyproline and C-terminal phenylalanine (**Appendix F**)

Methods

The purchased sodium hypochlorite stock was stored at 4 °C. The pK_a of HOCl is 7.5 resulting in almost equal concentrations of hypochlorous acid and its conjugate base, hypochlorite, at physiological pH. The term “hypochlorous acid” is thus used to refer to both the acid and its conjugate base. The concentration of the sodium hypochlorite stock was determined daily using the absorbance at 290 nm ($\epsilon_{290\text{ nm}} = 350\text{ M}^{-1}\text{cm}^{-1}$) for a fresh dilution of the stock into 0.1 M NaOH.⁴⁵ Dilutions of HOCl stock were then made into 20 mM phosphate buffer at pH 7.4. The stock concentrations of peptides containing Tyr or NO₂Tyr were determined following dilution into 0.1 M HCl and using UV/vis spectroscopy with molar absorptivity values of $\epsilon_{275\text{ nm}} = 1368\text{ M}^{-1}\text{cm}^{-1}$ and $\epsilon_{360\text{ nm}} = 2790\text{ M}^{-1}\text{cm}^{-1}$, respectively.^{46, 47}

Reaction of Peptides with HOCl

200 μL of HOCl was reacted with an equal volume of excess peptide at concentrations of 10 - 120 μM HOCl and 20 – 240 μM peptide in 10 mM phosphate buffer at pH 7.4. Reactants were rapidly mixed in 1.5 mL glass vials in an aluminum block at 37 °C and the reaction was stopped by the addition of 200 μL of 10-fold excess cysteine at time points between 5 s and 12 hr.

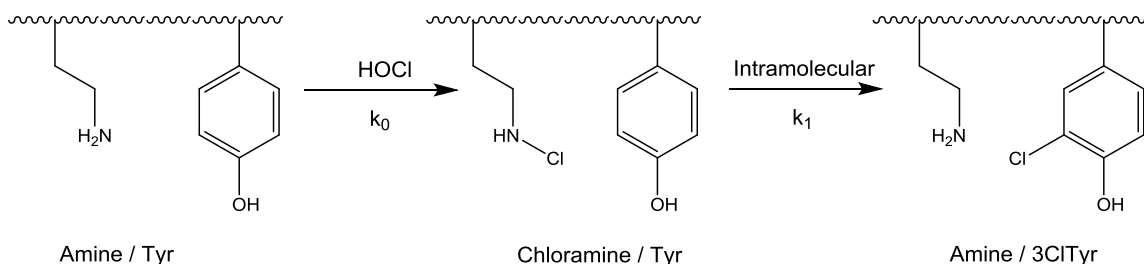
HPLC Quantitation of Reaction Products

The concentration of products and reactants in kinetic samples were measured using a ThermoFinnigan (Waltham, MA) Surveyor HPLC system with a MS Pump, Autosampler, and PDA detector (200-600 nm). The solvent gradients used for peptides containing tyrosine or NO₂Tyr are described in Chapters 2 and 3, respectively. Kinetic samples were run directly on the HPLC without further dilution. The Qual browser module of Xcalibur, ver. 1.3 (Thermo-Finnigan, Ontario, Canada) was used to analyze the HPLC chromatogram. Standard curves using N-acetylated analogues of tyrosine, 3ClTyr, and Cl₂Tyr or NO₂Tyr and N-acetyl-3-chloro-5-nitrotyrosine (ClNO₂Tyr) were obtained periodically to ensure that measured concentrations were accurate. ClNO₂Tyr was synthesized as previously described.⁴⁰

Analysis of Kinetics Data and Determination of Rate Constants

Microsoft Excel was used to analyze all kinetic data using a model comparison method.⁴⁸ The kinetic scheme and the differential equations used to model the rate constant are described in **Figure 2**. A time interval of 0.1 s was used to numerically model the differential equations. The sum of the squared differences (SSD) was calculated between the experimental and modeled concentrations for time points in a kinetics experiment. The Solver tool in Excel was used to determine the optimized second order rate constants that minimized the SSD giving SSD_{opt}. The error in each rate constant was estimated by determining the rate constant that gave SSD = SSD_{opt}*(F(P/(N-P))+1) where F is the critical value of the F distribution, P is the number of model parameters, and N is the number of data points. We chose a value of F

A. Scheme of Intramolecular Tyr or NO₂Tyr Chlorination



B. Differential Equations

$$\frac{d[\text{Chloramine/Tyr}]}{dt} = -k_1 * [\text{Chloramine/Tyr Peptide}]$$

$$\frac{d[\text{Amine/3ClTyr}]}{dt} = +k_1 * [\text{Chloramine/Tyr Peptide}]$$

Figure 2: Kinetic Scheme of Intramolecular Tyrosine Chlorination. (A) The chlorination of tyrosine or NO₂Tyr by HOCl in a lysine-containing peptide is through a chloramine intermediate. Lysine's side-chain amine is chlorinated quickly relative to the rate of tyrosine chlorination, such that any HOCl rapidly chlorinates the amine to form a chloramine. Therefore, the amount of Chloramine / Tyr peptide is equivalent to the amount of HOCl added, provided the peptide is available in excess. (B) Differential equations were used to solve for the intramolecular rate constant, k_1 , as described in the Methods section.

corresponding to the 95% confidence level. The rate constant values are reported as middle value $\pm \frac{1}{2}$ *range; the middle value was calculated from the high and low SSD values that defined the range of certainty (95% confidence level) and were within 1% of the optimized value in all cases.

Characterization of Secondary Structure by Circular Dichroism

CD samples were prepared by diluting concentrated peptide stock of a known concentration into 200 mM phosphate buffer, pH 7.4, to obtain a final concentration of 200 μ M peptide in a cell with a path length of 0.1 cm. The concentration of the stock solutions was determined by UV/vis spectroscopy using the molar absorptivity of tyrosine ($\epsilon_{275 \text{ nm}} = 1368 \text{ M}^{-1}\text{cm}^{-1}$).⁴⁶ CD spectra were recorded using a JASCO model J720 spectropolarimeter with a nitrogen flow rate of 5 L/min. Typical spectral accumulation parameters were a time constant of 1 sec and a scan rate of 100 nm/min with a 0.5 nm step resolution over the range of 195-350 nm with 12 scans averaged for each spectrum. The accumulated average spectra were trimmed at a dynode voltage of 700 prior to baseline subtraction and smoothing using the reverse Fourier transform procedure in the KASCO software. CD spectral values for peptides were expressed in units of residue molar ellipticity ($\text{deg} \cdot \text{cm}^2 / \text{residue dmol}$). The temperature of the CD cell was equilibrated at each temperature for 15 min prior to acquisition of the spectra. The initial temperature was 5 °C and was increased in 10 °C increments to 65 °C.

Results

Spacing of Lysine and Tyrosine Residues Alters Rate of Chlorination

To examine the effect that the spacing between the chloramine and the NO₂Tyr residue had on the rate of chlorination, we synthesized peptides with 0-3 residues between the lysine and NO₂Tyr residues. These peptides were characterized and shown to have very similar pK_a values around 6.9 and CD spectra analysis showed all peptides were unstructured (**Appendix G**). Each peptide was reacted with HOCl at 37 °C, in 10 mM phosphate buffer at pH 7.4 to calculate the initial rate of ClNO₂Tyr production. The reactions were stopped by introducing excess cysteine, which rapidly reacts with lysine chloramine at a rate of about 10⁸ M⁻¹s⁻¹,^{28, 29} and the resulting peptides were quantitated by HPLC. The initial reaction kinetics were all independent of peptide concentration and first order with respect to HOCl concentration, as seen previously in linear peptides containing histidine chloramine and NO₂Tyr.⁴⁰ The rate constants and pK_a values for the four peptides containing NO₂Tyr used in this study are summarized in **Table 1**.

CD Spectra of Cyclic Peptide Indicates Gramicidin S Homology

The CD spectra of cyclo-P(OH)TKL^DFP(OH)TYL^DF in aqueous phosphate buffer at pH 7.4 was determined at temperature ranging from 5 °C to 65 °C (**Figure 3**). The negative minima around 200 and 220 nm are similar to those exhibited by cyclic gramicidin S analogues, as previously reported.^{44, 49, 50} According to the work of Jelokhani-Niaraki *et al.*, gramicidin S analogues with distorted sheet and turn structures exhibit more negative ellipticities around 200 nm than 220 nm and vary more with temperatures compared to gramicidin S analogues with more stable antiparallel beta-

Table 1. Rate Constants for Chlorination of NO₂Tyr by Lysine Chloramine within a Peptide^a

Peptide Sequence	Residues between Lys and NO ₂ Tyr	Rate Constant (s ⁻¹)	pK _a
Ac-GNK- Y (NO ₂)-AE-NH ₂	0	6.18 ± 0.18 x 10 ⁻⁵	6.8 ± 0.1
Ac-GKN- Y (NO ₂)-AE-NH ₂	1	7.05 ± 0.22 x 10 ⁻⁵	6.8 ± 0.1
Ac- KGN - Y (NO ₂)-AE-NH ₂	2	2.54 ± 0.03 x 10 ⁻⁵	6.9 ± 0.1
Ac- KGNA - Y (NO ₂)-E-NH ₂	3	1.96 ± 0.09 x 10 ⁻⁵	6.9 ± 0.1

^aReactions were performed at 37 °C, pH 7.4 in 10 mM phosphate buffer.

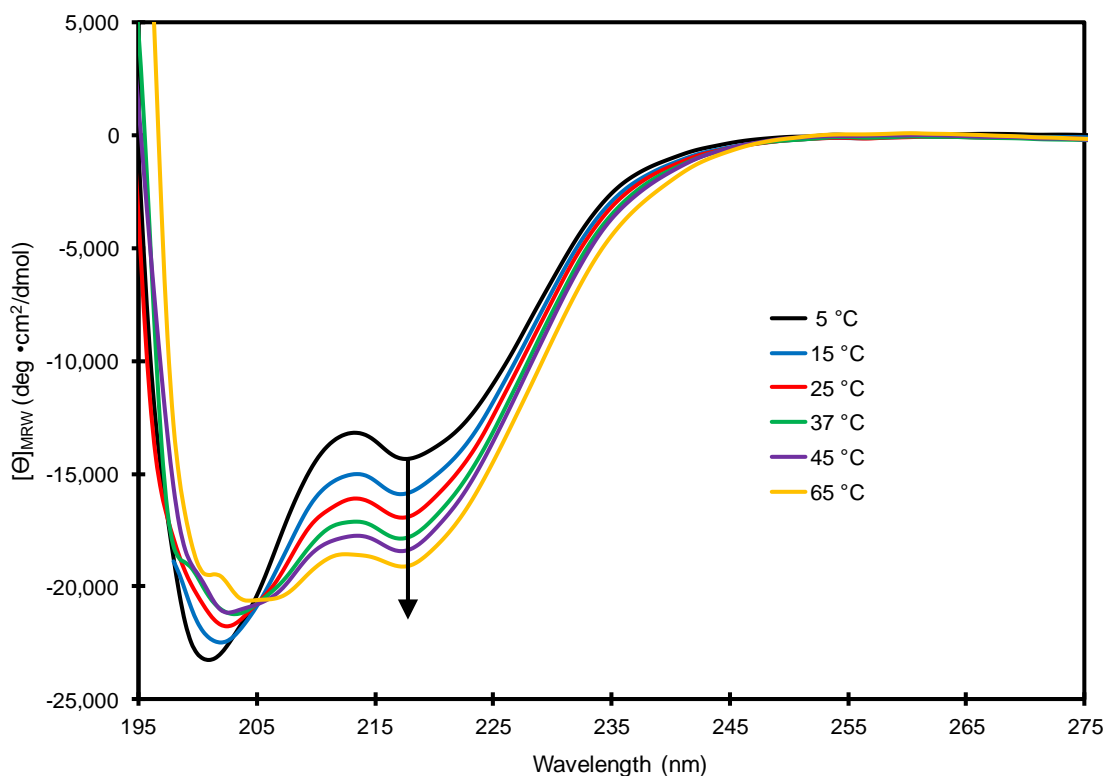


Figure 3: CD Spectra of cyclo-P(OH)TKL^DFP(OH)TYL^DF. The secondary structure of the gramicidin-S analogue, cyclo-P(OH)TKL^DFP(OH)TYL^DF, was analyzed by CD spectroscopy at a concentration of 200 μ M in 200 mM phosphate buffer at pH 7.4. The arrow indicates the change in the CD spectra as the temperature of the sample was increased from 5 °C (bold) to 15, 25, 37, 45, and 65 °C, consecutively. Cooling the temperature back to 5 °C indicated no significant change from the initial measurement (data not shown). The large negative ellipticities around 200 and 220 are similar to those exhibited by cyclic gramicidin S analogues as previously reported.⁴⁹

sheets which have double minima at 205 and 220 nm with comparable ellipticities and have minimal changes in secondary structure with temperature changes.⁴⁹ Our gramicidin S analogue, cyclo-P(OH)TKL^DFP(OH)TYL^DF, shows characteristics more in common with the distorted gramicidin S analogues, though the CD spectra of the peptide at 65 °C has minima at 205 and 220 nm that may be consistent with the antiparallel beta-sheets in gramicidin S.

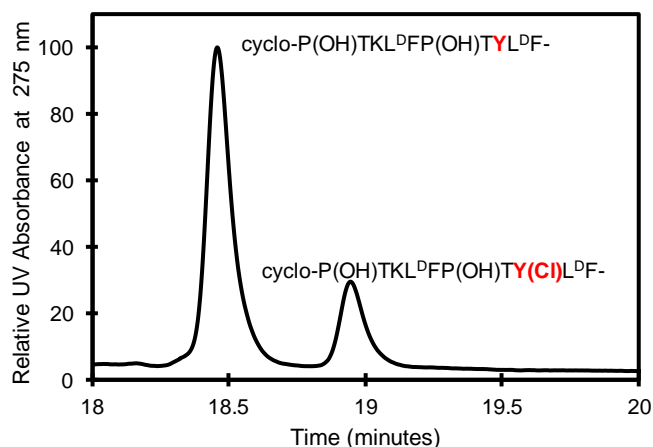
Rate of Tyrosine Chlorination by Lysine Chloramine Increased in Cyclic Peptide

Approximately 75 µM of the cyclic peptide cyclo-P(OH)TKL^DFP(OH)TYL^DF was reacted with 50 µM HOCl in 10 mM phosphate buffer at pH 7.4 at 37 °C. The reaction was stopped by the addition of excess cysteine at varying time points and the tyrosine- and 3ClTyr-containing peptides were quantitated by HPLC (**Figure 4A**). The product peak was confirmed to contain 3ClTyr by its UV-spectra and its mass by LC-MS (data not shown). The loss of tyrosine-containing peptide and growth of 3ClTyr-containing peptide were modelled according to our kinetic scheme in Figure 2 and the rate constant was determined to be $1.02 \times 10^{-3} \text{ s}^{-1}$ (**Figure 4B**).

Discussion

The biomarker 3ClTyr is formed when HOCl, the unique product of MPO, chlorinates the phenol ring of tyrosine. HOCl can also chlorinate amino groups on the side-chains of lysine or histidine. While it has been postulated previously that the chlorination of tyrosine *in vivo* is through chloramine intermediates, the rate of chlorination of free tyrosine by free chloramine is slow.²⁹ Studies have since shown that, in proteins, 3ClTyr formation is favored in tyrosine residues that are located near a lysine

A. HPLC of cyclo-P(OH)TKL^DFP(OH)TYL^DF + HOCl



B. Kinetics of cyclo-P(OH)TKL^DFP(OH)TYL^DF + HOCl

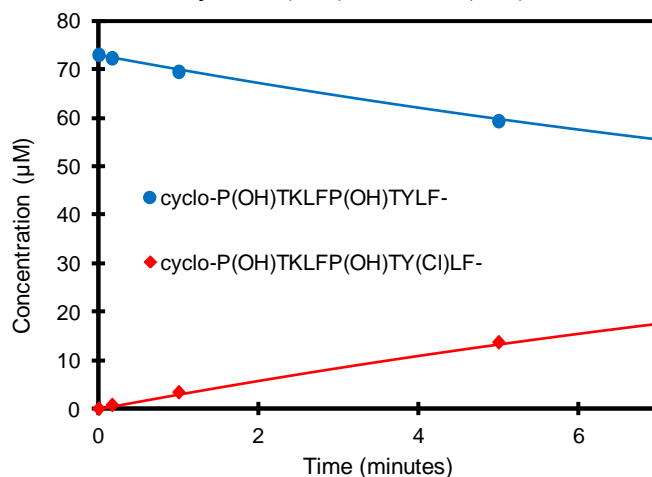


Figure 4: Kinetics of cyclo-P(OH)TKL^DFP(OH)TYL^DF Chlorination by HOCl. 75 μM of the peptide cyclo-P(OH)TKL^DFP(OH)TYL^DF was reacted with 50 μM HOCl at in 10 mM phosphate buffer at pH 7.4 at a temperature of 37 $^{\circ}\text{C}$ and the reaction was stopped by the addition of excess cysteine at set time points. (A) HPLC was used to monitor the decrease of cyclo-P(OH)TKL^DFP(OH)TYL^DF at and the increase of the chlorinated product cyclo-P(OH)TKL^DFP(OH)TY(CI)L^DF. This shows the amount of product formation after 5 minutes. (B) The concentration of each species was quantitated from the UV-HPLC and were modeled to determine the rate constant of chlorination. The solid lines represent the modeled reaction progress with an optimized rate constant. The intramolecular rate of chlorination in this peptide was determined to be $1.02 \times 10^{-3} \text{ s}^{-1}$.

or histidine residue.^{33, 39} The proposed reason for these increased yields of chlorination is that the restriction in freedom between lysine and tyrosine allows the likelihood of their collision to increase and favoring their reaction together (**Figure 2**).^{37, 40} For example, Bergt *et al.* discovered that tyrosine residues in alpha-helices are preferentially chlorinated when in the sequence motif KxxY or KxxxY, where x is a residue that is unreactive with HOCl.³⁸ These studies only looked at the yields of 3ClTyr in simple systems. In order to be able to predict how likely 3ClTyr formation would be in a more complicated system, such as in the human cell where antioxidants are present, we need to determine how the rate of chlorination can change with structure.

To investigate how spacing between lysine and tyrosine can affect the rate of chlorination, we synthesized peptides containing a varying amount of residues between NO₂Tyr and lysine. Chlorination of NO₂Tyr by HOCl or chloramines has been previously determined to follow the same mechanism as chlorination of tyrosine and is approximately three-fold slower,⁴⁰ which allows us to more easily follow the growth of chlorinated product over time. The rate constants of these peptides were determined and are shown in **Table 1**. We see that the sequence motif that had the fastest rate of chlorination was KxY(NO₂), followed by KY(NO₂), KxxY(NO₂), and KxxxY(NO₂), respectively. The fastest rate constant was only approximately 3.5-fold faster than the slowest in these motifs. The effect of sequence on the intramolecular kinetics of chlorination is independent of a defined peptide secondary structure since all peptides examined in this report have negligible helical structure as shown by circular dichroism spectroscopy (**Appendix G**). If we were to extrapolate from this model to the chlorination of tyrosine and formation of 3ClTyr, the fastest rate of chlorination in the

KxY motif would be approximately $2 \times 10^{-4} \text{ s}^{-1}$. Based on previous trends,^{37, 40} this may be enhanced 1000-fold by replacing lysine with histidine, up to a rate of about 0.2 s^{-1} in a HxY motif.

Our determination that the KxY(NO₂) sequence motif has the fastest rate of chlorination seemingly contradicts the previous study that identifies KxxY and KxxxY as having the greatest yields of 3ClTyr.³⁸ We believe that this discrepancy lies in the secondary structure of the peptides being studied. Bergt *et al.* were studying peptide fragments from apolipoprotein A-I which are known to lie in regions with alpha-helix characteristics.⁵¹ In an alpha-helical structure, residues that are spaced with two or three residues between them appear on the same face of the helix.^{52, 53} Our own peptides in this study were completely unstructured and therefore present only the effect of the amino acid sequence on 3ClTyr formation. This suggests that secondary structure may play a significant role in the rate of tyrosine chlorination and warrants further investigation.

To investigate the role of secondary structure on tyrosine chlorination by HOCl-induced lysine chloramine, we attempted to synthesize a peptide that restricted lysine and tyrosine closely in space to increase the reaction kinetics. Our peptide, cyclo-P(OH)TKL^DFP(OH)TYL^DF (**Figure 1**), was based on the structure of the cyclic decapeptide gramicidin S, which is known to have a beta-pleated sheet motif with several hydrogen bonds between the parallel strands.^{41, 42, 54} To verify that our peptide was properly cyclized and had the appropriate beta-sheet characteristics, we characterized the peptide by LC-MS/MS (**Appendix F**) and circular dichroism (**Figure 3**). These studies indicated that our peptide was cyclized correctly and had strong homology to gramicidin S. These characteristics theoretically favor the intramolecular transfer of chlorine from

the lysine chloramine. The kinetic study was performed and the rate constant was determined to be $1.02 \times 10^{-3} \text{ s}^{-1}$ (**Figure 4**). This is about 5-fold faster than the proposed rate of chlorination in a KxY motif we extrapolated above.

In the human cell, there are a plethora of available reactants for HOCl that compete with tyrosine. Reduction of HOCl by antioxidants such as glutathione or the sulfur-containing amino acids methionine and glutathione are rapid with rate constants ranging from 10^5 to $10^8 \text{ M}^{-1}\text{s}^{-1}$.^{28,31} These are significantly faster than the rate of chlorination of tyrosine by HOCl at $71 \text{ M}^{-1}\text{s}^{-1}$.³⁷ However, the reaction of HOCl with histidine or lysine to form chloramines at 10^4 to $10^5 \text{ M}^{-1}\text{s}^{-1}$,^{27,28} is better able to compete with the antioxidants. Furthermore, the accelerated chlorination of tyrosine residues nearby histidine or lysine discovered in this study would further increase the incidence of 3ClTyr formation even in the presence of antioxidants. This evidence suggests that chloramines play a significant role in formation of the biomarker 3ClTyr *in vivo* and that the majority of 3ClTyr formed will be protein-bound and will not exist as free amino acids.

Additionally, the regioselectivity of tyrosine chlorination seen in this study has implications in the formation of the 3ClTyr byproduct Cl₂Tyr. Several studies have shown that concentrations of 3ClTyr in polypeptides will plateau then decrease as increasing amount of HOCl are added.^{33,55,56} The loss of 3ClTyr is accounted for if Cl₂Tyr is concurrently measured.³⁷ Because the chlorination of 3ClTyr by HOCl or chloramines undergoes the same mechanism of chlorination as tyrosine, the same regioselectivity applies. In other words, peptide primary or secondary structures that position chloramine and tyrosine close together and favor 3ClTyr formation will also

favor Cl₂Tyr formation. It is our recommendation that any study that measures 3ClTyr to correlate it to MPO activity must also measure Cl₂Tyr in order to avoid underestimating the degree of inflammation.

References

1. Fang, F. C. (2004) Antimicrobial reactive oxygen and nitrogen species: concepts and controversies. *Nature reviews. Microbiology*, 2, 820-832.
2. Dukan, S., Belkin, S., and Touati, D. (1999) Reactive oxygen species are partially involved in the bacteriocidal action of hypochlorous acid. *Archives of biochemistry and biophysics*, 367, 311-316.
3. Babior, B. M. (2000) Phagocytes and oxidative stress. *The American journal of medicine*, 109, 33-44.
4. Nauseef, W. M. (2007) How human neutrophils kill and degrade microbes: an integrated view. *Immunological reviews*, 219, 88-102.
5. Vieira, O. V., Botelho, R. J., and Grinstein, S. (2002) Phagosome maturation: aging gracefully. *The Biochemical journal*, 366, 689-704.
6. Weiss, S. J. (1989) Tissue destruction by neutrophils. *The New England journal of medicine*, 320, 365-376.
7. King, C. C., Jefferson, M. M., and Thomas, E. L. (1997) Secretion and inactivation of myeloperoxidase by isolated neutrophils. *Journal of leukocyte biology*, 61, 293-302.
8. Bradley, P. P., Christensen, R. D., and Rothstein, G. (1982) Cellular and extracellular myeloperoxidase in pyogenic inflammation. *Blood*, 60, 618-622.
9. Allen, L. A., Beecher, B. R., Lynch, J. T., Rohner, O. V., and Wittine, L. M. (2005) *Helicobacter pylori* disrupts NADPH oxidase targeting in human neutrophils to induce extracellular superoxide release. *Journal of immunology*, 174, 3658-3667.
10. Nauseef, W. M. (2004) Assembly of the phagocyte NADPH oxidase. *Histochemistry and cell biology*, 122, 277-291.
11. Zalavary, S., and Bengtsson, T. (1998) Modulation of the chemotactic peptide- and immunoglobulin G-triggered respiratory burst in human neutrophils by exogenous and endogenous adenosine. *European journal of pharmacology*, 354, 215-225.
12. Stocker, R., and Keaney, J. F., Jr. (2004) Role of oxidative modifications in atherosclerosis. *Physiological reviews*, 84, 1381-1478.
13. Daugherty, A., Dunn, J. L., Rateri, D. L., and Heinecke, J. W. (1994) Myeloperoxidase, a catalyst for lipoprotein oxidation, is expressed in human atherosclerotic lesions. *The Journal of clinical investigation*, 94, 437-444.
14. Sugiyama, S., Okada, Y., Sukhova, G. K., Virmani, R., Heinecke, J. W., and Libby, P. (2001) Macrophage myeloperoxidase regulation by granulocyte macrophage

- colony-stimulating factor in human atherosclerosis and implications in acute coronary syndromes. *The American journal of pathology*, 158, 879-891.
15. Halliwell, B. (2006) Oxidative stress and neurodegeneration: where are we now? *Journal of neurochemistry*, 97, 1634-1658.
 16. Choi, D. K., Pennathur, S., Perier, C., Tieu, K., Teismann, P., Wu, D. C., Jackson-Lewis, V., Vila, M., Vonsattel, J. P., Heinecke, J. W., and Przedborski, S. (2005) Ablation of the inflammatory enzyme myeloperoxidase mitigates features of Parkinson's disease in mice. *The Journal of neuroscience : the official journal of the Society for Neuroscience*, 25, 6594-6600.
 17. Green, P. S., Mendez, A. J., Jacob, J. S., Crowley, J. R., Growdon, W., Hyman, B. T., and Heinecke, J. W. (2004) Neuronal expression of myeloperoxidase is increased in Alzheimer's disease. *Journal of neurochemistry*, 90, 724-733.
 18. Nagra, R. M., Becher, B., Tourtellotte, W. W., Antel, J. P., Gold, D., Paladino, T., Smith, R. A., Nelson, J. R., and Reynolds, W. F. (1997) Immunohistochemical and genetic evidence of myeloperoxidase involvement in multiple sclerosis. *Journal of neuroimmunology*, 78, 97-107.
 19. Komatsu, N., and Takayanagi, H. (2012) Autoimmune arthritis: the interface between the immune system and joints. *Advances in immunology*, 115, 45-71.
 20. Edwards, S. W., Hughes, V., Barlow, J., and Bucknall, R. (1988) Immunological detection of myeloperoxidase in synovial fluid from patients with rheumatoid arthritis. *The Biochemical journal*, 250, 81-85.
 21. Haklar, G., Sayin-Ozveri, E., Yuksel, M., Aktan, A. O., and Yalcin, A. S. (2001) Different kinds of reactive oxygen and nitrogen species were detected in colon and breast tumors. *Cancer letters*, 165, 219-224.
 22. Reuter, S., Gupta, S. C., Chaturvedi, M. M., and Aggarwal, B. B. (2010) Oxidative stress, inflammation, and cancer: how are they linked? *Free radical biology & medicine*, 49, 1603-1616.
 23. Rainis, T., Maor, I., Lanir, A., Shnizer, S., and Lavy, A. (2007) Enhanced oxidative stress and leucocyte activation in neoplastic tissues of the colon. *Digestive diseases and sciences*, 52, 526-530.
 24. Roncucci, L., Mora, E., Mariani, F., Bursi, S., Pezzi, A., Rossi, G., Pedroni, M., Luppi, D., Santoro, L., Monni, S., Manenti, A., Bertani, A., Merighi, A., Benatti, P., Di Gregorio, C., and de Leon, P. M. (2008) Myeloperoxidase-positive cell infiltration in colorectal carcinogenesis as indicator of colorectal cancer risk. *Cancer epidemiology, biomarkers & prevention : a publication of the American Association for Cancer Research, cosponsored by the American Society of Preventive Oncology*, 17, 2291-2297.

25. Whiteman, M., Jenner, A., and Halliwell, B. (1997) Hypochlorous acid-induced base modifications in isolated calf thymus DNA. *Chemical research in toxicology*, 10, 1240-1246.
26. Badouard, C., Masuda, M., Nishino, H., Cadet, J., Favier, A., and Ravanat, J. L. (2005) Detection of chlorinated DNA and RNA nucleosides by HPLC coupled to tandem mass spectrometry as potential biomarkers of inflammation. *Journal of chromatography. B, Analytical technologies in the biomedical and life sciences*, 827, 26-31.
27. Prutz, W. A. (1996) Hypochlorous acid interactions with thiols, nucleotides, DNA, and other biological substrates. *Archives of biochemistry and biophysics*, 332, 110-120.
28. Pattison, D. I., and Davies, M. J. (2001) Absolute rate constants for the reaction of hypochlorous acid with protein side chains and peptide bonds. *Chemical research in toxicology*, 14, 1453-1464.
29. Pattison, D. I., and Davies, M. J. (2005) Kinetic analysis of the role of histidine chloramines in hypochlorous acid mediated protein oxidation. *Biochemistry*, 44, 7378-7387.
30. Hawkins, C. L., Pattison, D. I., and Davies, M. J. (2002) Reaction of protein chloramines with DNA and nucleosides: evidence for the formation of radicals, protein-DNA cross-links and DNA fragmentation. *The Biochemical journal*, 365, 605-615.
31. Peskin, A. V., and Winterbourn, C. C. (2001) Kinetics of the reactions of hypochlorous acid and amino acid chloramines with thiols, methionine, and ascorbate. *Free radical biology & medicine*, 30, 572-579.
32. Sochaski, M. A., Jarabek, A. M., Murphy, J., and Andersen, M. E. (2008) 3-chlorotyrosine and 3,5-dichlorotyrosine as biomarkers of respiratory tract exposure to chlorine gas. *Journal of analytical toxicology*, 32, 99-105.
33. Kang, J. I., Jr., and Neidigh, J. W. (2008) Hypochlorous acid damages histone proteins forming 3-chlorotyrosine and 3,5-dichlorotyrosine. *Chemical research in toxicology*, 21, 1028-1038.
34. Kettle, A. J. (1996) Neutrophils convert tyrosyl residues in albumin to chlorotyrosine. *FEBS letters*, 379, 103-106.
35. Aldridge, R. E., Chan, T., van Dalen, C. J., Senthilmohan, R., Winn, M., Venge, P., Town, G. I., and Kettle, A. J. (2002) Eosinophil peroxidase produces hypobromous acid in the airways of stable asthmatics. *Free radical biology & medicine*, 33, 847-856.

36. Chapman, A. L., Hampton, M. B., Senthilmohan, R., Winterbourn, C. C., and Kettle, A. J. (2002) Chlorination of bacterial and neutrophil proteins during phagocytosis and killing of *Staphylococcus aureus*. *The Journal of biological chemistry*, 277, 9757-9762.
37. Curtis, M. P., Hicks, A. J., and Neidigh, J. W. (2011) Kinetics of 3-chlorotyrosine formation and loss due to hypochlorous acid and chloramines. *Chemical research in toxicology*, 24, 418-428.
38. Bergt, C., Fu, X., Huq, N. P., Kao, J., and Heinecke, J. W. (2004) Lysine residues direct the chlorination of tyrosines in YXXK motifs of apolipoprotein A-I when hypochlorous acid oxidizes high density lipoprotein. *The Journal of biological chemistry*, 279, 7856-7866.
39. Domigan, N. M., Charlton, T. S., Duncan, M. W., Winterbourn, C. C., and Kettle, A. J. (1995) Chlorination of tyrosyl residues in peptides by myeloperoxidase and human neutrophils. *The Journal of biological chemistry*, 270, 16542-16548.
40. Curtis, M. P., and Neidigh, J. W. (2014) Kinetics of 3-nitrotyrosine modification on exposure to hypochlorous acid. *Free radical research*, 48, 1355-1362.
41. Lee, D. L., and Hodges, R. S. (2003) Structure-activity relationships of de novo designed cyclic antimicrobial peptides based on gramicidin S. *Biopolymers*, 71, 28-48.
42. Grotenbreg, G. M., Spalburg, E., de Neeling, A. J., van der Marel, G. A., Overkleeft, H. S., van Boom, J. H., and Overhand, M. (2003) Synthesis and biological evaluation of novel turn-modified gramicidin S analogues. *Bioorganic & medicinal chemistry*, 11, 2835-2841.
43. Peng, Z. H. (1999) Solid phase synthesis and NMR conformational studies on cyclic decapeptide template molecule. *Biopolymers*, 49, 565-574.
44. Wadhvani, P., Afonin, S., Ieronimo, M., Buerck, J., and Ulrich, A. S. (2006) Optimized protocol for synthesis of cyclic gramicidin S: starting amino acid is key to high yield. *The Journal of organic chemistry*, 71, 55-61.
45. Morris, J. C. (1966) Acid Ionization Constant of HOCl from 5 to 35 Degrees. *J. Phys. Chem-US*, 3798-3805.
46. Hunt, S. (1984) Halogenated tyrosine derivatives in invertebrate scleroproteins: isolation and identification. *Methods in enzymology*, 107, 413-438.
47. Riordan, J. F., Sokolovsky, M., and Vallee, B. L. (1967) Environmentally sensitive tyrosyl residues. Nitration with tetranitromethane. *Biochemistry*, 6, 358-361.

48. Motulsky, H. C., A. (2005) Fitting Models to Biological Data Using Linear and Nonlinear Regression. GraphPad Software, San Diego, CA.
49. Jelokhani-Niaraki, M., Prenner, E. J., Kondejewski, L. H., Kay, C. M., McElhaney, R. N., and Hodges, R. S. (2001) Conformation and other biophysical properties of cyclic antimicrobial peptides in aqueous solutions. *The journal of peptide research : official journal of the American Peptide Society*, 58, 293-306.
50. Jelokhani-Niaraki, M., Prenner, E. J., Kay, C. M., McElhaney, R. N., and Hodges, R. S. (2002) Conformation and interaction of the cyclic cationic antimicrobial peptides in lipid bilayers. *The journal of peptide research : official journal of the American Peptide Society*, 60, 23-36.
51. Borhani, D. W., Rogers, D. P., Engler, J. A., and Brouillette, C. G. (1997) Crystal structure of truncated human apolipoprotein A-I suggests a lipid-bound conformation. *Proceedings of the National Academy of Sciences of the United States of America*, 94, 12291-12296.
52. Brouillette, C. G., Anantharamaiah, G. M., Engler, J. A., and Borhani, D. W. (2001) Structural models of human apolipoprotein A-I: a critical analysis and review. *Biochimica et biophysica acta*, 1531, 4-46.
53. Segrest, J. P., Jones, M. K., De Loof, H., Brouillette, C. G., Venkatachalapathi, Y. V., and Anantharamaiah, G. M. (1992) The amphipathic helix in the exchangeable apolipoproteins: a review of secondary structure and function. *Journal of lipid research*, 33, 141-166.
54. Yamada, K., Unno, M., Kobayashi, K., Oku, H., Yamamura, H., Araki, S., Matsumoto, H., Katakai, R., and Kawai, M. (2002) Stereochemistry of protected ornithine side chains of gramicidin S derivatives: X-ray crystal structure of the bis-Boc-tetra-N-methyl derivative of gramicidin S. *Journal of the American Chemical Society*, 124, 12684-12688.
55. Whiteman, M., and Spencer, J. P. (2008) Loss of 3-chlorotyrosine by inflammatory oxidants: implications for the use of 3-chlorotyrosine as a bio-marker in vivo. *Biochemical and biophysical research communications*, 371, 50-53.
56. Drabik, G., and Naskalski, J. W. (2001) Chlorination of N-acetyltyrosine with HOCl, chloramines, and myeloperoxidase-hydrogen peroxide-chloride system. *Acta biochimica Polonica*, 48, 271-275.

CHAPTER FIVE

DISCUSSION

Loss of 3ClTyr and NO₂Tyr by HOCl

3-Chlorotyrosine (3ClTyr) and 3-nitrotyrosine (NO₂Tyr) are useful as markers of myeloperoxidase (MPO) activity in inflammatory tissue because they are stable and readily measurable. Two studies called into question their stability as concentrations of these markers decrease upon exposure to hypochlorous acid (HOCl), the unique product of MPO.^{1,2} If the rate of decrease is sufficiently fast, it would implicate that any previous study measuring these markers potentially underestimated the activity of MPO. In our study we identify the products of 3ClTyr or NO₂Tyr reacting with HOCl and determine the kinetics of chlorination, summarized in **Figure 1**.

The product of HOCl reacting with 3ClTyr is 3,5-dichlorotyrosine (Cl₂Tyr), as reported by several previous studies.³⁻⁶ The rate constant of chlorination of 3ClTyr was determined to be 238 M⁻¹s⁻¹, approximately 3-fold faster than the rate of chlorination of tyrosine at 71 M⁻¹s⁻¹. Although the rate constant is greater, there are several orders of magnitude more tyrosine than 3ClTyr in a cell; studies *in vivo* observe 0-1000 μmol of 3ClTyr per mol of Tyr.⁷⁻¹¹ This would suggest that HOCl reacting with 3ClTyr would be insignificant. However, in the few studies that measured Cl₂Tyr *in vivo*, the amount observed is similar to the amount of 3ClTyr.¹²⁻¹⁴

Pattison *et al.*, who had previously overestimated the rate of tyrosine chlorination by HOCl,¹⁵ have since accepted our determined rate constants.¹⁶ They, and others, have since used these values to argue that previous studies only measuring 3ClTyr without Cl₂Tyr may be underestimating the degree of MPO activity.¹⁶⁻¹⁸ We agree with this

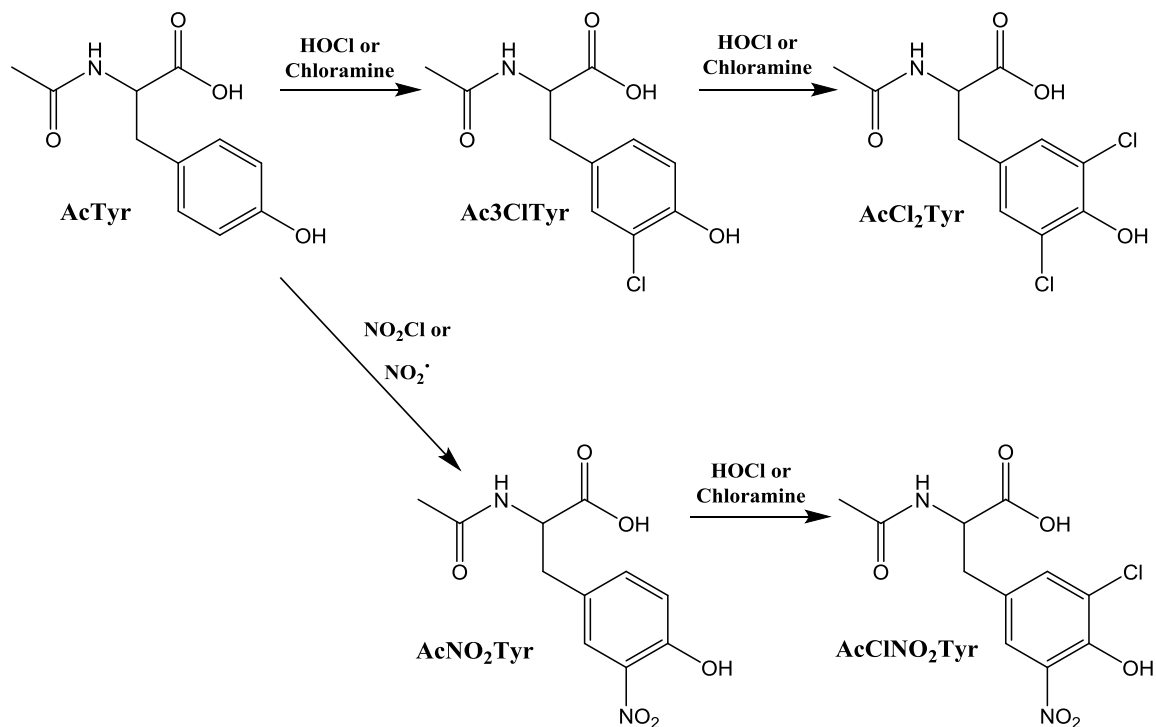


Figure 1: Products of 3ClTyr and NO₂Tyr Reacting with HOCl or Chloramines. N-acetylated analogues of tyrosine were used in these studies to prevent oxidation of the amino-group of tyrosine. Ac3ClTyr, N-acetyl-3-chlorotyrosine; AcCl₂Tyr, N-acetyl-dichlorotyrosine; AcClNO₂Tyr, N-acetyl-3-chloro-5-nitrotyrosine; AcNO₂Tyr, N-acetyl-3-nitrotyrosine; AcTyr, N-acetyltirosine; HOCl, hypochlorous acid; NO₂^{*}, nitrogen dioxide; NO₂Cl, nitryl chloride.

assessment that MPO activity has likely been underestimated. Because of the increased rate of 3ClTyr chlorination by HOCl and the high yields of Cl₂Tyr observed *in vivo*, we recommend that any future studies that measure 3ClTyr should also measure Cl₂Tyr simultaneously.

The product of HOCl reacting with NO₂Tyr is 3-chloro-5-nitrotyrosine (ClNO₂Tyr). The rate of NO₂Tyr chlorination by HOCl was determined to be 24.5 M⁻¹s⁻¹, three-fold slower than the chlorination of tyrosine by HOCl. These slower kinetics, combined with the fact that regioselectivity of tyrosine chlorination differs from that of tyrosine nitration, suggest the ClNO₂Tyr formation is likely to be insignificant *in vivo*.^{6, 19} Furthermore, NO₂Tyr formation is not specific to MPO activity; tyrosine can be nitrated by peroxynitrite, which is formed with superoxide reacts with nitric oxide independent of MPO.²⁰ In fact, one study has determined that tyrosine nitration is predominantly mediated in peroxynitrite-dependent pathways in human cells.²¹ No studies to date have tried to measure ClNO₂Tyr *in vivo* and, based on these results, we do not recommend it as a future study direction.

Chlorination of Tyrosine by Chloramines

Chlorination of tyrosine by HOCl (71 M⁻¹s⁻¹) is much slower than the reduction of HOCl by antioxidants such as glutathione (~10⁸ M⁻¹s⁻¹) or sulfur-containing amino acids like cysteine and methionine (~10⁷ M⁻¹s⁻¹).¹⁵ As such, it has been argued that any 3ClTyr measured *in vivo* only occurs after the oxidation of all available antioxidants.²² One proposed alternative explanation is that HOCl-induced chloramines, such as histidine or lysine chloramine, are intermediates in the chlorination of tyrosine. This is evidenced by

the preferential chlorination of tyrosine on proteins that are nearby histidine or lysine residues.^{5, 6, 23}

The rates of tyrosine chlorination by histidine and lysine chloramines as free amino acids ($3 \text{ M}^{-1}\text{s}^{-1}$ and $0.004 \text{ M}^{-1}\text{s}^{-1}$, respectively) determined in this study are significantly slower than direct chlorination of tyrosine by HOCl. This alone cannot explain the preferential chlorination of tyrosine near these residues in peptide. However, when tyrosine and lysine are constrained in close proximity within a peptide, the rate of chlorination increases significantly. Our study of chlorination of the peptide Ac-KGNYAE-NH₂ by HOCl showed an initial velocity (V_0) 600-fold greater than an analogous amino acid mixture (see **Chapter 2, Figure 7**). This is likely due to the reduced degrees of freedom of the tyrosine and lysine side-chains when they are confined to the same peptide. The intermolecular kinetics of tyrosine analogue chlorination by HOCl or chloramines are summarized in **Table 1**.

Additionally, lysine chloramine may protect chlorination potential from reduction by antioxidants such as glutathione. The fast reaction of HOCl to form lysine chloramine ($\sim 10^5 \text{ M}^{-1}\text{s}^{-1}$) better competes with the antioxidant glutathione ($\sim 10^8 \text{ M}^{-1}\text{s}^{-1}$) than the direct chlorination of tyrosine analogues ($\sim 10^2 \text{ M}^{-1}\text{s}^{-1}$). The lysine chloramine would then be able to undergo intramolecular chlorination of tyrosine prior to reduction by glutathione, provided the intramolecular kinetics are sufficiently fast.^{24, 25} **Figure 2** provides a schematic highlighting the relevant kinetics.

Table 1: Summary of Tyrosine Analogue Chlorination as Free Amino Acids. All reactions were performed at 37 °C in 100 mM phosphate buffer at pH 7.4.

Chlorinating Species	AcTyr (M⁻¹s⁻¹)	Ac3ClTyr (M⁻¹s⁻¹)	AcCl₂Tyr (M⁻¹s⁻¹)	AcNO₂Tyr (M⁻¹s⁻¹)
HOCl	71 ± 8	238 ± 27	32 ± 6	24.5 ± 1.2
HisCl	3.0 ± 0.3	10.4 ± 1.0	1.7 ± 0.2	1.1 ± 0.2
LysCl	0.004 ± 0.003	0.008 ± 0.002	0.003 ± 0.002	ND ^a

^aNo significant amount of product was detected after two hours of reaction

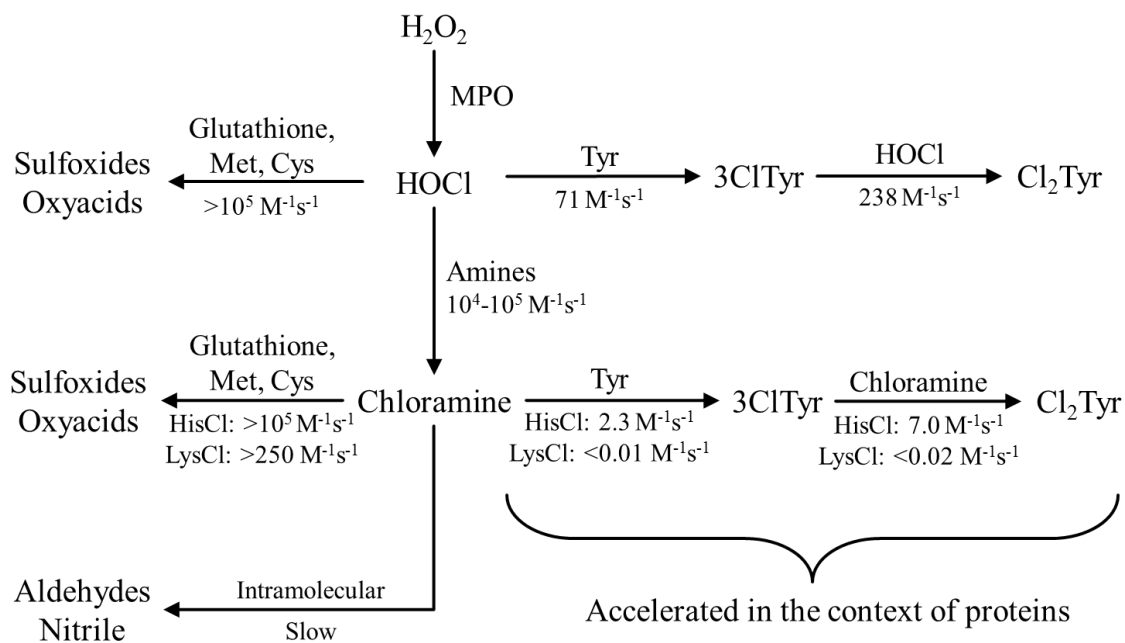


Figure 2: Summary of Reactions by HOCl that Compete with 3ClTyr Formation. All rate constants are for individual amino acid analogues. The rate constants for HOCl or chloramines reacting with sulfur containing amino acids or glutathione and primary amines reacting with HOCl are published elsewhere.^{15, 26} The remaining rate constants are from Table 1.

Effect of Peptide Primary Structure on Tyrosine Chlorination by HOCl

It has been determined previously that tyrosine is preferentially chlorinated by HOCl if it is on a peptide and near a lysine or histidine residue.^{5, 6} Bergt *et al.* in particular created several peptide fragments in an alpha-helical arrangement that separated tyrosine from lysine by varying residues.⁶ They saw that peptides with a KxxY or KxxxY motif (where x is a residue unreactive with HOCl) showed the greatest yields of 3ClTyr, though the kinetics were not determined. In addition, their observation that tyrosine at residue 192 on apolipoprotein A-I was preferentially chlorinated was attributed to a KxxY motif, which ignored the fact that histidine on residue 193 also contributes to 3ClTyr formation.²³

Our study set out to determine what effect changing the spacing between tyrosine and lysine had on the rate of chlorination in a simple, unstructured peptide. Using peptides with a varying number of residues between lysine and NO₂Y (NO₂Y rather than tyrosine was used because its slower rate of chlorination and unique UV-spectra assisted with analysis), we determined the rate constants of tyrosine chlorination. The effect of lysine positioning on the rate of NO₂Y chlorination was such that KxY > KY > KxxY > KxxxY. The rates of the four peptides studied varied minimally, with the fastest at $7 \times 10^{-5} \text{ s}^{-1}$ being only 3.5-fold faster than the slowest. Additionally, replacing a lysine residue with histidine accelerated the chlorination kinetics 1000-fold more, suggesting that histidine chloramine is the more likely cause of 3ClTyr formation at residue 192 of apolipoprotein A-I. **Table 2** summarizes the kinetics of tyrosine chlorination in the peptides we synthesized in these studies.

Table 2: Summary of Tyrosine Analogue Chlorination in Peptides. All reactions were performed at 37 °C in 10 mM phosphate buffer at pH 7.4.

Peptide Sequence	Rate Constant (s ⁻¹)
Ac- H GNY(NO ₂)AE-NH ₂	2.60 ± 0.53 x 10 ⁻²
Ac-GN K Y(NO ₂)AE-NH ₂	6.18 ± 0.18 x 10 ⁻⁵
Ac-G K NY(NO ₂)AE-NH ₂	7.05 ± 0.22 x 10 ⁻⁵
Ac- K GNY(NO ₂)AE-NH ₂	2.54 ± 0.03 x 10 ⁻⁵
Ac- K GN A Y(NO ₂)E-NH ₂	1.96 ± 0.09 x 10 ⁻⁵
Ac- K GN A YAE-NH ₂	2.38 ± 0.07 x 10 ⁻⁴
cyclo-P(OH)TKL ^D FP(OH)TYL ^D F-	1.02 x 10 ⁻³

Our results demonstrating that the KxY motif is faster than the KxxY or KxxxY motifs may appear to contradict what was reported by Bergt *et al.*⁶ However, their study utilized peptide fragments that were alpha-helical analogues and had even greater alpha-helical characteristic while lipid-associated, increasing ClTyr yields. In an alpha helix, the lysine residues would appear on the same face as the tyrosine residues when spaced three or four residues away. Additionally, the structure of the apolipoprotein A-I fragment they synthesized had its crystal structure analyzed previously, demonstrating that the tyrosine and lysine alpha-carbons are only 4.5 Å from each other.^{27, 28} These results suggest that the secondary structure of a protein may be more important to the chloramine-induced formation of 3ClTyr than the primary structure, and warranted further study.

Effect of Peptide Secondary Structure on Tyrosine Chlorination by HOCl

Our final study was to determine how the secondary structure could affect the rate of tyrosine chlorination by HOCl-induced chloramines. Ideally, the structure would place a chloramine near the tyrosine phenol ring and constrict the degrees of freedom to further facilitate chlorination. We synthesized the peptide cyclo-P(OH)TKL^DFP(OH)TYL^DF which is based on gramicidin S, a short peptide known to have a beta-pleated sheet motif.²⁹ Beta-turns in this peptide are induced by Pro-^DPhe bonds, with the hydrogen bonds between the anti-parallel strands further stabilizing the structure.^{30, 31} We modified the structure to include lysine and tyrosine on opposite strands, as well as using hydroxyproline and threonine to add hydrophilic characteristics to the peptide, allowing us to perform kinetics under the same conditions as our previous studies. CD spectroscopy of

this peptide indicated that it was homologous to other gramicidin S analogues and has slightly disorganized beta-sheet structure and beta turns as opposed to the anti-parallel beta-sheets seen in native gramicidin S (see **Chapter 4, Figure 3**).

We determined the rate of tyrosine chlorination by lysine chloramine in cyclo-P(OH)TKL^DFP(OH)TYL^DF to be $1 \times 10^{-3} \text{ s}^{-1}$. This is approximately 5-fold faster than the rate of tyrosine chlorination by lysine chloramine in the simple unstructured peptide Ac-KGNYAE-NH₂. While we expected a more significant increase in the rate of chlorination, this does support the hypothesis that secondary structure can facilitate an increased rate of chlorination of tyrosine by lysine chloramine. Additionally, if we extrapolate the difference between AcTyr chlorination by lysine chloramine versus histidine chloramine, we expect the intramolecular rate of tyrosine chlorination by histidine in a similar cyclic peptide to be 1000-fold greater at 1 s^{-1} . Our kinetic studies support the claims of other researchers that propose that formation of 3ClTyr *in vivo* is predominantly facilitated by intramolecular chlorination by chloramines in a peptide.^{5, 6}
³² Furthermore, the regioselectivity of specific tyrosine residues in a protein would favor further chlorination of the same tyrosine residue, suggesting that measurement of protein-bound Cl₂Tyr may be a relevant marker of inflammation.

Overall Trends in the Kinetics of Chlorination of Tyrosine Analogues

Table 1 provides a summary of the chlorination of tyrosine analogues from Chapters 2 and 3. The rate of direct chlorination of tyrosine is approximately 22-fold greater than by histidine chloramine and 21,000-fold greater than by lysine chloramine, averaged across all tyrosine analogues. Chlorination of AcTyr across all chlorinating

species is approximately 3.4-fold slower than Ac3ClTyr chlorination, 2-fold faster than AcCl₂Tyr oxidation, and 2.8-fold faster than AcNO₂Tyr chlorination.

In the context of peptides, this trend between the rate of chlorination by histidine chloramine and lysine chloramine holds true. Comparing the rate of chlorination of the peptides Ac-HGNY(NO₂)AE-NH₂ and Ac-KGNY(NO₂)AE-NH₂ (**Table 2**), there is an approximately 1000-fold difference between the rate of chlorination. This is similar to the difference between the rates of chlorination of AcTyr, Ac3ClTyr, and AcCl₂Tyr by histidine and lysine chloramines.

This same trend does not hold true for the difference between tyrosine and NO₂Tyr chlorination in lysine-containing peptides. Comparing the rate of chlorination in Ac-KGNYAE-NH₂ and Ac-KGNY(NO₂)AE-NH₂ (**Table 2**) demonstrates that tyrosine is chlorinated about 9-fold faster than NO₂Tyr. However, as free amino acids, AcTyr is chlorinated about 3-fold faster. This discrepancy has several potential explanations. First, our peptide reactions used a lower concentration of phosphate buffer than our amino acid reactions (10 mM and 100 mM, respectively). If the pH were slightly closer to 8.5, this would cause an increase in the rate of tyrosine chlorination and a decrease in the chlorination of NO₂Tyr (see **Chapter 2, Figure 6** and **Appendix E**). Second, the steric effect of the nitro-group on NO₂Tyr may affect the secondary structure of the linear peptide in ways that unmodified tyrosine would not, such that lysine chloramine had easier access to tyrosine to facilitate chlorination. Another possible explanation is variance due to human error.

The third explanation, human error, is the most likely. It may be that we did not perform the kinetic study of Ac-KGNYAE-NH₂ carefully enough. It was the first peptide

we studied and was before we learned that one must be rapidly mixing the reaction vessels with stir bars to uniformly distribute HOCl and prevent HOCl from being present in excess, both of which lead to HOCl chlorinating tyrosine in a bimolecular reaction. Support of this occurring is in the presence of peptide containing Cl₂Tyr (see **Chapter 2, Figure 7**) which should be impossible if only an intramolecular reaction between lysine chloramine and tyrosine occurred. Before any comparisons can be made in this regard, the peptide Ac-KGNYAE-NH₂ would need to be resynthesized and the kinetic study repeated.

Future Directions

First, to prepare our latest study for publication, we intend to further characterize the secondary structure of the cyclic peptide by measuring changes in chemical shift deviation by NMR versus temperature.³³ Further controls may also be added to the study, such as determining kinetics of unstructured, linear analogues of our cyclic peptides. It would also be of interest to determine whether a histidine analogue of our cyclic peptide truly exhibits the 1000-fold increase in kinetics that we expect.

Our next goal would be to establish the link between HOCl concentration and the amount of 3ClTyr and Cl₂Tyr in human cells. Currently, there are no accurate estimates of the amount of HOCl in inflamed tissue, though estimates have been made based on the capability of neutrophils to generate HOCl over time.³⁴⁻³⁶ By exposing human cells to HOCl and quantitating the amount of 3ClTyr and Cl₂Tyr per mol of tyrosine using previously established methods,³⁷ we can begin to better correlate these markers to MPO activity. Additionally, due to the rapid reduction of reactive species in the cytoplasm, it is

thought that significant quantities of HOCl have difficulty making it to the nucleus.³⁸ It would be informative to measure 3ClTyr and Cl₂Tyr quantities in histones of cells exposed to HOCl and compare those to overall levels.

Lastly, we would want to take the methods we've developed in the previous studies and measure the biomarkers 3ClTyr and Cl₂Tyr in human samples. We have already discussed with clinicians and other researchers the possibility of analyzing serum samples of patients with sepsis or of hypoxic newborns to determine the level of MPO activity through 3ClTyr and Cl₂Tyr measurement. These can be compared to the current clinical standards of inflammation such as the erythrocyte sedimentation rate and C-reactive protein, both of which can have limited sensitivity at early stages of disease and are nonspecific.^{39, 40} The measurement of 3ClTyr in conjunction with Cl₂Tyr within proteins of the serum may provide us a means of detecting inflammatory states earlier than with the current clinical methods and perhaps provide insight into the mechanism of pathogenesis. With LC-MS detection of chlorinated tyrosine becoming as sensitive as GC-MS methods^{17, 41} and the growth of LC-MS/MS machines in hospitals capable of these measurements,⁴² we believe that 3ClTyr and Cl₂Tyr are promising markers of inflammation for the clinical setting.

References

1. Whiteman, M., and Spencer, J. P. (2008) Loss of 3-chlorotyrosine by inflammatory oxidants: implications for the use of 3-chlorotyrosine as a bio-marker in vivo. *Biochemical and biophysical research communications*, 371, 50-53.
2. Whiteman, M., and Halliwell, B. (1999) Loss of 3-nitrotyrosine on exposure to hypochlorous acid: implications for the use of 3-nitrotyrosine as a bio-marker in vivo. *Biochemical and biophysical research communications*, 258, 168-172.
3. Chapman, A. L., Senthilmohan, R., Winterbourn, C. C., and Kettle, A. J. (2000) Comparison of mono- and dichlorinated tyrosines with carbonyls for detection of hypochlorous acid modified proteins. *Archives of biochemistry and biophysics*, 377, 95-100.
4. Fu, S., Wang, H., Davies, M., and Dean, R. (2000) Reactions of hypochlorous acid with tyrosine and peptidyl-tyrosyl residues give dichlorinated and aldehydic products in addition to 3-chlorotyrosine. *The Journal of biological chemistry*, 275, 10851-10858.
5. Kang, J. I., Jr., and Neidigh, J. W. (2008) Hypochlorous acid damages histone proteins forming 3-chlorotyrosine and 3,5-dichlorotyrosine. *Chemical research in toxicology*, 21, 1028-1038.
6. Bergt, C., Fu, X., Huq, N. P., Kao, J., and Heinecke, J. W. (2004) Lysine residues direct the chlorination of tyrosines in YXXK motifs of apolipoprotein A-I when hypochlorous acid oxidizes high density lipoprotein. *The Journal of biological chemistry*, 279, 7856-7866.
7. Bergt, C., Pennathur, S., Fu, X., Byun, J., O'Brien, K., McDonald, T. O., Singh, P., Anantharamaiah, G. M., Chait, A., Brunzell, J., Geary, R. L., Oram, J. F., and Heinecke, J. W. (2004) The myeloperoxidase product hypochlorous acid oxidizes HDL in the human artery wall and impairs ABCA1-dependent cholesterol transport. *Proceedings of the National Academy of Sciences of the United States of America*, 101, 13032-13037.
8. Buss, I. H., Senthilmohan, R., Darlow, B. A., Mogridge, N., Kettle, A. J., and Winterbourn, C. C. (2003) 3-Chlorotyrosine as a marker of protein damage by myeloperoxidase in tracheal aspirates from preterm infants: association with adverse respiratory outcome. *Pediatric research*, 53, 455-462.
9. Citardi, M. J., Song, W., Batra, P. S., Lanza, D. C., and Hazen, S. L. (2006) Characterization of oxidative pathways in chronic rhinosinusitis and sinonasal polyposis. *American journal of rhinology*, 20, 353-359.

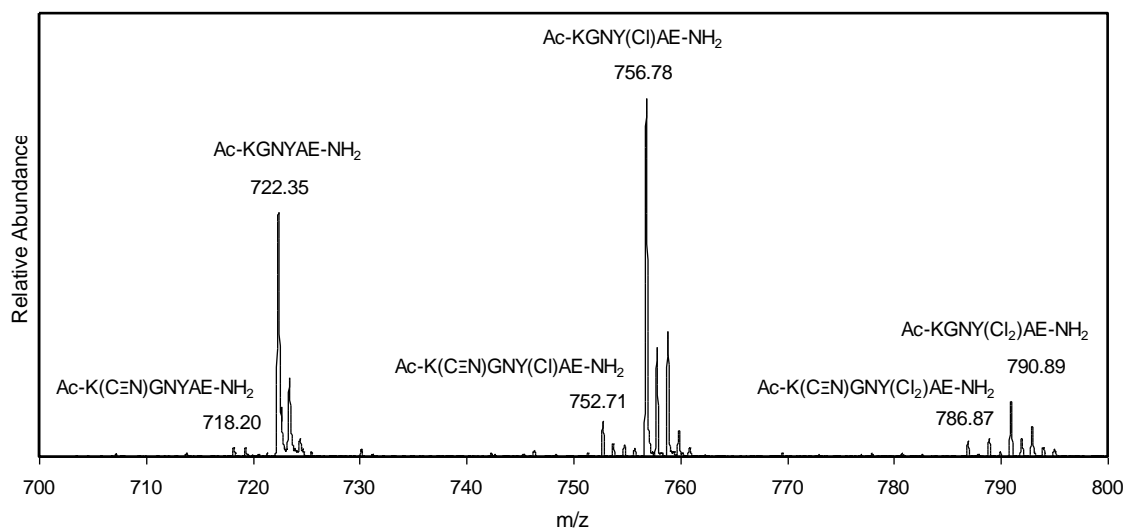
10. Himmelfarb, J., McMenamin, M. E., Loseto, G., and Heinecke, J. W. (2001) Myeloperoxidase-catalyzed 3-chlorotyrosine formation in dialysis patients. *Free radical biology & medicine*, 31, 1163-1169.
11. Shao, B., Oda, M. N., Oram, J. F., and Heinecke, J. W. (2010) Myeloperoxidase: an oxidative pathway for generating dysfunctional high-density lipoprotein. *Chemical research in toxicology*, 23, 447-454.
12. Sochaski, M. A., Jarabek, A. M., Murphy, J., and Andersen, M. E. (2008) 3-chlorotyrosine and 3,5-dichlorotyrosine as biomarkers of respiratory tract exposure to chlorine gas. *Journal of analytical toxicology*, 32, 99-105.
13. Chapman, A. L., Hampton, M. B., Senthilmohan, R., Winterbourn, C. C., and Kettle, A. J. (2002) Chlorination of bacterial and neutrophil proteins during phagocytosis and killing of *Staphylococcus aureus*. *The Journal of biological chemistry*, 277, 9757-9762.
14. Aldridge, R. E., Chan, T., van Dalen, C. J., Senthilmohan, R., Winn, M., Venge, P., Town, G. I., and Kettle, A. J. (2002) Eosinophil peroxidase produces hypobromous acid in the airways of stable asthmatics. *Free radical biology & medicine*, 33, 847-856.
15. Pattison, D. I., and Davies, M. J. (2001) Absolute rate constants for the reaction of hypochlorous acid with protein side chains and peptide bonds. *Chemical research in toxicology*, 14, 1453-1464.
16. Pattison, D. I., Davies, M. J., and Hawkins, C. L. (2012) Reactions and reactivity of myeloperoxidase-derived oxidants: differential biological effects of hypochlorous and hypothiocyanous acids. *Free radical research*, 46, 975-995.
17. Kettle, A. J., Albrett, A. M., Chapman, A. L., Dickerhof, N., Forbes, L. V., Khalilova, I., and Turner, R. (2014) Measuring chlorine bleach in biology and medicine. *Biochimica et biophysica acta*, 1840, 781-793.
18. Maghzal, G. J., Cergol, K. M., Shengule, S. R., Suarna, C., Newington, D., Kettle, A. J., Payne, R. J., and Stocker, R. (2014) Assessment of myeloperoxidase activity by the conversion of hydroethidine to 2-chloroethidium. *The Journal of biological chemistry*, 289, 5580-5595.
19. Souza, J. M., Daikhin, E., Yudkoff, M., Raman, C. S., and Ischiropoulos, H. (1999) Factors determining the selectivity of protein tyrosine nitration. *Archives of biochemistry and biophysics*, 371, 169-178.
20. Pietraforte, D., Salzano, A. M., Marino, G., and Minetti, M. (2003) Peroxynitrite-dependent modifications of tyrosine residues in hemoglobin. Formation of tyrosyl radical(s) and 3-nitrotyrosine. *Amino acids*, 25, 341-350.

21. Galinanes, M., and Matata, B. M. (2002) Protein nitration is predominantly mediated by a peroxynitrite-dependent pathway in cultured human leucocytes. *The Biochemical journal*, 367, 467-473.
22. Peskin, A. V., and Winterbourn, C. C. (2001) Kinetics of the reactions of hypochlorous acid and amino acid chloramines with thiols, methionine, and ascorbate. *Free radical biology & medicine*, 30, 572-579.
23. Pattison, D. I., and Davies, M. J. (2005) Kinetic analysis of the role of histidine chloramines in hypochlorous acid mediated protein oxidation. *Biochemistry*, 44, 7378-7387.
24. Winterbourn, C. C., and Kettle, A. J. (2000) Biomarkers of myeloperoxidase-derived hypochlorous acid. *Free radical biology & medicine*, 29, 403-409.
25. Pattison, D. I., Hawkins, C. L., and Davies, M. J. (2003) Hypochlorous acid-mediated oxidation of lipid components and antioxidants present in low-density lipoproteins: absolute rate constants, product analysis, and computational modeling. *Chemical research in toxicology*, 16, 439-449.
26. Prutz, W. A. (1996) Hypochlorous acid interactions with thiols, nucleotides, DNA, and other biological substrates. *Archives of biochemistry and biophysics*, 332, 110-120.
27. Segrest, J. P., Jones, M. K., De Loof, H., Brouillette, C. G., Venkatachalapathi, Y. V., and Anantharamaiah, G. M. (1992) The amphipathic helix in the exchangeable apolipoproteins: a review of secondary structure and function. *Journal of lipid research*, 33, 141-166.
28. Borhani, D. W., Rogers, D. P., Engler, J. A., and Brouillette, C. G. (1997) Crystal structure of truncated human apolipoprotein A-I suggests a lipid-bound conformation. *Proceedings of the National Academy of Sciences of the United States of America*, 94, 12291-12296.
29. Lee, D. L., and Hodges, R. S. (2003) Structure-activity relationships of de novo designed cyclic antimicrobial peptides based on gramicidin S. *Biopolymers*, 71, 28-48.
30. Grotenbreg, G. M., Spalburg, E., de Neeling, A. J., van der Marel, G. A., Overkleeft, H. S., van Boom, J. H., and Overhand, M. (2003) Synthesis and biological evaluation of novel turn-modified gramicidin S analogues. *Bioorganic & medicinal chemistry*, 11, 2835-2841.
31. Peng, Z. H. (1999) Solid phase synthesis and NMR conformational studies on cyclic decapeptide template molecule. *Biopolymers*, 49, 565-574.

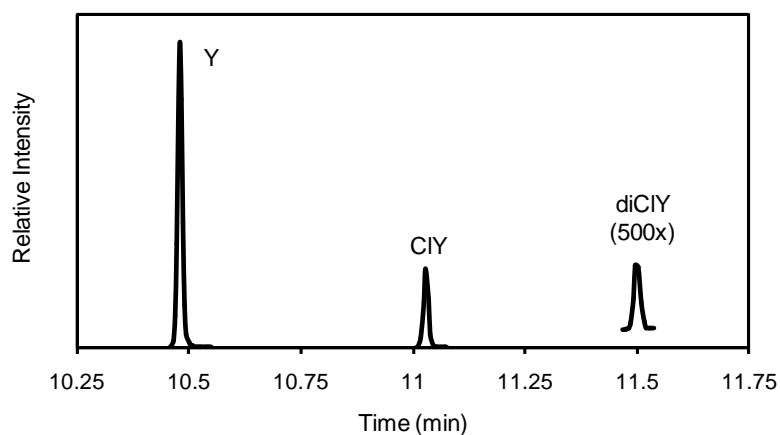
32. Domigan, N. M., Charlton, T. S., Duncan, M. W., Winterbourn, C. C., and Kettle, A. J. (1995) Chlorination of tyrosyl residues in peptides by myeloperoxidase and human neutrophils. *The Journal of biological chemistry*, 270, 16542-16548.
33. Neidigh, J. W., Fesinmeyer, R. M., Prickett, K. S., and Andersen, N. H. (2001) Exendin-4 and glucagon-like-peptide-1: NMR structural comparisons in the solution and micelle-associated states. *Biochemistry*, 40, 13188-13200.
34. Babior, B. M. (2000) Phagocytes and oxidative stress. *The American journal of medicine*, 109, 33-44.
35. King, C. C., Jefferson, M. M., and Thomas, E. L. (1997) Secretion and inactivation of myeloperoxidase by isolated neutrophils. *Journal of leukocyte biology*, 61, 293-302.
36. Test, S. T., and Weiss, S. J. (1986) The generation of utilization of chlorinated oxidants by human neutrophils. *Advances in Free Radical Biology & Medicine*, 2, 91-116.
37. Hazen, S. L., Crowley, J. R., Mueller, D. M., and Heinecke, J. W. (1997) Mass spectrometric quantification of 3-chlorotyrosine in human tissues with attomole sensitivity: a sensitive and specific marker for myeloperoxidase-catalyzed chlorination at sites of inflammation. *Free radical biology & medicine*, 23, 909-916.
38. Suquet, C., Warren, J. J., Seth, N., and Hurst, J. K. (2010) Comparative study of HOCl-inflicted damage to bacterial DNA *ex vivo* and within cells. *Archives of biochemistry and biophysics*, 493, 135-142.
39. Mussap, M. (2012) Laboratory medicine in neonatal sepsis and inflammation. *The journal of maternal-fetal & neonatal medicine : the official journal of the European Association of Perinatal Medicine, the Federation of Asia and Oceania Perinatal Societies, the International Society of Perinatal Obstet*, 25 Suppl 4, 32-34.
40. Batlivala, S. P. (2009) Focus on diagnosis: the erythrocyte sedimentation rate and the C-reactive protein test. *Pediatrics in review / American Academy of Pediatrics*, 30, 72-74.
41. Zheng, L., Nukuna, B., Brennan, M. L., Sun, M., Goormastic, M., Settle, M., Schmitt, D., Fu, X., Thomson, L., Fox, P. L., Ischiropoulos, H., Smith, J. D., Kinter, M., and Hazen, S. L. (2004) Apolipoprotein A-I is a selective target for myeloperoxidase-catalyzed oxidation and functional impairment in subjects with cardiovascular disease. *The Journal of clinical investigation*, 114, 529-541.
42. Grebe, S. K., and Singh, R. J. (2011) LC-MS/MS in the Clinical Laboratory - Where to From Here? *The Clinical biochemist. Reviews / Australian Association of Clinical Biochemists*, 32, 5-31.

APPENDICES

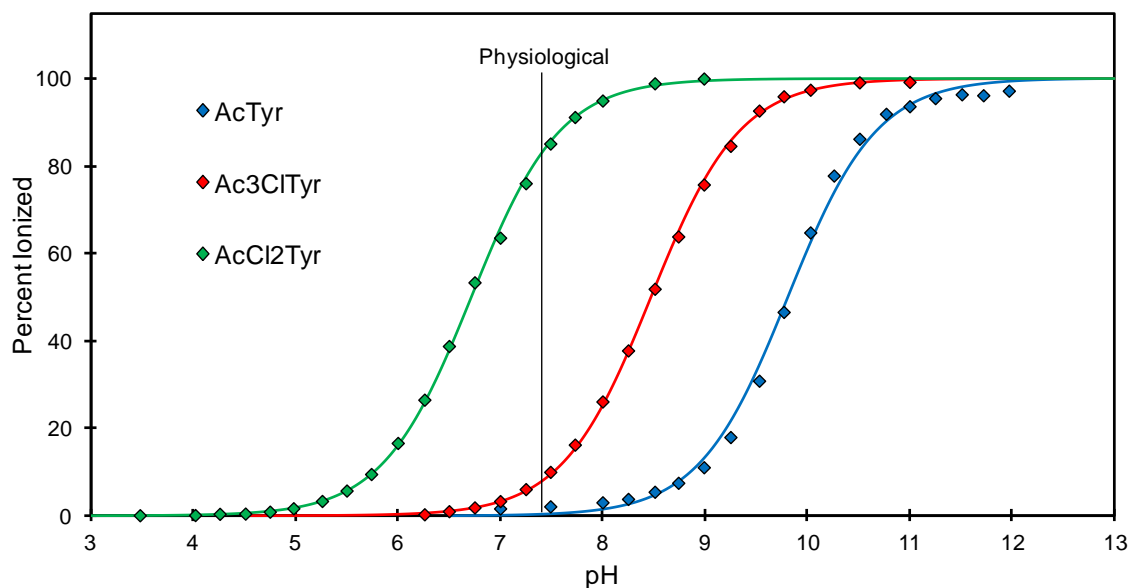
A. Characterization of Ac-KGNYAE-NH ₂ Chlorination Products by MALDI-TOF.....	130
B. GC-MS of Tyr, 3ClTyr, and Cl ₂ Tyr.....	131
C. Chlorination of Tyrosine Lowers the pK _a Value of the Phenol Hydroxyl	132
D. Chlorination of AcNO ₂ Tyr Lowers the pK _a Value of the Phenol Hydroxyl	133
E. pH-Dependence of the Apparent Rate Constant of AcNO ₂ Tyr Chlorination by HOCl.....	134
F. Confirmation of Cyclic Structure of cyclo-P(OH)TKL ^D FP(OH)TYL ^D F- by MS/MS	135
G. CD Spectra of Peptides Containing Lysine and NO ₂ Y	136



Appendix A: Characterization of Ac-KGNYAE-NH₂ Chlorination Products by MALDI-TOF. MALDI-TOF was used to identify products of the reaction of Ac-KGNYAE-NH₂ with HOCl. MALDI samples were prepared using the dried-droplet method and 2,5-dihydroxybenzoic acid as the matrix. Samples were analyzed in negative-ion reflectron mode by a Bruker Autoflex MALDI-TOF. The mass-to-charge ratio was calibrated using a commercially-available peptide solution containing angiotensin I and II, substance P, bombesin, clipped ACTH residues 1-17 and 18-39, and somatostatin. Due to the weak signal of these standards in negative-ion mode, we also added the previously characterized peptide Ac-KGNYAE-NH₂ (MH⁻ ion at 722.3468 m/z) to the standard mix to achieve a more accurate standard curve. This shows the final products when 260 μM HOCl reacts with 125 μM Ac-KGNYAE-NH₂ at 37 °C for 1 hr. Peaks at 722.4, 756.8, and 790.9 m/z correspond to the MH⁻ ions of the peptide containing tyrosine, 3-chlorotyrosine, and 3,5-dichlorotyrosine, respectively. Peaks at 718.2, 752.7, and 786.9 m/z correspond to the lysine nitrile form of the peptide with tyrosine, 3-chlorotyrosine, and 3,5-dichlorotyrosine, respectively.

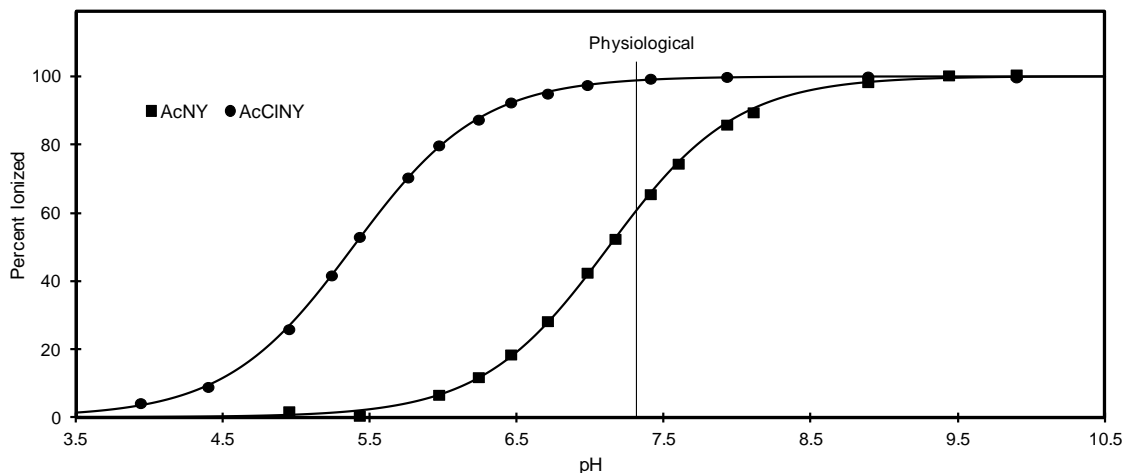


Appendix B: GC-MS of Tyr, 3ClTyr, and Cl₂Tyr. Approximately 100 μM of the peptide Ac-KGN₃YAE-NH₂ was reacted with 50 μM of HOCl at 37 °C and quenched with methionine after one hour. An internal standard of isotope-labelled labeled [¹³C₉]Tyr, [¹³C₆]3ClTyr, and [¹³C₉]Cl₂Tyr was added and the samples dried down. The peptide was then hydrolyzed with HBr and phenol at 120 °C overnight before being dried down again. The residues were then derivatized with propanol and heptafluorobutyric anhydride, as previously described (Hazen *et al.*, Free Radic Biol Med, 1997. 23(6): 909-916). The resulting *n*-propyl, per-heptafluorobutyric derivatives of Tyr, 3ClTyr, and Cl₂Tyr were detected using an Agilent 6890N GC/5973N MSD instrument in negative chemical ionization mode, as seen in the above figure. Quantitation of the tyrosine residues was achieved by creating a standard curve based on the ratios of 417/426, 451/457, and 683/692 *m/z* for tyrosine, 3ClTyr, and Cl₂Tyr, respectively. The amount of analyte detected using this GC-MS method was not significantly different from the amount of analyte calculated using our HPLC method described in Chapter 2.

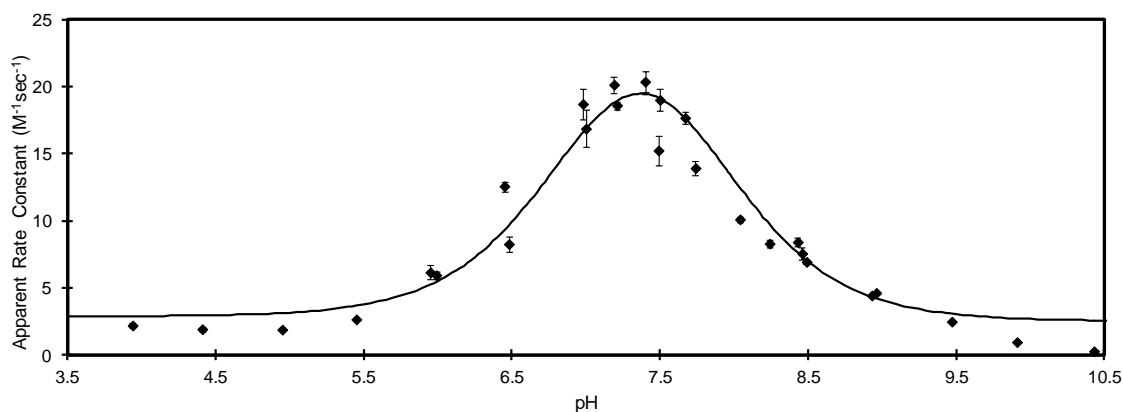


Appendix C: Chlorination of Tyrosine Lowers the pK_a Value of the Phenol Hydroxyl.

The curves plot the following function: percent ionized = $(100 \times 10^{(\text{pH} - \text{pK}_a)}) / (1 + 10^{(\text{pH} - \text{pK}_a)})$, where the pK_a value was fitted to the experimental data. The 100% ionized and 0% ionized absorbance values were fitted to the experimental values at 242, 244, and 246 nm for N-acetyltyrosine, N-acetyl-3-chlorotyrosine, and N-acetyl-3,5-dichlorotyrosine, respectively. The calculated pK_a values for N-acetyltyrosine, N-acetyl-3-chlorotyrosine, and N-acetyl-3,5-dichlorotyrosine are 9.8, 8.5, and 6.7, respectively.



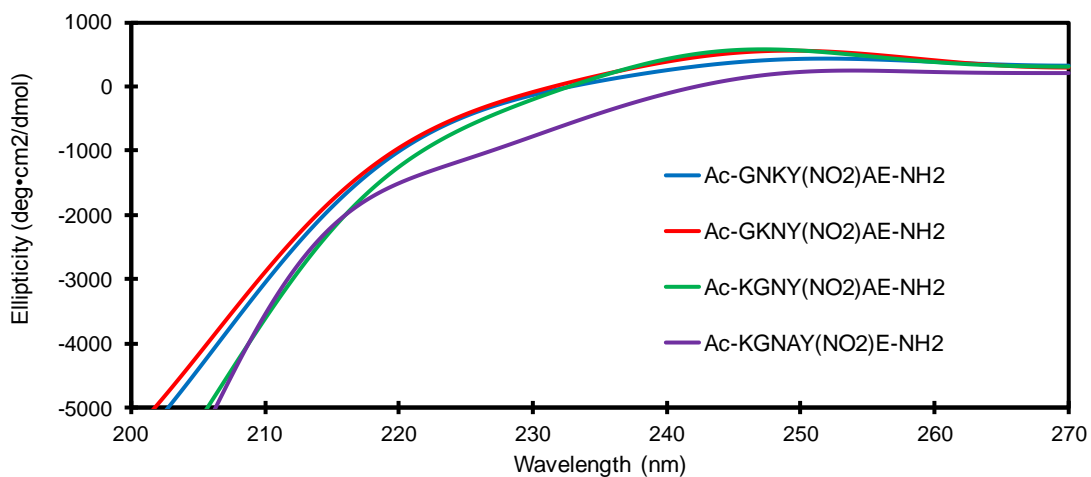
Appendix D: Chlorination of AcNO₂Tyr Lowers the pK_a Value of the Phenol Hydroxyl. Approximately 300 μM of AcNO₂Tyr or AcClNO₂Tyr were suspended in 100 mM phosphate buffer at the indicated pH values and the absorbance was measured by UV/Vis spectroscopy. The absorbance at 430 nm for both compounds in 0.1 M NaOH was assumed to represent 100% ionized while the absorbance value while in 0.1 M HCl was assumed to represent 0% ionized. The curves plot the function, percent ionized = $(100 \cdot 10^{(pH-pK_a)}) / (1 + 10^{(pH-pK_a)})$ where the pK_a value was optimized to minimize differences between the calculated and experimental values. The calculated pK_a values for AcNO₂Tyr and AcClNO₂Tyr are 7.1 ± 0.1 and 5.4 ± 0.1, respectively.



Appendix E: pH-Dependence of the Apparent Rate Constant of AcNO₂Tyr Chlorination by HOCl. 750 μM AcNO₂Tyr was reacted with 100 μM HOCl at the specified pH for 5, 10, 15, 30, 45, and 60 s. The observed rate constant and error was obtained by modeling the HPLC results as described in the Experimental Procedures. The solid curve models the pH dependence of the apparent rate constant as $k_x[\text{phenol}][\text{HOCl}] + k_y([\text{phenol}][\text{OCl}^-] + [\text{phenolate}][\text{HOCl}]) + k_z[\text{phenolate}][\text{OCl}^-]$. The pK_a value for AcNO₂Tyr and HOCl used to calculate the relative concentrations of the acid and conjugate base were 7.1 and 7.5, respectively. Due to the similarity in pK_a values, it was necessary to combine the rate constants of the phenol reacting with HOCl and the phenolate reacting with OCl⁻. The rate constants are $k_x = 2.9 \pm 1.0$; $k_y = 35.6 \pm 1.8$; and $k_z = 1.6 \pm 0.9 \text{ M}^{-1}\text{s}^{-1}$. The preferred species for the chlorination reaction are either the phenol reacting with OCl⁻ or the phenolate reacting with HOCl.

Peptide Sequence	Theoretical Mass (m/z)	Actual Mass (m/z)
L ^D FP(OH)TYL ^D F-P(OH)T	1112.6	1112.1
L ^D F-P(OH)TKL ^D FP(OH)T	1077.6	1077.3
L ^D FP(OH)TYL ^D F-P(OH)	1011.5	1011.4
^D FP(OH)TYL ^D F-P(OH)T	999.5	999.3
L ^D F-P(OH)TKL ^D FP(OH)	976.6	976.4
^D F-P(OH)TKL ^D FP(OH)T	964.5	964.1
P(OH)TYL ^D F-P(OH)T	852.4	852.2
^D F-P(OH)TKL ^D F	750.4	750.2
YL ^D F-P(OH)	537.3	536.9

Appendix F: Confirmation of Cyclic Structure of cyclo-P(OH)TKL^DFP(OH)TYL^DF- by MS/MS. The purified, cyclic peptide, cyclo-P(OH)TKL^DFP(OH)TYL^DF-, was analyzed using a ThermoFinnigan LCQ Deca XP mass spectrometer and confirmed to have a mass of 1240.7 m/z. The original linear peptide sequence was NH₂-P(OH)TKL^DFP(OH)TYL^DF-CO₂ and has a mass of 1258.7 m/z. To determine whether cyclization occurred between the N-terminal hydroxyproline and the C-terminal phenylalanine, we examined the daughter ions of the 1240.7 m/z mass and identified peptide sequences that are only possible if the peptide is cyclized appropriately, shown below. The results confirm the intended cyclic peptide was synthesized. Theoretical masses were determined using the ProteinProspector tool from prospector.ucsf.edu.



Appendix G: CD Spectra of Peptides Containing Lysine and NO₂Y. Four indicated peptides were diluted into 10 mM phosphate buffer at pH 7.4 with a final peptide concentration ranging from 270 to 430 μ M. The concentration was determined by measuring the UV/Vis absorbance at 360 nm of similarly diluted samples in 0.1 M HCl. The CD spectrum was measured on a JASCO model J720 spectropolarimeter at 37 °C with samples in a 1 mm-width cell. Data was measured between 200 and 270 nm in 0.5 nm increments with 1 nm band width and 1 s dwell time. The CD was converted to ellipticity by dividing by the path length, the concentration of the peptide, and the number of residues in the peptide. The spectrum of all four peptides is typical of a disordered secondary structure.